

DEVELOPMENT OF MEMBRANE CHROMATOGRAPHIC SEPARATION

DEVELOPMENT OF MEMBRANE CHROMATOGRAPHIC SEPARATION AND THEIR
APPLICATION FOR BIOPHARMACEUTICAL (THERAPEUTIC MONOCLONAL
ANTIBODIES AND T7 BACTERIOPHAGE) PURIFICATION

BY

ROXANA ROSHANKHAH, B.Sc.

A THESIS

SUBMITTED TO THE SCHOOL OF CHEMICAL ENGINEERING
AND THE SCHOOL OF GRADUATE STUDIES
IN PARTIAL FULFILMENT OF THE REQUIREMENTS
FOR THE DEGREE OF
MASTER OF APPLIED SCIENCE

Hamilton, Ontario

Examining Committee:

Supervisors: Dr. Raja Ghosh, Dr. Robert Pelton

Committee: Dr. Amin Reza Rajabzadeh

Master of Applied Science (2022)

School of Chemical Engineering

McMaster University, Hamilton, Ontario, Canada

TITLE:	Development of membrane chromatographic separation and their application for biopharmaceutical (therapeutic monoclonal antibodies and T7 bacteriophage) purification
AUTHOR:	Roxana Roshankhah, B.Sc.
SUPERVISOR:	Dr. Raja Ghosh, Dr. Robert Pelton
NUMBER OF PAGES:	89, xv

Abstract

Biopharmaceuticals, produced and extracted from living cells and organisms, are targeted treatments for a variety of medical conditions and diseases, some of which have no other available treatments. The manufacturing of biopharmaceuticals consists of upstream and downstream processes. The downstream operation includes several steps, such as purification and quality controls, among others. The purification process is crucial in the production of biopharmaceuticals, as a high impurity rate renders the treatment unusable. The production of therapeutic biopharmaceuticals is bounded by the efficiency of the purification process. Due to its close connection to the purification process, industrial solutions such as Chromatography purification became significantly important, with several qualitative and quantitative techniques for mixture components identification, separation, and purification, was introduced and adopted within this field.

In this thesis, the Trastuzumab purification process is investigated using cation-exchange z^2 Laterally-Fed Membrane Chromatography (z^2 LFMC) purification technique. z^2 LFMC is a purification device that leverages z^2 flow distribution characteristics to enhance the separation efficiency of a laterally-fed membrane chromatography. Exploring the performance discrepancy between z^2 LFMC and affinity chromatography (Considers as one of the most diverse and powerful chromatographic methods for purification) in the process of Trastuzumab purification. The experimental evaluation highlights that both chromatography methods (z^2 LFMC and protein A) achieve more than 95% purity efficiency. However, the recovery rate of z^2 LFMC was noticeably higher (90.4% in comparison with 81.7%).

Bacteriophages were widely used to treat various bacterial diseases in people and animals. Further, the purification of T7 bacteriophage membrane chromatography by anion exchange z^2 LFMC shows a promising research direction. The results show that following anion exchange z^2 LFMC enables a recovery rate of up to 89.0%, and a 71.2% endotoxin removal rate.

This thesis further explores the potential enhancements in the separation process. In particular, Computational Fluid Dynamic (CFD) modeling is utilized toward developing several design variations of the z^2 LFMC. This thesis highlights that the biopharmaceuticals purification process is nowhere optimized, and several state-of-the-art approaches, including z^2 LFMC, can be used to significantly increase the efficiency of the purification process.

Key words: Purification, Chromatography, Membrane, Column, Laterally Fed Membrane Chromatography, LFMC, z²LFMC, Monoclonal Antibodies, Computational Fluid Dynamics, CFD, Bacteriophage, T7, Impurities

Acknowledgments

All the praises and thanks be to God, the Most Merciful, the Most Gracious.

This thesis would not be possible without the support and contributions of several individuals. Chief among them is Dr. Raja Ghosh, who I would like to thank for readily providing patience, guidance, and support for the past several years of my academic career. His advice and constant help in these 3 years helped me to gain confidence in my path.

I would also like to thank Dr. Robert Pelton, my co-supervisor, and his group for all the help and equipment they provided while I was performing my tests.

I am thankful to Dr. Zeinab Hosseini Doust and Kyle Jackson for their help in our collaboration project.

I would like to thank my collaborators in Dr. Ghosh group, Dr. Guoqiang Chen, Dr. Karina Kawka for helping me to set up my experiments whenever I was desperately finding a solution. Thanks to Yating Xu for her encouragement during this path.

I would like to thank my parents and my brother for their support without them, this day would not have been possible. No amount of words will be enough to tell how grateful I am to them.

And finally, I would like to thank McMaster University to give me this opportunity to do my Master's. Definitely, being at McMaster was the best time in my life.

Table of Contents

Chapter 1	2
Introduction	2
Biopharmaceuticals Purification Process	2
Purification of Monoclonal Antibodies	2
Purification of T7 Bacteriophage.....	3
Chromatography.....	3
LFMC, z ² LFMC.....	4
CFD Simulation & Modeling	4
Thesis Structure	5
Chapter 2.....	5
Chapter 3.....	5
Chapter 4.....	5
Chapter 5.....	5
References.....	6
Chapter 2.....	9
Abstract	11
Introduction	12
Experimental.....	17
Materials	17
Membrane Chromatography Device	17
Methods.....	18
Results and Discussion.....	19
Conclusion	31
CRediT Authorship Contribution Statement.....	33
Declaration of Competing Interest.....	33
Acknowledgments.....	33
Data availability	33
References.....	34
Chapter 3.....	42
Abstract:	43
Introduction	43
Materials.....	45
Results and Discussion.....	47

Conclusion	58
Acknowledgment.....	59
References.....	60
Chapter 4.....	64
Abstract	65
Introduction	65
Materials and Methods.....	67
Phage Propagation and Filtering	67
Double Overlay Phage Titer Assay	68
Endotoxin Quantification Assay	68
Materials.....	69
Results and Discussion.....	69
Conclusion	80
Acknowledgement	81
References.....	82
Chapter 5.....	87
Conclusion	87
Future work	88
Appendix.....	89

List of Abbreviations

mAb	Monoclonal Antibodies
LFMC	Laterally-Fed Membrane Chromatography
E-Coli	Escherichia Coli
kb	Kilobase
DNA	Deoxyribonucleic Acid
HIC	Hydrophobic Interaction Chromatography
CHO	Chinese Hamster Ovary
BSA	Bovine Serum Albumin
CFD	Computational Fluid Dynamics
SEC	Size Exclusion Chromatography
CV	Colum Volume
PBS	Phosphate Buffered Saline
SDS-PAGE	Sodium Dodecyl Sulfate Polyacrylamide Gel Electrophoresis
HPLC	High Performance Liquid Chromatography

Da	Dalton
UV	Ultraviolet
HMW	High Molecular Weight
LMW	Low Molecular Weight
AUC	Area Under Curve
HCP	Host Cell Protein
DLS	Dynamic Light Scattering
S	Sulfonic Functional
MALDI-Tof	Matrix-Assisted Laser Desorption/Ionization – Time of Flight
Q	Quaternary Ammonium
FEM	Finite Element Method
FT	Flow-Through
E	Eluate
HETP	Height Equivalent to Theoretical plates
CVM	Column Volume per Minute
TFF	Tangential Flow Filtration

LPS	Lipopolysaccharide
MC	Membrane Chromatography
NSERC	Natural Sciences and Engineering Research Council of Canada
pI	Isoelectric Point
EU	Endotoxin Unit
Pg	Porphyromonas Gingivalis
PFU	Plaque-Forming Unit
PEG	Polyethylene Glycol
AEC	Anion Exchange Chromatography
RPM	Revolutions Per Minute
UF	Ultra Filtration
LAL	Limulus Amoebocyte Lysate
Cond	Conductivity

List of Figures/ Tables

Figure 1: A. Schematic representation of fluid flow in a z ² LFMC device. B. Photograph of a z ² LFMC device.	16
Figure 2 Chromatogram obtained during purification of Trastuzumab from CHO cell culture supernatant using MabSelect SuRe affinity column	20
Figure 3 SEC chromatogram obtained with Trastuzumab purified using MabSelect SuRe column-based affinity chromatography (mobile phase: Phosphate Buffered Saline (pH 7.4), column: TSK-Gel G3000SWXL; flow rate: 0.5 mL/min; sample volume: 50 µL).....	21
Figure 4 Effect of dilution factor on the fraction of mAb recovered during Trastuzumab purification from CHO cell culture supernatant using the S z ² LFMC device at pH 5.5.....	24
Figure 5 Chromatogram obtained during the purification of Trastuzumab from CHO cell culture supernatant using the S z ² LFMC device	25
Figure 6 Close-ups of the eluted mAb peaks obtained during Trastuzumab purification using the S z ² LFMC device, the mAb being eluted with three different linear gradients, i.e., 25 mL (A), 50 mL (B), and 100 mL (C)	25
Figure 7 SEC chromatograms obtained during purification of Trastuzumab from CHO cell culture supernatant using S z ² LFMC device. A. Flow through sample. B. Eluted mAb.....	26
Figure 8 Chromatogram obtained during purification of Trastuzumab from CHO cell culture supernatant using the Capto S ImpAct column.....	27
Figure 9 Close-ups of the eluted mAb peaks obtained during Trastuzumab purification using the Capto S ImpAct column at two different flow rates, i.e., 5 mL/mL (A), and 10 mL/min (B)	28

Figure 10 SEC chromatograms obtained during purification of Trastuzumab from CHO cell culture supernatant using Capto S ImpAct column. A. Flow through sample. B. Eluted mAb 28

Figure 11 Analysis of purified Trastuzumab samples obtained by MabSelect SuRe, Capto S ImpAct, and S z²LFMC based purification methods using 10% reducing SDS-PAGE..... 29

Figure 12 Membrane chromatography devices with equal bed height. A) Stacked disk membrane B) Radial flow membrane chromatography 48

Figure 13 Laterally fed membrane chromatography in three different generations..... 48

Figure 14 Concentration of solute (mol/m³) on stacked-disc device on the time of 15 seconds. 49

Figure 15 Concentration of solute (mol/m³) on radial flow device on the time of 15 seconds. 50

Figure 16 Concentration of solute (mol/m³) on LFMC device on the time of 15 seconds... 51

Figure 17 Concentration of solute (mol/m³) on z²LFMC-rectangular design device on the time of 15 seconds. 52

Figure 18 Concentration of solute (mol/m³) on z²LFMC-square design device on the time of 15 seconds 52

Figure 19 Concentration of solute (mol/m³) on z²LFMC-square design device on the time of 15 seconds 55

Figure 20 Concentration of solute (mol/m³) on z²LFMC-square design device on the time of 15 seconds 56

Figure 21 Tracer profiles for 5 different membrane chromatography at 500mL/min 57

Figure 22 Effect of the curvature on tracer profile at 100 mL/min 58

Figure 23 Diameter of primary and secondary channels in the rectangular and square z ² LFMC devices.....	70
Figure 24 Optimizing the gradient for releasing pure phage.....	72
Figure 25 Optimizing pH for releasing pure phage	72
Figure 26 Optimization regarding the pH and Gradient. Further investigation on A) Eluate peak ratio and B) PFU Recovery	75
Figure 27 Conductivity in AKTA of different dilutions (1 in 2, 1 in 4, 1 in 8, 1 in 20) of phage in FT	75
Figure 28 Effect of dilution (1 in 2, 1 in 4, 1 in 8, 1 in 20) on peak area ratio.....	76
Figure 29 Single and multi-injection phage on z ² LFMC.....	77
Figure 30 Single and multi-injection phage on z ² LFMC.....	78
Figure 31 PFU recovery and Endotoxin removal based on previous chromatographs	79
Figure 32 Super loop by loading 100 mL phage 1:1 with optimized conditions, B) Super loop by loading 15 mL phage 1:1.....	79

Table 1 Effect of flow rate on the number of theoretical plates per unit bed height in the 5 mL S z ² LFMC device and the 5 mL Capto S ImpAct.....	22
Table 2 Attributes of the mAb peaks and mAb recovery obtained during purification experiments carried out using the MabSelect SuRe column, the S z ² LFMC device, and the Capto S ImpAct column.....	30
Table 3 Parameters used in CFD experiment.....	46
Table 4 Diameter of primary and secondary channels in the rectangular and square z ² LFMC devices.....	53
Table 5 Number of plates/m obtained with the 5 mL Q z ² LFMC device in different flowrates (5, 10, 12 and 15 mL)	71
Table 6 Comparing endotoxin removal percentage in UF Centrifuge, UF stirred filter and Sartobind Q z ² LFMC.....	80

Chapter 1

Introduction

Biopharmaceuticals Purification Process

The upstream process of biopharmaceutical manufacturing produces monoclonal antibodies and bacteriophages. Based on the nature of the used biopharmaceuticals, there are several production types. For instance, monoclonal antibodies and bacteriophages are produced using cell culture in a bioreactor. The downstream process occurs after the upstream process, encompasses three main steps, namely, initial recovery (i.e., extraction/isolation), purification (i.e., removal of most contaminants), and polishing (i.e., removal of specified contaminants and that may have formed during isolation and purification) [2].

The purification step within the downstream process consists of multiple operation units, working parallelly to purify a biological product from cell culture. This step involves capturing the target biomolecule and removing impurities like host cell proteins, DNA, process-related impurities, including buffers and antifoam, as well as product-related impurities, such as aggregates [1].

The purification step can either be simple, or complex by design, where several approaches are introduced in the literature, including but not limited to, filtration, centrifugation, chromatography, and precipitation.

Purification of Monoclonal Antibodies

Over the past few decades, the therapeutic use of monoclonal antibodies for various treatments has been approved [3][4]. Highly purified monoclonal antibodies are crucial for human use, particularly in treatments targeting cancer, autoimmune disorders, cardiovascular disease, chronic illnesses, and infectious diseases [5]. The purification of monoclonal antibodies is crucial due to (i) the recent growth in the produced capacity for monoclonal antibodies (mAbs) from a few milligrams to grams per liter, and (ii) the need for various combinations of doses in the treatment process. Due to these changes, the purification processes are tested under various constraints to ensure an efficient production cycle [6]. This includes the separation of antibodies based on size, charge, or chemical properties.

Purification of T7 Bacteriophage

Bacteriophage is a virus with the ability to infect bacteria and destroy their functional components. Bacteriophage infects most strains of *Escherichia coli* and relies on these hosts to propagate. The virulent T7 phage is one of seven phages first identified in 1945 [7]. The genome of T7 phages is approximately 40 kb in size, and is packed into the polyhedral head, formed by the capsid proteins [8].

With the recent rise in antibiotic resistance to bacterial pathogens, it become essential to develop novel infection-control strategies. Despite being a newly emerging method, the bacteriophage is widely developed across several countries to treat patients that suffer from antibiotic resistance. However, the lysis procedure of bacteriophages contains several harmful impurities, such as endotoxin, produced by gram-negative bacteria. Due to that, recent efforts focus on advancing downstream processes, including the purification process, enabling wide use of bacteriophage for treatments with reduced risks.

Chromatography

Among purification methods, chromatography is a traditional technique [9] consisting of several purification approaches, including affinity, ion-exchange, hydrophobic interactions, size exclusion, and mixed-mode chromatography [10][11]. Affinity chromatography, for example, is based on reversible biological interactions between two molecules, such as enzyme-substrate interactions or antibody-antigen interactions [12]. On the other hand, the driving force of ion-exchange chromatography is the electrostatic interaction between the target molecule and the stationary media [13]. For instance, in cation-exchange chromatography, the base is negatively charged, while the target molecule in the feed is positively charged. Charging the target molecule, however, is still ongoing research, with several proposed solutions. For instance, a charge can be set in stationary media based on pH levels, where a positive charge is assigned when the pH level is below an isoelectric point (pI), and a negative charge is assigned when the pH is above the pI threshold. Moreover, Hydrophobic Interaction Chromatography (HIC) is widely used to purify biopharmaceuticals based on their hydrophobic interaction with the coupled hydrophobic ligands.

LFMC, z²LFMC

LFMC is a new design to increase the protein purification efficiency using a stack of microporous membranes, enabling a fast and scalable alternative solution to column chromatography. As the fluid enters from the inlet, it passes through the membrane stack at various points along its length while moving along the tapers. The fluid then exits the outlet on the other side of the membrane stack, located at the bottom port. The literature highlighted the capabilities of LFMC, not limited to resolution and stability of protein separation process, but also achieving higher theoretical plates in comparison with resin-based membrane stacked disks [14][15][16][17][18][19]. In this thesis, various enhancements of the purification resolution is proposed by removing the tapered design in LFMC. These enhancements are referred to as the second generation of LFMC (i.e., z²LFMC), as the flow is a combination of two z-patterns [20]. This module is designed to overcome the limitations that exist in LFMC, and is accompanied by several CFD simulations and lab experiments across this thesis.

CFD Simulation & Modeling

CFD is the process of mathematically modeling physical and chemical problems in an attempt of solving them numerically [21]. CFD is an efficient computerized method of studying fluid mechanics based on numerical analyses, removing some of the complexities associated with experimental approaches, allowing for extensive analysis of three-dimensional bioreactors flow fields [22] [23]. CFD starts with creating and meshing the model. The geometry is discretized into a collection of discrete, finite volumes by the mesh. Then, initial and boundary conditions are applied to the mesh solution domain. Once inputted to the system, the solver engine iteratively solves the specified physical models in each mesh cell until the solution domain's set convergence requirements are reached. To this end, the computation results are extracted and displayed in appropriate format (streamlines, contours, etc.), providing a better end-user understanding of the simulation outcomes [24].

In this thesis, CFD simulations are configured based on the mass and momentum conservation principles. Given that all the tests are associated with chromatography, the Navier-Stokes (conservation of momentum), conservation of mass and Brinkman Equations are

used. Along with this thesis, the two physics that were used in simulations are “laminar flow” and “transport of diluted species in porous media physics”.

Thesis Structure

The remaining of this thesis consists of published and ongoing projects.

Chapter 2

In this chapter, the efficiency of protein affinity chromatography, resin based column, and LFMC, for purification of monoclonal antibodies are investigated to find alternatives for high-resolution protein separation. This chapter was published in Biochemical Engineering Journal.

Chapter 3

In this chapter, CFD is used to compare various designs of LFMC modules, comparing the performance against radial flow and stacked disk devices.

Chapter 4

This chapter explores the feasibility of using z²LFMC for T7 Bacteriophage purification, supported by extensive analytical results.

Chapter 5

In this chapter, the main insights and findings are reported, alongside the ongoing projects and future research directions.

References

- [1] A.F. Jozala, D.C. Geraldés, L.L. Tundisi, V.A. Feitosa, C.A. Breyer, S.L. Cardoso, P.G. Mazzola, L. Oliveira-Nascimento, C.O. Rangel-Yagui, P.O. Magalhães, M.A. Oliveira, A. Pessoa, Biopharmaceuticals from microorganisms: from production to purification, *Braz. J. Microbiol.*, 47 Suppl 1(2016), pp. 51-63
- [2] A.M. Azevedo, P.A. Rosa, I.F. Ferreira, M.R. Aires-Barros, Chromatography-free recovery of biopharmaceuticals through aqueous two-phase processing, *Trends. Biotechnol.*, 27(4)(2009), pp. 240-247
- [3] L.M. Weiner, Fully human therapeutic monoclonal antibodies, *J. Immunother.*, 29(1)(2006), pp. 1–9
- [4] J.M. Reichert, V.E. Valge-Archer, Development trends for monoclonal antibody cancer therapeutics, *Nat. Rev. Drug. Discov.*, 6(5)(2007), pp. 349–356
- [5] A.B. Mahmuda, F. Bande, K.J. Kadhim Al-Zihiry, N. Abdulhaleem, R.A. Majid, R.A. Hamat, W.O. Abdullah, Z. Unyah, Monoclonal antibodies: a review of therapeutic applications and future prospects, *Trop. J. Pharm. Res.*, 16 (2017), pp. 713-722
- [6] D.S. Chahar, S. Ravindran, S.S. Pisal, Monoclonal antibody purification and its progression to commercial scale, *J. Biol. Stand.*, 63(2020), pp. 1–13
- [7] M. Demerec, U. Fano, Bacteriophage-resistant mutants in *Escherichia coli*, *Genetics.*, 30(1945), pp. 119–136
- [8] H. Xu, X. Bao, W. Hong, A. Wang, K. Wang, H. Dong, J. Hou, R. Govinden, B. Deng, H.Y. Chenia, Biological Characterization and Evolution of Bacteriophage T7- Δ holin During the Serial Passage Process, *Front. Microbiol.*, 12(2021), pp. 705310

[9] E. Karlsson, L. Ryden, J. Brewer, Protein purification. Principles, High Resolution Methods, and Applications (2nd Edition), Ion exchange chromatography, New York: Wiley (1998)

[10] H. Rusli, R.M. Putri, A. Alni, Recent Developments of Liquid Chromatography Stationary Phases for Compound Separation: From Proteins to Small Organic Compounds. *Molecules.*, 27(3)(2022), pp. 907

[11] M. Saraswat, L. Musante, A. Ravidá, B. Shortt, B. Byrne, H. Holthofer, Preparative purification of recombinant proteins: current status and future trends, *Biomed. Res. Int.*, 2013 (2013), pp. 1-18

[12] M. Urh, D. Simpson, K. Zhao, Affinity chromatography: general methods, *Meth. Enzymol.*, 463(2009), pp. 417–438

[13] S. Fekete, A. Beck, J. Fekete, D. Guillarme, Method development for the separation of monoclonal antibody charge variants in cation exchange chromatography, Part I: salt gradient approach, *J. Pharm. Biomed. Anal.*, 102(2015), pp. 33–44

[14] P. Madadkar, R. Ghosh, High-resolution protein separation using a laterally-fed membrane chromatography device, *J. Membr. Sci.*, 499(2016), pp. 126-133

[15] P. Madadkar, S.L. Nino, R. Ghosh, High-resolution, preparative purification of PEGylated protein using a laterally-fed membrane chromatography device. *J. Chromatogr. B., Analytical technologies in the biomedical and life sciences*, 1035(2016), pp.1–7

[16] P. Madadkar, U. Umatheva, G. Hale, Y. Durocher, R. Ghosh, Ultrafast Separation and Analysis of Monoclonal Antibody Aggregates Using Membrane Chromatography, *Anal. Chem.*, 89(8)(2017), pp. 4716-4720

[17] P. Madadkar, Q. Wu, R. Ghosh, A laterally-fed membrane chromatography module, *J. Membr. Sci.*, 487(2015), pp. 173-179

- [18] R. Ghosh, P. Madadkar, Q. Wu, On the workings of laterally-fed membrane chromatography, *J. Membr. Sci.*, 516(2016), pp. 26-32
- [19] R. Sadavarte, P. Madadkar, C.D. Filipe, R. Ghosh, Rapid preparative separation of monoclonal antibody charge variants using laterally-fed membrane chromatography, *J. Chromatogr. B., Analytical technologies in the biomedical and life sciences*, 1073(2018), pp. 27–33
- [20] R. Ghosh, G. Chen, R. Roshankhah, U. Umatheva, P. Gatt, A z^2 laterally-fed membrane chromatography device for fast high-resolution purification of biopharmaceuticals, *J. Chromatogr. A.*, 1629(2020), pp. 461453
- [21] J. H. Ferziger, M. Peric, *Computational methods for fluid dynamics*. Springer, Berlin Heidelberg New York, (2002), pp. 217–259
- [22] D.W. Hutmacher, H. Singh, *Computational fluid dynamics for improved bioreactor design and 3D culture*, *Trends. Biotechnol.*, 26(4)(2008), pp. 166–172
- [23] A. John, *Computational Fluid Dynamics in Upstream Biopharma Manufacturing Processes*. Thomas Pharmaceutical Technology, *Pharm. Technol.*, 45(11)(2021), pp. 34-40
- [24] C. Johnson, V. Natarajan, C. Antoniou, Evaluating two process scale chromatography column header designs using CFD, *Biotechnol. Prog.*, 30(4)(2014), pp. 837–844

Chapter 2

Purification of Monoclonal Antibody using Cation Exchange z^2 Laterally-fed Membrane Chromatography – A Potential Alternative to Protein A Affinity Chromatography

Prior to any treatment with biopharmaceuticals, the target protein has to be separated from a complex mixture and that is the reason for having protein purification as the main application in biotechnology. A target protein can be separated from other mixtures based on their specific properties like charge, hydrophobicity or affinity to another molecule, whereas affinity is the most efficient method. One example is protein A (ligand), which can be utilized to purify immunoglobulin G antibodies (target protein). Ion exchange chromatography is a common and powerful purification technique in the production of monoclonal antibodies. Ion-exchange chromatography separates monoclonal antibodies based on their charge. Toward that, the S z^2 LFMC format was used to ensure high-speed and high-resolution purification in purifying trastuzumab from cell culture supernatant. In this experiment, the purity and recovery of mAb obtained with these two devices were compared.

In this project, I completed the experiments and was the primary author of the manuscript. Dr. Guoqiang Chen helped me with my initial understanding of the project and setting up the equipment. Yating Xu and Nikhila Butani helped me with the experiments when I was not available at McMaster University during my internship.

Dr. Yves Durocher and Dr. Robert Pelton provided the materials of the experiment and Dr. Raja Ghosh supervised the project and edited the manuscript.

This chapter was published in Biochemical Engineering Journal.

Roxana Roshankhah, Guoqiang Chen, Yating Xu, Nikhila Butani, Yves Durocher, Robert Pelton, Raja Ghosh,

Purification of monoclonal antibody using cation exchange z² laterally-fed membrane chromatography – A potential alternative to protein A affinity chromatography,

Biochemical Engineering Journal,

Volume 178,

2022,

108293,

ISSN 1369-703X,

<https://doi.org/10.1016/j.bej.2021.108293>.

(<https://www.sciencedirect.com/science/article/pii/S1369703X21003697>)

© Copyright by Roxana Roshankhah
All Rights Reserved

Purification of Monoclonal Antibody using Cation Exchange z^2 Laterally-fed Membrane Chromatography – A Potential Alternative to Protein A Affinity Chromatography

Roxana Roshankhah^a, Guoqiang Chen^a, Yating Xu^a, Nikhila Butani^a, Yves Durocher^{b,c}, Robert Pelton^a, Raja Ghosh^{a,*}

^a Department of Chemical Engineering, McMaster University, 1280 Main Street West, Hamilton, ON L8S 4L7, Canada

^b National Research Council of Canada, Montreal, QC H4P 2R2, Canada

^c Département de biochimie et médecine moléculaire, Faculté de médecine, Université de Montréal, Montreal, QC H3C 3J7, Canada

*Corresponding Author

Email: rghosh@mcmaster.ca

Phone: +1 905 525 9140 ext 27415

Abstract

Protein A affinity chromatography, which is the standard method for purifying monoclonal antibodies (mAbs) is expensive and involves elution at acidic pH, which could degrade the mAb. Moreover, it cannot be used to fractionate charge variants or to remove mAb aggregates. In this study, we examine the purification of Trastuzumab by cation-exchange z^2 laterally-fed membrane chromatography (or z^2 LFMC). It has been shown that z^2 LFMC is suitable for carrying out high-speed, high-resolution protein purification. The results discussed in this paper demonstrate that the purity of Trastuzumab obtained by the z^2 LFMC process was comparable to that obtained by protein A chromatography (i.e., >95% with both methods), while the recovery was significantly greater with z^2 LFMC (90.4% as opposed to 81.7%). Also, the z^2 LFMC process was faster, did not require acidic pH conditions for elution, and the mAb was eluted in 2.24 bed volumes as opposed to 2.74 bed volumes with protein

A chromatography. The mAb productivity obtained with the z²LFMC process was more than 3 times higher than that with the column-based purification process. The z²LFMC device is significantly cheaper than its equivalent protein A affinity column, and earlier studies have shown it to be suitable for separating mAb charge variants and aggregates. Therefore, the z²LFMC process could be evaluated as a cheaper and more efficient alternative to protein A affinity chromatography.

Key Words: Membrane chromatography, LFMC, Monoclonal antibody, Purification, z²LFMC

Introduction

Monoclonal antibodies (or mAbs) of the IgG class have been successfully adopted and used as biopharmaceuticals. The typical dosage of mAbs used to treat diseases such as cancer, autoimmune disorders, cardiovascular disease, chronic illnesses, and infectious diseases (including COVID- 19) ranges from hundreds of milligrams to several grams, and these are manufactured at scales ranging from hundreds of kilograms to several tons per year [1], [2], [3], [4], [5], [6], [7], [8], [9]. MAb comprise about 58% of the biopharmaceutical market, increasing from about \$50 billion to about \$90 billion between the years 2010 and 2015 [7]. The advent of Trastuzumab, an anticancer drug which is used to treat HER-2 positive breast cancer, led to rapid growth and development of mAb therapeutics [8], [10]. This molecule is widely used as a model for designing and developing mAb manufacturing processes. However, mAb therapy is very expensive [11], [12], [13]. The high cost for a biosimilar mAb like Trastuzumab is associated with the manufacturing cost, which consists of two components: (i) upstream cost, including the cost of raw materials such as cell culture media and the cost of running bioreactors, and (ii) downstream cost, which is the cost of purification and formulation. In a techno-economic analysis [14], the total capital investment for mAb manufacture was estimated at \$121.6 million, with upstream machinery cost being about 35%, with the remaining cost associated with the downstream machinery. There is consensus that the high downstream processing cost is primarily responsible for the high cost of biopharmaceuticals such as mAbs [15]. The main reason for the high cost of mAb purification is the complexity of the process, which sometimes involves more than 30 unit operations, including multiple chromatography steps, that are required to obtain safe and efficacious products [15], [16]. Moreover, most mAbs have some degree of

microheterogeneity, and tendency to form aggregates and these factors create additional challenges [17], [18].

Affinity chromatography is regarded as the gold standard technique for purifying mAbs [19], [20], [21], [22], [23], [24]. It utilizes immobilized ligands, such as protein A, protein G or protein L. Protein A interacts strongly and specifically with the Fc region of IgG mAbs. The use of such ligands makes it possible to remove up to 98% of impurities, even from very complex feed streams, such as cell culture harvest media. Protein A columns have been used by mAb manufacturers for many years despite challenges such as high cost, low reusability, and concerns over the clearance of leached ligand [19]. This is contributed to that protein A include high single-step purity, ease of use, high capacity, high recovery, broad applicability, familiarity, and availability from multiple suppliers [19], [25], [26]. However, using of protein A column has its own limitations and drawbacks, including the leakage of protein A, which is immunotoxic, and the acidic pH condition required for elution, which leads to antibody aggregation, or, in some cases, leading to chemical modification of the constituent amino acids [27], [28], [29]. Aggregates are also formed during cell culture, and several preliminary downstream processing steps, including centrifugation and microfiltration [30]. Note that Monoclonal antibody aggregates cannot be separated from non-aggregated mAb molecules by protein A chromatography, as both species bid to the ligand through their Fc domain [31]. When using protein A chromatography for purifying mAbs, additional steps, such as size exclusion chromatography, cation exchange chromatography, hydrophobic interaction chromatography or hydrophobic charge induction chromatography, are required for removing aggregates [31], [32]. Moreover, the price of protein A media is substantially higher than other types of chromatographic media. A protein A column with a diameter of 1 m and a bed height of 50 cm could cost up to several millions of US dollars, which is two times the cost of ion-exchange resin [16]. The dynamic mAb binding capacity of protein A resin is nearly half that of a typical cation exchange resin [33]. In addition, Protein A is unable to discriminate between mAb charge variants. Therefore, if acidic or basic mAb variants are present in the feed sample, they are co-eluted with the mAb. In the literature, it has been shown that a maximum of 50 cycles is possible with the best protein A column, With is significantly lower than ion-exchange columns [34]. Further, a major concern of using protein A resin is the associated risks when using cleaning agents [35], [36].

Considerable effort is currently being devoted to research on alternatives to protein A affinity chromatography [37], [38]. Biopharmaceutical companies were surveyed in 2016 to assess their motivation for replacing protein A columns [39]. The results showed that over half of the companies would consider replacing protein A with a suitable alternative, and nearly 20% reported that they were already in the process of finding alternatives [39]. Most humanized mAbs of IgG1 and IgG2 subclasses bind to cation exchange resins under low ionic strength conditions, and these can be eluted by increasing the conductivity or the pH of the eluting buffer. Cation exchange chromatography has been shown to be highly suitable for removing mAb aggregates, separating charge-variants, and removing DNA and leached protein A [23], [40]. Also, cation exchange resins are significantly more stable at acidic and alkaline conditions than protein A media [40]. For instance, membrane chromatography, which involves the use of porous membranes as chromatographic media has been found to be suitable for carrying out fast and scalable ion-exchange chromatographic separations [41], [42], [43], [44], [45]. The speed and scalability of membrane chromatography could be attributed to the predominance of convective mass transport within membranes. When compared to column chromatography, membrane chromatography is faster by more than an order to magnitude [43], [44]. The overall cost of running a membrane device is lower than that of a resin-based column due to a variety of factors which includes the lower equipment cost, and lower costs of buffer, maintenance and cleaning [45], [46]. As membranes can be disposed, expensive and time-consuming procedures such as cleaning and validation are eliminated. The use of cation-exchange membrane chromatography for purification of mAbs has been examined [41]. However, it was not found to be particularly suitable for process-scale antibody purification in the bind-and-elute mode. However, the study did show that the milder operating conditions during cation-exchange membrane chromatography resulted in better product stability in comparison to that with protein A chromatography [41].

Most commercial membrane chromatography devices currently used in the biopharmaceutical industry are of the radial flow type [23], [41], [42], [43], [44], [45], [47]. While these devices have been found to be suitable for fast separations in the flow through mode [41], they are totally unsuitable for high-resolution bind-and-elute separations due to non-uniform flow distribution [48], [49]. Flow non-uniformity results in a high degree of solute dispersion within the device, leading to broad and asymmetric peaks, and ultimately poor resolution in solute

separation. Laterally-fed membrane chromatography (or LFMC) devices developed in our group combine high-speed with high-resolution and have been shown to be particularly suitable for bind and elute separations [48], [49], [50], [51], [52], [53]. LFMC is based on the use of a stack of rectangular membrane sheets housed between two parallel plates, each plate containing a pillared lateral channel, one for flow distribution, the other for flow collection. The superior separation performance of the LFMC device vis-à-vis other membrane chromatography devices could be attributed to more uniform flow through the membrane stack, which resulted in lower solute dispersion within the device. Lower dispersion is indicated by a greater number of theoretical plates per unit membrane bed-height, and ultimately this results in better peak resolution in protein separation processes [48], [49], [50], [51], [52], [53]. In a recent paper, we have discussed a z^2 flow distribution and collection feature for improving the separation efficiency in resin-based chromatography [54]. More recently, we have demonstrated that the separation efficiency of an LFMC device could be further improved by incorporating the same z^2 flow distribution and collection feature. The resultant enhanced LFMC device is therefore designated as z^2 LFMC [55]. Flow distribution and collection in a z^2 LFMC device is achieved using two sets of primary and secondary flow channels as shown in Fig. 1A. Fig. 1B shows a photograph of an actual z^2 LFMC device. The fluid flowing through a z^2 LFMC device has three levels of hierarchy, i.e., primary flow through the primary channels, secondary flow through the secondary channels and tertiary (or normal) flow through the membrane stack [54], [55]. Such three-level hierarchy is sustained by designing the device in such a way that hydraulic resistance in the primary channels is lower than that in the secondary channels, which in turn is lower than that in the membrane stack [55]. If the resistance to flow within the membrane were lower than that within the primary and secondary channels, the fluid would “short-circuit” through the membrane stack, and the z^2 LFMC device would perform very poorly. As can be inferred from Fig. 1A, all hypothetical flow paths within the z^2 LFMC device are of identical length. Also, as the lengths of primary, secondary and tertiary flow path components in all these hypothetical pathways are the same, the hydraulic resistances along these could be expected to be identical [55]. Therefore, the residence time along these pathways could also be expected to be identical. As can be seen from Fig. 1A, the flow distribution and collection system of the z^2 LFMC device is based on straight flow channels. Hence, the extent of back mixing within these could be expected to be very low. Also, as explained in our previous paper [55], a z^2 LFMC device is very scalable and compact, and has a

narrower solute residence time distribution than the older LFMC device. The z^2 LFMC device has been shown to be suitable for separating mAb charge variants and mAb aggregates [55] from protein A purified mAb samples. In our current study, we focus on the use of cation exchange z^2 LFMC for mAb purification from cell culture supernatant in a capture chromatography mode, i.e., as an alternative to protein A based affinity chromatography.

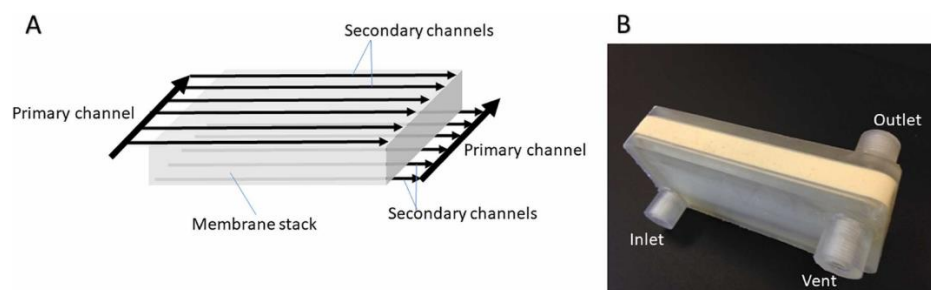


Fig. 1. A. Schematic representation of fluid flow in a z^2 LFMC device. B. Photograph of a z^2 LFMC device.

This paper discusses the feasibility of developing a capture-type process for purification of a mAb (Trastuzumab) from CHO cell culture media, in the bind-and-elute mode, using a cation exchange z^2 LFMC device [55]. As mentioned earlier, the overall objective of this study is to develop a viable alternative to protein A based mAb purification, the numerous motivations for which have already been elaborated. The z^2 LFMC device used in this study had a membrane bed volume of 5 mL and contained a stack of strong cation exchange (Mustang S) membranes. In our paper on the design and development of the z^2 LFMC device [55], we have discussed the effect of membrane pore-size on the efficiency of protein separation. The Mustang S membrane was chosen as it had an average pore size of 0.8 μm , due to which, very high resolution could be expected. A 5 mL protein A column containing MabSelect SuRe resin served as the primary control device, while a 5 mL column containing strong cation exchange Capto S ImpAct media was used as a secondary control device. Separation process parameters such as feed conditioning, flow rate and elution conditions were systematically examined. The purity and recovery of mAb obtained with these three devices along with other separation efficiency metrics are compared.

Experimental

Materials

Trastuzumab containing cell culture supernatant (lot: 20170920 BC), produced using Chinese Hamster Ovary (CHO) cell line was kindly donated by the National Research Council Canada, Montreal, QC, Canada. HiTrap Capto S ImpAct column (5 mL volume, 50 μm resin particle diameter, 16 mm column diameter, 25 mm bed height, GE17-3717-55) and protein A affinity MabSelect SuRe resin (GE17-5438-03) were purchased from GE Healthcare Biosciences, QC, Canada. Mustang S cation-exchange membrane sheets (MSTG25S6) were purchased from Pall Corporation (New York, NY, USA). The membrane has a thickness of 0.1375 mm and an average pore-size of 0.8 μm . The IgG binding capacity of the Mustang S membrane is reported to be about 20 mg/mL (manufacturer's data). Citric acid (C0759), sodium citrate (S4641), sodium phosphate monobasic (S0751), sodium phosphate dibasic (S0875), and sodium chloride (S7653) were purchased from Sigma-Aldrich (St. Louis, MO, USA). All buffers and the solutions used in our experiments were prepared using ultra-pure water (18.2 M Ω cm) obtained from a SIMPLICITY 185 water purification unit (Millipore, Molsheim, France). MF-Millipore™ Membrane Filter, 0.45 μm pore size (Catalogue Number: HAWP04700) was used for micro-filtering and degassing buffers. A size exclusion chromatography (SEC) column (TSK-Gel G3000SWXL, 7.8 mm \times 300 mm, Tosoh Bioscience, Montgomeryville, PA, USA) was used analyzing mAb samples using an Alliance HPLC system (Waters Corporations, Milford, MA, USA). Freeman 1085 Polyurethane Elastomer (Batch # 77032) consisting of resin (part A) and hardener (part B) was purchased from Freeman Manufacturing and Supply Company, Avon, OH, USA. A 5 mL custom-designed column, having a bed-height of 25 mm and diameter of 16 mm was used for carrying out protein A affinity chromatography with MabSelect SuRe resin.

Membrane Chromatography Device

The details of the design of z²LFMC device used in this study (see Fig. 1A and B) are described in our previous paper [55]. Briefly, the z²LFMC device consisted of a top plate, a membrane stack and a bottom plate held together using elastomer resin (Freeman Polyurethane) [55]. The membrane stack was prepared using 26 rectangular pieces of Mustang S membrane (each 20 mm \times 70 mm), the membrane bed-height being 3.6 mm, and the membrane bed-volume being

5 mL. The Mustang S membrane has sulfonic acid cation exchange ligand. The plates were 3-D printed with a Form 2 3-D printer (Formlabs, Somerville, MA, USA) using Formlabs Standard resin. Fluid entering the device was directed to a primary channel (circular cross-section of 0.75 mm diameter), which was located at a slight offset from the membrane stack. The fluid is then directed to a set of semi-circular secondary channels of 0.75 mm diameter each, from where it entered the top of the membrane stack. The fluid leaving the membrane stack was collected using a second set of secondary channels, and from there to a second primary channel, and thence to the outlet. These plates were provided with vents for priming the device prior to use, and for removing entrapped bubbles. These vents were kept closed during the chromatography experiments. The membrane chromatography device used in this study will henceforth be referred to as S z²LFMC.

Methods

The column and membrane-based chromatography experiments were carried out using an AKTA Prime Plus liquid chromatography system (GE Healthcare Biosciences, Montreal, QC, Canada). The performance of chromatography devices is frequently quantified in terms of the number of theoretical plates within them. Theoretical plate measurement was carried out using 0.4 M NaCl solution as mobile phase and 0.8 M NaCl solution as tracer. The volume of the tracer solution injected was 50 μ L. The number of theoretical plates (N) was calculated using the equation shown below:

$$N = 5.545 \left(\frac{V_R}{w_{0.5}} \right) \quad (1)$$

Where V_R is the peak retention volume, while $w_{0.5}$ is the peak width at half height.

All solutions used in the mAb purification experiments were prepared using micro-filtered and degassed buffers. The mAb feed solutions were injected using appropriate sample loops.

Chromatograms were obtained by monitoring the effluent from the membrane device (or the column) at 280 nm wavelength. Samples corresponding to the different separated peaks obtained during the mAb purification experiments were collected and analyzed using size exclusion chromatography and sodium dodecyl sulfate polyacrylamide gel electrophoresis (SDS-PAGE).

Size exclusion chromatography (or SEC) analysis was carried out using a TSK-Gel G3000SWXL column fitted to an Alliance HPLC system. All SEC experiments were done at 0.5 mL/min flow rate by injecting 50 μ L samples, and the chromatograms were obtained by monitoring the column effluent at 280 nm wavelength. PBS (Phosphate Buffered Saline, pH 7.4) was used as mobile phase for SEC analysis. Prior to SEC analysis, all samples were filtered through a 0.45 μ m pore size membrane to remove particles. The SEC method was able to separate the mAb (~150 kDa molecular weight) from impurities such as media proteins, host cell proteins and product related impurities such as aggregates.

The feed (microfiltered CHO cell culture supernatant) and purified mAb samples collected during the purification experiments were analyzed by 10% SDS-PAGE under reducing conditions according to the method reported by Laemmli [56]. The SDS-PAGE experiments were carried out with a Hoefer MiniVE system (GE Healthcare Bio-Sciences, Baie-d'Urfe, QC, Canada) using Tris-glycine running buffer (pH 8.3) at 140 V constant voltage. The volume of sample loaded in each lane was 10 μ L. The gel was stained using Coomassie Brilliant Blue dye and destained with a mixture of methanol, acetic acid and water.

Results and Discussion

MabSelect SuRe resin, which is widely used for large-scale commercial manufacturer of mAbs is prepared using recombinant protein A ligand expressed in *Escherichia coli* [57]. This resin is known to be more alkali stable and has a higher mAb binding capacity compared to other protein A resins. In addition, this resin is reported to have low ligand leakage and is based on a rigid base matrix [57]. Hence, MabSelect SuRe resin was used as the benchmark (or primary control) to compare the performance of the S z²LFMC device examined in this study. Fig. 2 shows the chromatogram obtained during purification of Trastuzumab from CHO cell culture supernatant using a 5 mL MabSelect SuRe resin column. The separation, which took less than 12 min, was

carried out using 150 mM sodium phosphate buffer (pH 7.2) as binding buffer, and 0.1 citrate buffer (pH 3) as eluting buffer, at a flow rate of 5 mL/min. The feed sample consisted of CHO cell culture supernatant, diluted 1:1 in binding buffer, and 2 mL of this feed sample was loaded on the column. Elution was achieved using a sharp 50 mL linear gradient. The impurities appeared as a flow through peak between 5 and 15 mL effluent volume, while the mAb was eluted between 45 and 55 mL effluent volume. The area under the curve (or AUC) of the eluted mAb peak was about 10.02% (average value based on duplicate experiments) of the total AUC in the chromatograms (i.e., the sum of the AUCs of the flow through and eluted peaks). Therefore, it may be inferred that the mAb comprised about 10.02% of the UV (280 nm) absorbing species (i.e., proteins, and others) present in the CHO cell culture supernatant. The purified mAb obtained by protein A affinity chromatography was analyzed by SEC (see Fig. 3). The mAb appeared as a major peak around 17.5 min retention time, and peak area integration results suggested that the purity was greater than 95% (based on peak forming species). The purified mAb was virtually free of high molecular weight (HMW) impurities and had very miniscule amount of low molecular weight (LMW) impurities.

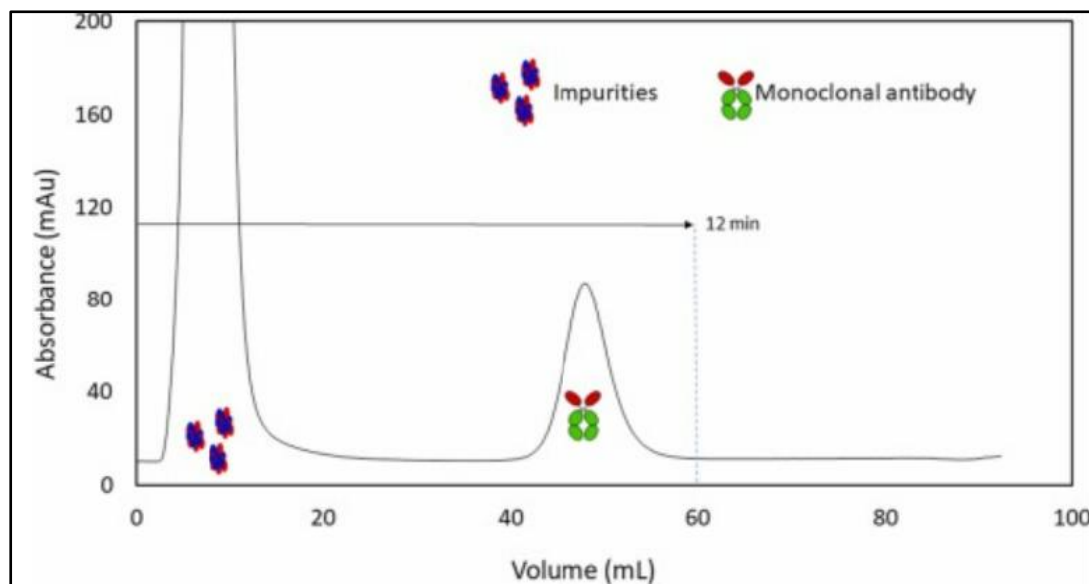


Fig. 2. Chromatogram obtained during purification of Trastuzumab from CHO cell culture supernatant using MabSelect SuRe affinity column (column volume: 5 mL; binding buffer: 150 mM sodium phosphate pH 7.2; eluting buffer: 100 mM citrate buffer pH 3; feed: CHO cell culture supernatant diluted 1:1 in binding buffer; volume of sample loaded: 2 mL; flow rate: 5 mL/min; linear gradient length: 50 mL).

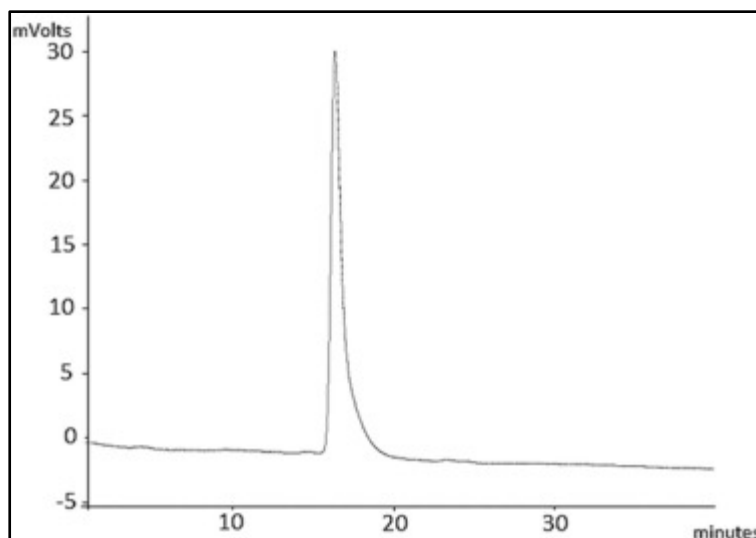


Fig. 3. SEC chromatogram obtained with Trastuzumab purified using MabSelect SuRe column-based affinity chromatography (mobile phase: Phosphate Buffered Saline (pH 7.4), column: TSK-Gel G3000SWXL; flow rate: 0.5 mL/min; sample volume: 50 μ L).

Before carrying out mAb purification using the S z²LFMC device and the Capto S ImpAct column, these were tested for their respective separation efficiencies in terms of their number of theoretical plates. Table 1 shows the number of the theoretical plates per unit bed height at different flow rates for the Capto S ImpAct column and the S z²LFMC device. The number of theoretical plates for the Capto S ImpAct column remained largely similar at the two flow rates examined. With the S z²LFMC device, the number of theoretical plates increased with increase in flow rates. This trend was consistent with that observed in an earlier study [55]. The number of theoretical plates in a membrane chromatography device depends primarily on four factors, i.e., eddy dispersion, axial diffusion, resistance to mass transfer, and macroscale convective dispersion [55]. With the z²LFMC device, the first, third and fourth factors are expected to remain largely unaffected by the flow rate. However, the extent of axial diffusion could be expected to decrease with increase in flow rate, particularly as a highly diffusible tracer species (i.e., sodium chloride) was used for measuring the number of theoretical plates. Therefore, the increase in the number of theoretical plates with increase in flow rate was due to lower axial diffusion of the tracer. The efficiencies of the two devices could be objectively compared at 10 mL/min flow rate, i.e., the higher flow rate used with the column and the lowest flow rate used with the S z²LFMC device. At this flow rate, the number of plates/m obtained with the S z²LFMC

device was 10.8 time greater than that with the column, the bed-height of the two devices being 3.6 mm and 25 mm respectively. Also, the operating flow rate range of the S z²LFMC device was greater than that of the column. The S z²LFMC device could be operated at 20 mL/min flow rate without any problems. In fact, the number of theoretical plates obtained at this flow rate was greater than those obtained at the lower flow rates, i.e., 10 and 15 mL/min.

Table 1. Effect of flow rate on the number of theoretical plates per unit bed height in the 5 mL S z²LFMC device and the 5 mL Capto S ImpAct column.

Flow rate (mL/min)	Column volumes per minute (CVM)	N/m S z ² LFMC device	N/m Capto S ImpAct column
5	1	---	3544
10	2	37768	3483
15	3	41755	---
20	4	51822	---

Optimization of cation-exchange chromatography (and indeed any type of chromatography) is a stepwise process, where different process parameters need to be taken into consideration. Preliminary experiments were carried out to determine the binding capacity of Trastuzumab on the cation exchange membrane housed within the S z²LFMC device. These experiments were carried out using pure Trastuzumab feed solution (5 mg/mL in 10 mM sodium phosphate buffer, pH 5.5). The 10% breakthrough binding capacity was found to be 10.58 mg of Trastuzumab per mL of membrane bed volume. The typical binding capacity of human IgG on the Mustang S membrane is reported to be around 20 mg/mL (manufacturer's data). Binding of target proteins on ion-exchange media is particularly sensitive to the solution pH and the ionic strength of the feed solution. Preliminary experiments showed that pH 5.5. was suitable for mAb binding on both, the S z²LFMC device and the Capto S ImpAct column (data not shown). Preliminary experiments also indicated that the high ionic strength of the Trastuzumab containing CHO cell culture supernatant used in the current study made it unsuitable for mAb binding on both the cation exchange chromatography devices examined, i.e., the S z²LFMC device and the Capto S ImpAct column. Therefore, the cell culture supernatant had to be appropriately diluted using low ionic strength buffer to bring down the effective ionic strength of the feed solution, and thereby facilitate

mAb capture. The extent to which the cell culture supernatant was diluted was quantified in terms of the dilution factor, which is defined as the volume of cell culture supernatant used divided by the total volume after dilution with low ionic strength buffer, i.e., the undiluted cell culture supernatant had a dilution factor of 1, and a numerically lower dilution factor would indicate greater dilution with low ionic strength buffer. The extent to which the dilution factor affected mAb binding on the cation exchange media was in turn quantified in terms of the fraction of mAb recovered in the eluate, which was obtained by dividing the amount of mAb recovered in the eluate by the amount of mAb present in the feed. In these experiments, the amount of mAb in the feed solution was significantly lower than the mAb binding capacity of the cation exchange membrane. Therefore, the fraction of mAb recovered in these experiments would depend primarily on the ionic strength of the feed solution. Fig. 4 shows the effect of dilution factor on the fraction of mAb recovered with the S z²LFMC device. In these experiments 20 mM sodium phosphate (pH 5.5) was used as the low ionic strength diluting buffer. Based on these results, a dilution factor of 0.5 (i.e., 1:1 vol/volume dilution) was chosen for feed preparation in all subsequent mAb purification experiments using cation exchange chromatography (both column and membrane based). At dilution factors higher than 0.5, the extent of mAb binding was very significantly affected by the high ionic strengths of the feed solutions. On the other hand, at dilution factors lower than 0.25, the lower mAb concentration in the feed solution led to lower mAb binding (as could be expected based on an adsorption isotherm). When similar binding experiments were carried out at pH 6.0, the fraction of mAb recovered at a dilution factor of 0.5 was 0.27, i.e., the mAb binding was significantly lower than that at pH 5.5 for the same dilution factor. The feed sample used for purification of Trastuzumab using MabSelect SuRe resin-based protein A chromatography (see Fig. 2) was also prepared by using a dilution factor of 0.5. Hence, all three devices used in this study were compared using feed containing the same mAb concentration. The cation exchange column or membrane-bound mAb was eluted using 1 M NaCl solution as eluent.

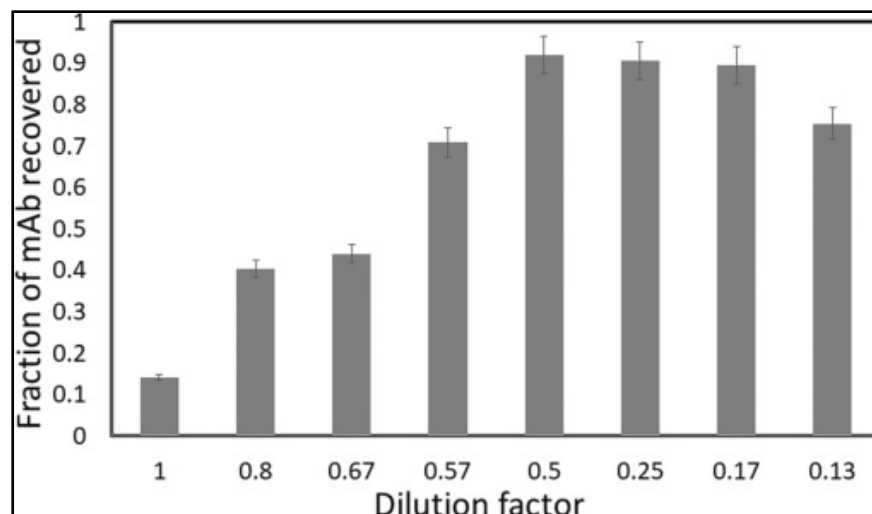


Fig. 4. Effect of dilution factor on the fraction of mAb recovered during Trastuzumab purification from CHO cell culture supernatant using the S z²LFMC device at pH 5.5.

Preliminary experiments carried out using the S z²LFMC device showed that the best separation of mAb was obtained at 10 mL/min flow rate. At 5 mL/min flow rate the separation was quite unsatisfactory, while at 15 and 20 mL/min flow rates, the separation was marginally inferior to that obtained at 10 mL/min flow rate. These results show that the number of theoretical plates data obtained using sodium chloride as tracer cannot always be used to predict performance in protein purification experiments. Fig. 5 shows the chromatogram obtained during purification of Trastuzumab from CHO cell culture supernatant with the S z²LFMC device, using 2 mL of 1:1 diluted CHO cell culture supernatant as feed (i.e., using a dilution factor of 0.5). Both binding and elution were carried out at a flow rate of 10 mL/min, the binding buffer being 20 mM sodium phosphate (pH 5.5), and the eluting buffer being 1 M NaCl solution prepared in binding buffer. The elution was carried out using a 100 mL linear gradient from binding to eluting buffer. The impurities appeared in the flow through peak between 7 and 35 mL effluent volume while the mAb was eluted around 77 mL effluent volume. In addition to the main eluted mAb peak, there was a shoulder around 85–90 mL effluent volume and another small peak around 120 mL effluent volume. The gradient length used in this particular experiment was chosen based on optimization experiments carried out using different gradient lengths. Fig. 6 shows the close-ups of the eluted mAb peaks obtained using 3 different linear gradient lengths, i.e., 25 mL, 50 mL, and 100 mL. In this figure, volume* indicates the effluent volume after the start of the salt gradient used for

elution, i.e., 0 mL corresponded to the point at which a gradient was started. When a gradient of 25 mL length was used, the shoulder (indicated by the dashed ellipse) followed the mAb peak very closely. With increase in the gradient length, the shoulder moved further away, indicating better separation between the mAb and the species present in the shoulder.

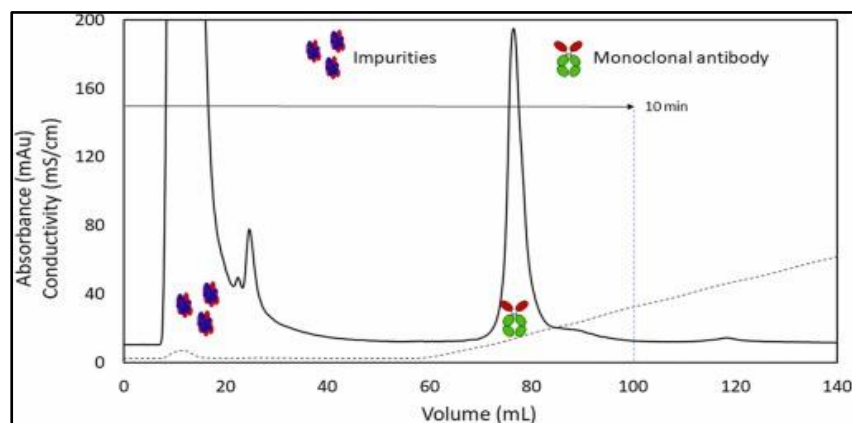


Fig. 5. Chromatogram obtained during the purification of Trastuzumab from CHO cell culture supernatant using the S^2 LFCM device (membrane bed volume: 5 mL; binding buffer: 20 mM sodium phosphate buffer pH 5.5; eluting buffer: binding buffer + 1 M NaCl; feed: CHO cell culture supernatant diluted 1:1 in binding buffer; volume of sample loaded: 2 mL; flow rate: 10 mL/min; linear gradient length: 100 mL; solid line: UV absorbance; dashed line: conductivity).

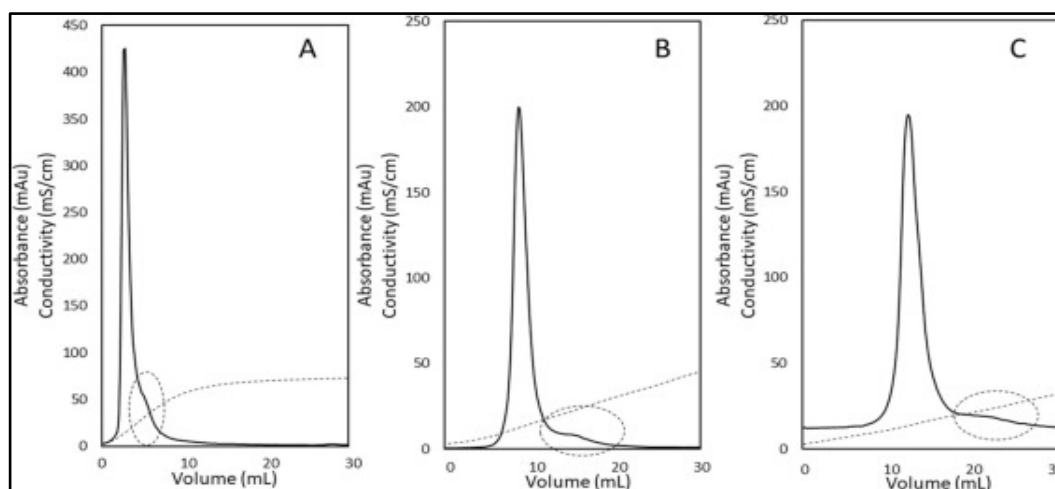


Fig. 6. Close-ups of the eluted mAb peaks obtained during Trastuzumab purification using the S^2 LFCM device, the mAb being eluted with three different linear gradients, i.e., 25 mL (A), 50 mL (B), and 100 mL (C) (membrane bed volume: 5 mL; binding buffer: 20 mM sodium phosphate buffer pH 5.5; eluting buffer: binding buffer + 1 M NaCl; feed: CHO cell culture supernatant diluted 1:1 in binding buffer; volume of sample loaded: 2 mL; flow rate: 10 mL/min; solid line: UV absorbance; dashed line: conductivity).

Samples corresponding to the flow through, and the main mAb peak (without the shoulder) from the mAb purification experiment carried out with the S z²LFMC device at the optimized conditions (see Fig. 5) were analyzed by SEC. The results obtained by SEC analysis are summarized in Fig. 7. The flow through (see Fig. 7A) consisted primarily of low molecular proteins and other UV absorbing impurities (i.e., those with greater than 20 min retention time) typically present in the cell culture supernatant. There was a very tiny peak around 17.5 min (corresponding to the mAb retention time) which indicated that only a miniscule amount of mAb escaped in the flow through, i.e., the recovery of mAb was high. The SEC chromatogram obtained with the purified mAb sample (see Fig. 7B) showed that the sample was very pure (>95%), i.e., the mAb purity was comparable to that obtained using protein A affinity chromatography (see SEC chromatogram in Fig. 3 for comparison).

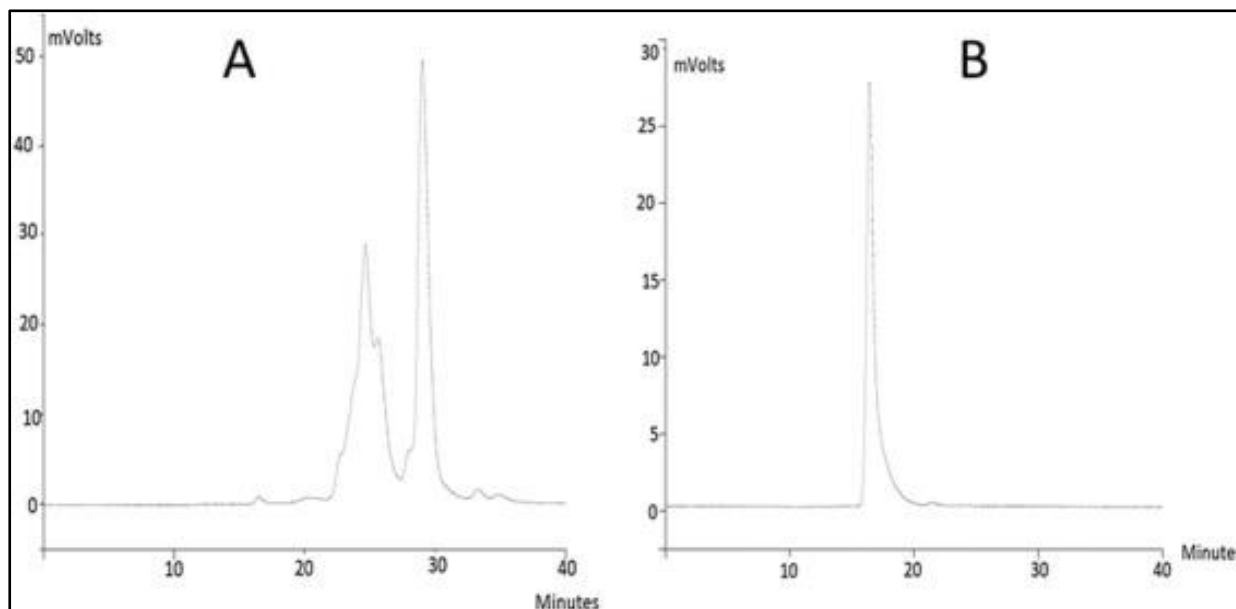


Fig. 7. SEC chromatograms obtained during purification of Trastuzumab from CHO cell culture supernatant using S z²LFMC device. A. Flow through sample. B. Eluted mAb (mobile phase: Phosphate Buffered Saline (pH 7.4), column: TSK-Gel G3000SWXL; flow rate: 0.5 mL/min; sample: 50 μ L).

Fig. 8 shows the chromatogram obtained during purification of Trastuzumab from CHO cell culture supernatant using the Cpto S ImpAct column. This experiment was carried out at a flow rate of 5 mL/min, the feed being identical to that used for mAb purification using the S z²LFMC device, i.e., 2 mL of 1:1 diluted CHO cell culture supernatant. The binding and eluting buffers were also the same as those used with the S z²LFMC device, i.e., 20 mM sodium phosphate (pH 5.5)

and 1 M NaCl solution (prepared in binding buffer) respectively. The elution was carried out using a 100 mL linear gradient from binding to eluting buffer. The impurities appeared in the flow through peak between 5 and 15 mL effluent volume while the mAb was eluted as a single peak around 71 mL effluent volume. Fig. 9 shows close-ups of the eluted mAb peaks obtained with the Capto S ImpAct column at two different flow rates, i.e., 5 mL/min and 10 mL/min, in each case, elution being carried out using 100 mL linear gradient. The eluted mAb peak obtained at 5 mL/min flow rate was significantly sharper and higher than that obtained at 10 mL/min.

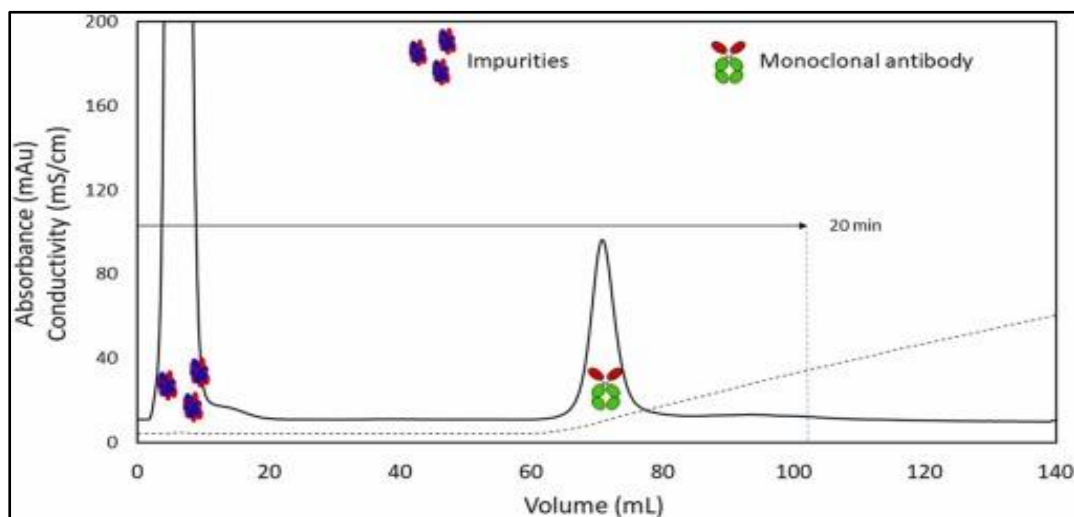


Fig. 8. Chromatogram obtained during purification of Trastuzumab from CHO cell culture supernatant using the Capto S ImpAct column (column volume: 5 mL; binding buffer: 20 mM sodium phosphate buffer pH 5.5; eluting buffer: binding buffer + 1 M NaCl; feed: CHO cell culture supernatant diluted 1:1 in binding buffer; volume of sample loaded: 2 mL; flow rate: 5 mL/min; linear gradient length: 100 mL; solid line: UV absorbance; dashed line: conductivity).

The flow through and eluted mAb peak samples obtained during purification of Trastuzumab from CHO cell culture supernatant using the Capto S ImpAct column at 5 mL/min flow rate were analyzed by SEC (see Fig. 10). Unlike the flow through obtained with the S z²LFMC device (see Fig. 7A), the flow through obtained with the Capto S ImpAct column (see Fig. 10A) had significant amounts of mAb present (17.5 min retention time). Therefore, the mAb recovery obtained with the Capto S ImpAct column was definitely lower than that obtained with the S z²LFMC device. Also, the purified mAb sample (see Fig. 10B) contained some low molecular weight (LMW)

impurities and therefore had a slightly lower purity (about 95%) than that obtained with the S^zLFMC device (see Fig. 7B).

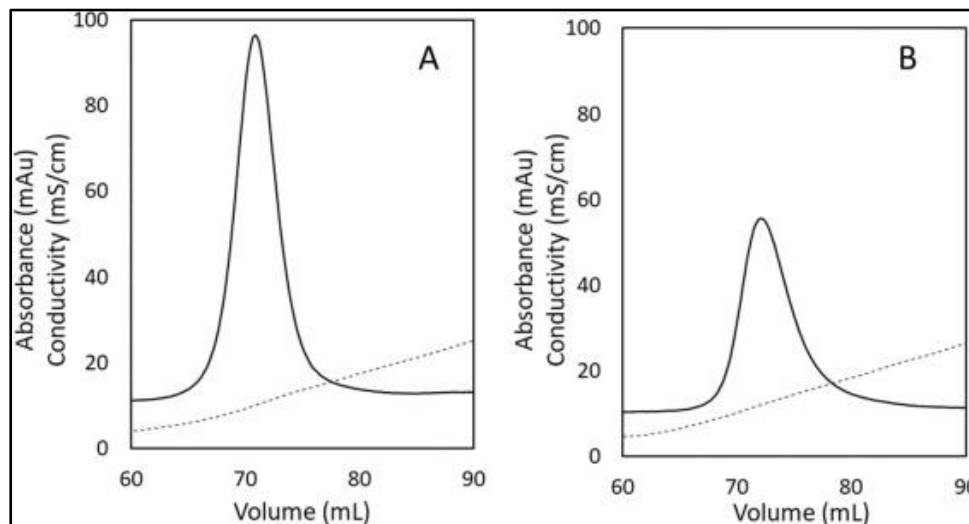


Fig. 9. Close-ups of the eluted mAb peaks obtained during Trastuzumab purification using the Capto S ImpAct column at two different flow rates, i.e., 5 mL/mL (A), and 10 mL/min (B) (column volume: 5 mL; binding buffer: 20 mM sodium phosphate buffer pH 5.5; eluting buffer: binding buffer + 1 M NaCl; feed: CHO cell culture supernatant diluted 1:1 in binding buffer; volume of sample loaded: 2 mL; linear gradient length: 100 mL; solid line: UV absorbance; dashed line: conductivity).

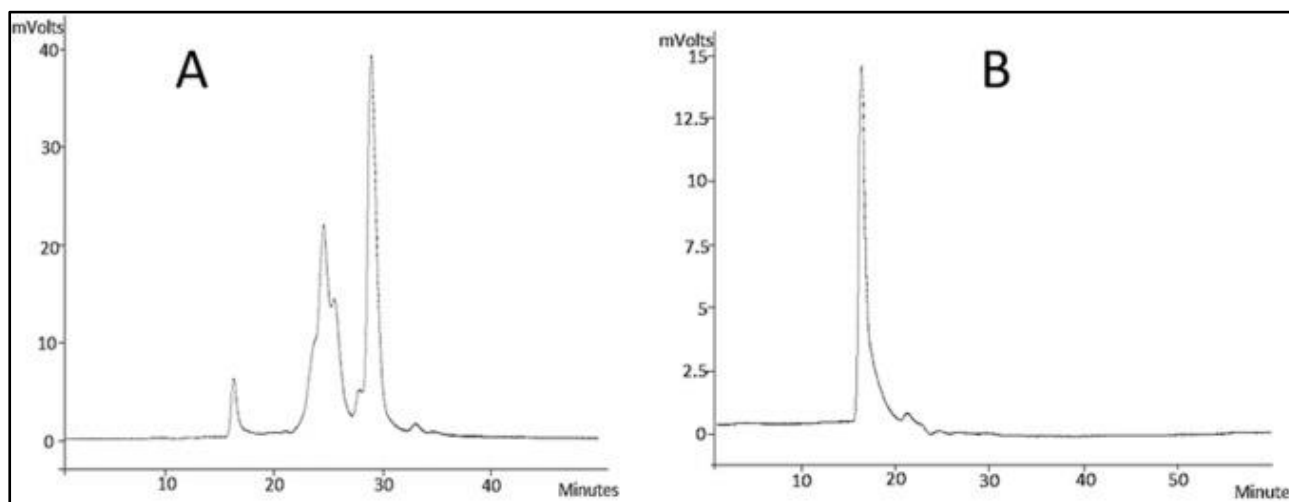


Fig. 10. SEC chromatograms obtained during purification of Trastuzumab from CHO cell culture supernatant using Capto S ImpAct column. A. Flow through sample. B. Eluted mAb (mobile phase: Phosphate Buffered Saline (pH 7.4), column: TSK-Gel G3000SWXL; flow rate: 0.5 mL/min; sample injected: 50 μ L).

Fig. 11 shows the image of the stained SDS-PAGE gel obtained with purified Trastuzumab samples from the MabSelect SuRe, S z²LFMC, and Capto S ImpAct based purification experiments. The two bands corresponding to molecular weights of 25 kDa and 50 kDa observed in purified Trastuzumab sample lanes correspond respectively to the light and the heavy chains of the mAb. The SDS-PAGE results indicate that the mAb samples obtained using all three techniques were qualitatively pure.

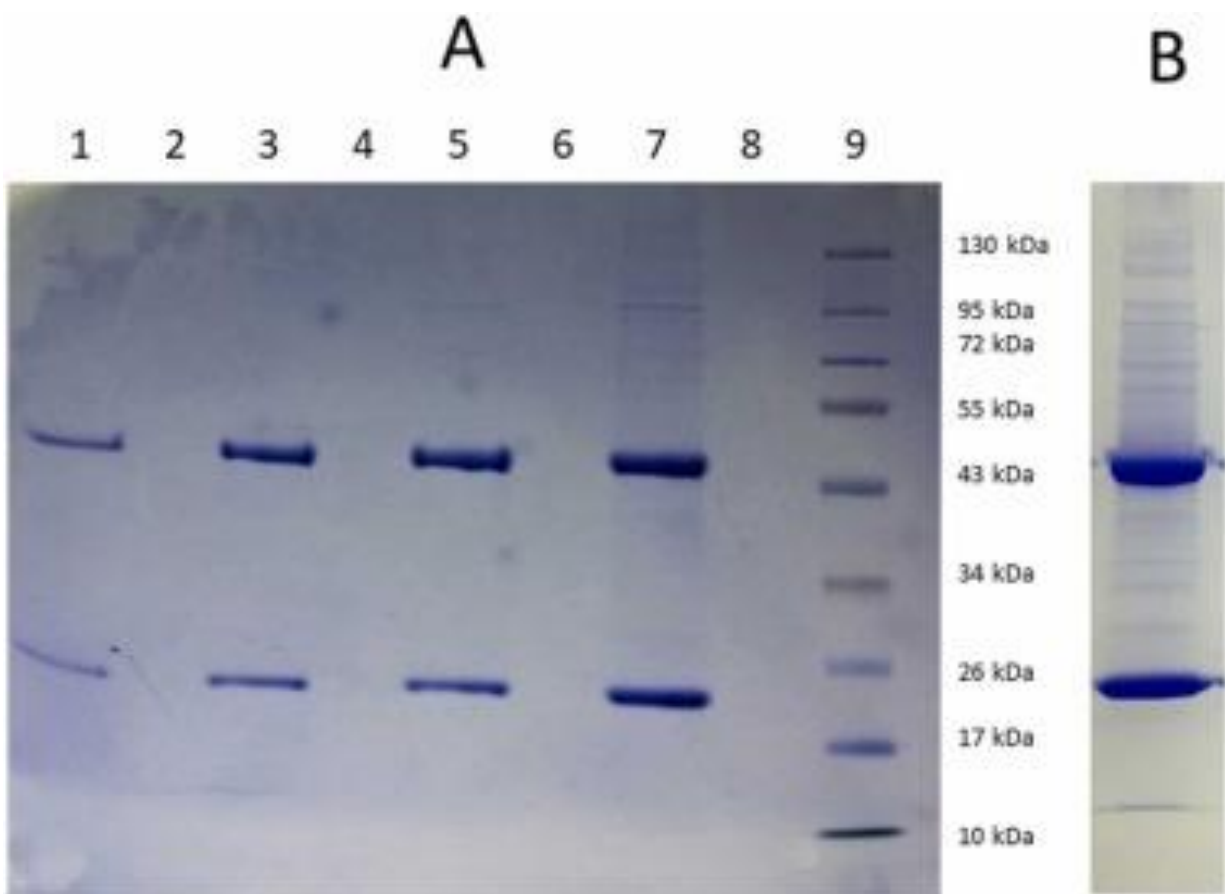


Fig. 11. Analysis of purified Trastuzumab samples obtained by MabSelect SuRe, Capto S ImpAct, and S z²LFMC based purification methods using 10% reducing SDS-PAGE. (A) lane 1: purified mAb obtained by Capto S ImpAct based purification method, lane 2: blank, lane 3: purified mAb obtained by S z²LFMC based purification method, lane 4: blank, lane 5: purified mAb obtained by MabSelect SuRe based affinity chromatography, lane 6: blank, lane 7: microfiltered and diluted CHO cell culture supernatant, lane 8: blank, lane 9: molecular weight markers, (B) undiluted cell culture supernatant.

From the chromatograms shown in Figs. 2, 5 and 8, it may be inferred that the separation obtained with the S z²LFMC device was better than that obtained using either the MabSelect SuRe resin column (the primary control) or the Capto S ImpAct column (the secondary control). To begin with, the fastest separation was obtained with the S z²LFMC device (less than 10 min), followed by the MabSelect SuRe resin column (about 12 min) and then by the Capto S ImpAct column (less than 20 min). The eluted mAb peak obtained with the S z²LFMC device was taller and sharper, which indicated lower dispersion, which could be attributed to superior fluidics within the separation media and the device. Secondly, the area under the curve (AUC) of the eluted mAb peak obtained with the S z²LFMC device was greater than that obtained using the two other devices, indicating superior mAb recovery with the former. Table 2 summarizes area under the curve data and related information for the mAb peaks, and the mAb recovery data for purification experiments carried out using the MabSelect SuRe column (see Fig. 2), the S z²LFMC device (see Fig. 5), and the Capto S ImpAct column (see Fig. 9). These results show that the highest mAb recovery was obtained with the S z²LFMC device, followed by the MabSelect SuRe resin column, and then the Capto S ImpAct column. The sharpest mAb peak was obtained with the S z²LFMC device (2.24 membrane-bed volumes), followed by the MabSelect SuRe resin column (2.74 column volumes), and the Capto S ImpAct column (2.86 column volumes). The mAb productivity in the three purification processes compared above were calculated by dividing the mass of mAb recovered in each case by its peak volume, the time over which each peak was eluted, and the bed-volume of the device (which was 5 mL in all three cases). These were found to be 0.42, 1.38 and 0.35 mg/mL/h/mL device volume respectively for the MabSelect SuRe column, the S z²LFMC device, and the Capto S ImpAct column.

Table 2. Attributes of the mAb peaks and mAb recovery obtained during purification experiments carried out using the MabSelect SuRe column, the S z²LFMC device, and the Capto S ImpAct column.

Device	Peak area (mAu mL)	Peak width at half height (mL)	Peak volume (mL)	Recovery of mAb (%)
MabSelect SuRe column	439.28	5.3	13.7	81.7
S z ² LFMC device	486.18 ^a	3.2	11.2 ^a	90.4
Capto S ImpAct column	397.51	4.0	14.3	73.9

a: Excluding shoulder.

Conclusion

The results discussed above clearly indicate that Trastuzumab could be purified from cell culture supernatant using the S z²LFMC device. However, it should be pointed out that this is an initial feasibility study, and more detailed and rigorous experiments would be required before the method could be claimed as a viable alternative to protein A based affinity chromatography. Experiments that would need to be carried out include determination of mAb binding capacity of the S z²LFMC device (from cell culture supernatant), and its comparison with the binding capacities of the MabSelect SuRe resin column and the Capto S ImpAct column. In the current study, we demonstrated equivalence in mAb purity based on robust primary techniques such as SEC and SDS-PAGE. Additional techniques such as those used for showing host cell protein (or HCP) and endotoxin clearance would also be required. Other analytical techniques that would be required at the next stage of development of the S z²LFMC based process include matrix-assisted laser desorption/ionization – time of flight (or MALDI-Tof) and dynamic light scattering (or DLS) to detect aggregates, and assays to demonstrate equivalence in biological activity. The main advantages of the S z²LFMC device over the MabSelect SuRe resin column are lower media cost, faster separation, and gentler operating conditions, i.e., no requirement for elution under acidic pH conditions. As discussed in the introduction, other potential advantages of the membrane chromatography-based purification process include lower buffer consumption, lower operating cost, and elimination of steps such as cleaning and validation. Also, as discussed in a previous paper [55], the S z²LFMC device is suitable to fractionating mAb charge variants (if present), and for the removal of mAb aggregates. The mAb examined in the current study did not have any noticeable charge variants or aggregates. However, in cases where variants and aggregates do exist, the S z²LFMC device-based purification process could combine two steps, i.e., capture and polishing in one. One of the disadvantages of using cation exchange chromatography for mAb purification is the need for the dilution of the feed sample. With protein A affinity chromatography, clarified cell culture supernatant can be directly loaded on the column. Any potential advantage of using the S z²LFMC device should be weighed against this disadvantage. When using protein A affinity chromatography for purifying mAbs, viral inactivation is carried out by holding the acidic eluate for specified duration before neutralization. While this may appear convenient, the acidic pH condition could result in protein aggregation, denaturation and other forms of chemical degradation [58], [59]. When using the S z²LFMC device for purifying

mAbs, alternative virus inactivation/removal methods such as those involving membrane adsorbers may need to be used [60]. Anion and cation exchange membranes have been used for generation and purification of antibody fragments such as Fab [61] and F(ab')₂ [62]. A z²LFMC device housing within it a stack of appropriate membrane sheets could therefore be used as an efficient integrated reactor-separation system for producing and purifying antibody fragments.

Membrane fouling is frequently observed during processing of biological material such as proteins. In future studies, membrane fouling would need to be systematically studied, and if significant, mitigation measures would have to be implemented. The z²LFMC device used in the current study proved to be suitable for its intended application. In an earlier study [55] it was shown that it was relatively easy to scale up the z²LFMC device by maintaining the same length to width aspect ratio. However, while designing very large z²LFMC devices, a wider range of factors would need to be considered. For instance, the aspect ratio could potentially affect pressure drop, and thereby flow uniformity in large membrane chromatography devices. This in turn could potentially affect separation performance. Therefore, the aspect ratio would need to be optimized for the specific scale under consideration. Also, the relative size of the primary and secondary flow channels used in a device could affect separation performance. Screening and optimization of design attributes could be quite time consuming and expensive. Computational fluid dynamic (CFD) simulations could potentially be used for preliminary screening and optimization [63], before embarking on actual device fabrication.

The overall objective of the current study was to develop an alternative to protein A affinity chromatography. Cation exchange separation chemistry was chosen to overcome some of the inherent limitation of the protein A resin. The z²LFMC format for membrane chromatography was chosen for ensuring high-speed and high-resolution. Trastuzumab could be purified from cell culture supernatant using the S z²LFMC device. The S z²LFMC device based mAb purification process was faster than those based on the MabSelect SuRe resin column and the Capto S ImpAct column. The eluted mAb peak obtained with the S z²LFMC device was taller and sharper than those obtained with the other devices. The mAb recovery obtained with the S z²LFMC device was higher than that obtained with either the MabSelect SuRe resin column or the Capto S ImpAct column. With the S z²LFMC device, the purified mAb was obtained in 2.24 membrane

bed volumes. The corresponding values for the MabSelect SuRe resin column and the Capto S ImpAct column were 2.74 column volumes and 2.86 column volumes respectively. The main advantages of cation exchange membrane chromatography over protein A affinity chromatography include lower media cost, faster separation, and gentler operating conditions. Other potential advantages include lower buffer consumption, lower operating cost, and elimination of steps such as cleaning and validation. More detailed and rigorous experiments would be required before the S z²LFMC based method could be claimed as a viable alternative to protein A based affinity chromatography for mAb purification.

CRedit Authorship Contribution Statement

Roxana Roshankhah: Experiments; Data curation; Formal analysis; Validation; Investigation; Methodology; Roles/Writing – original draft; Guoqiang Chen: Experiments, Yating Xu: Experiments, Nikhila Butani: Experiments, Yves Durocher: Resources; Roles/Writing – review & editing, Robert Pelton: Project administration; Funding acquisition; Resources; Roles/Writing – review & editing, Raja Ghosh: Conceptualization; Design of equipment; Funding acquisition; Project administration; Resources; Supervision; Visualization; Roles/Writing – review & editing.

Declaration of Competing Interest

The authors declare the following financial interests/personal relationships which may be considered as potential competing interests: There is no immediate competing interest but a provisional US patent application for the z²LFMC device used in this study has been filed.

Acknowledgments

This project is funded by the Natural Sciences and Engineering Research Council (NSERC) of Canada NSERC. We thank Paul Gatt (Department of Chemical Engineering, McMaster University) for fabricating the z²LFMC device used in this study.

Data availability

Research data will be available on request from corresponding author.

References

- [1] R. Hooft van Huijsduijnen, S. Kojima, D. Carter, H. Okabe, A. Sato, W. Akahata, T.N.C. Wells, K. Katsuno, Reassessing therapeutic antibodies for neglected and tropical diseases, *PLoS. Negl. Trop. Dis.*, 14 (2020), Article e0007860
- [2] R. Niwa, M. Satoh, The current status and prospects of antibody engineering for therapeutic use: focus on glycoengineering technology, *J. Pharm. Sci.*, 104 (2015), pp. 930-941
- [3] H.M. Shepard, G.L. Phillips, C.D. Thanos, M. Feldmann, Developments in therapy with monoclonal antibodies and related proteins, *Clin. Med*, 17 (2017), pp. 220-232
- [4] S. Fekete, A. Gassner, R. Serge, J. Schapple, D. Guillarme, Analytical strategies for the characterization of therapeutic monoclonal antibodies, *TrAC. Trends Anal. Chem.*, 42 (2013), pp. 4-83
- [5] A.B. Mahmuda, F. Bande, K.J. Kadhim Al-Zihiry, N. Abdulhaleem, R.A. Majid, R.A. Hamat, W.O. Abdullah, Z. Unyah, Monoclonal antibodies: a review of therapeutic applications and future prospects, *Trop. J. Pharm. Res.*, 16 (2017), pp. 713-722
- [6] M. Marovich, J.R. Mascola, M.S. Cohen, Monoclonal antibodies for prevention and treatment of COVID-19, *JAMA*, 324 (2020), pp. 131-132
- [7] R.M. Lu, Y.C. Hwang, I.J. Liu, C.C. Lee, H.Z. Tsai, H.J. Li, H.C. Wu, Development of therapeutic antibodies for the treatment of diseases, *J. Biomed. Sci.*, 27 (2020), pp. 1
- [8] R.O. Dillman, Magic bullets at last! Finally—approval of a monoclonal antibody for the treatment of cancer!!!, *Cancer Biother. Radiopharm.*, 12 (1997), pp. 223-225

[9] C. Wang, W. Li, D. Drabek, N.M. Okba, R. van Haperen, A.D.M.E. Osterhaus, F.J.M. van Kuppeveld, B.L. Haagmans, F. Grosveld, B.J. Bosch, A human monoclonal antibody blocking SARS-CoV-2 infection, *Nat. Commun.*, 11 (2020), pp. 1-6

[10] R.K. Murthy, S. Loi, A. Okines, E. Paplomata, E. Hamilton, S.A. Hurvitz, N.U. Lin, V. Borges, V. Abramson, C. Anders, P.L. Bedard, M. Oliveira, E. Jakobsen, T. Bachelot, S.S. Shachar, V. Müller, S. Braga, F.P. Duhoux, R. Greil, D. Cameron, L.A. Carey, G. Curigliano, K. Gelmon, G. Hortobagyi, I. Krop, S. Loibl, M. Pegram, D. Slamon, M.C. Palanca-Wessels, L. Walker, W. Feng, E.P. Winer, Tucatinib, trastuzumab, and capecitabine for HER2-positive metastatic breast cancer, *N. Engl. J. Med.*, 382 (2020), pp. 597-609

[11] A. Drucker, C. Skedgel, K. Virik, D. Rayson, M. Sellon, T. Younis, The cost burden of trastuzumab and bevacizumab therapy for solid tumours in Canada, *Curr. Oncol.*, 15 (2008), pp. 136-142

[12] S.C. Seferina, B.L.T. Ramaekers, M. de Boer, M.W. Dercksen, F. van den Berkmortel, R.J.W. van Kampen, A.J. van de Wouw, A.C. Voogd, V.C.G. Tjan Heijnen, M.A. Joore, Cost and cost-effectiveness of adjuvant trastuzumab in the real world setting: a study of the Southeast Netherlands Breast Cancer Consortium, *Oncotarget*, 8 (2017), pp. 79223-79233

[13] L.M. Fleck, The costs of caring: who pays? Who profits? Who panders?, *Hastings Cent. Rep.*, 36 (2006), pp. 13-17

[14] S. Nandi, A.T. Kwong, B.R. Holtz, R.L. Erwin, S. Marcel, K.A. McDonald, Techno-economic analysis of a transient plant-based platform for monoclonal antibody production, *MAbs*, 8 (2016), pp. 1456-1466

[15] M. Franzreb, E. Muller, J. Vajda, Cost estimation for Protein A chromatography: An in silico approach to MAb purification strategy, *BioProcess Int.*, 12 (2014), pp. 44-52

- [16] J. Wang, J. Zhou, Y.K. Gowtham, S.W. Harcum, S.M. Husson, Antibody purification from CHO cell supernatant using new multimodal membranes, *Biotechnol. Prog.*, 33 (2017), pp. 658-665
- [17] G. Kohler, C. Milstein, Continuous cultures of fused cells secreting antibody of predefined specificity, *Nature*, 256 (1975), pp. 495-497
- [18] S. Fekete, B. Alain, D. Guillarme, Chromatographic characterization of biopharmaceuticals: recent trends and new tools, *Am. Pharm. Rev.*, 18 (2015), pp. 59-63
- [19] D. Low, R. O'Leary, N.S. Pujar, Future of antibody purification, *J. Chromatogr. B*, 848 (2007), pp. 48-63
- [20] M.C. Flickinger, *Downstream Industrial Biotechnology: Recovery and Purification (First ed.)*, John Wiley & Sons, New York (2013)
- [21] R.L. Fahrner, D.H. Whitney, M. Vanderlaan, G.S. Blank, Performance comparison of protein A affinity-chromatography sorbents for purifying recombinant monoclonal antibodies, *Biotechnol. Appl. Biochem.*, 30 (1999), pp. 121-128
- [22] P.L. Ey, S.J. Prowse, C.R. Jenkin, Isolation of pure IgG1, IgG2a and IgG2b immunoglobulins from mouse serum using protein A-sepharose, *Immunochemistry*, 15 (1978), pp. 429-436
- [23] H.F. Liu, J. Ma, C. Winter, R. Bayer, Recovery and purification process development for monoclonal antibody production, *MAbs*, 2 (2010), pp. 480-499
- [24] D.K. Follman, R.L. Fahrner, Factorial screening of antibody purification processes using three chromatography steps without protein A, *J. Chromatogr. A*, 1024 (2004), pp. 79-85
- [25] Protein A. [〈https://bioprocessintl.com/〉](https://bioprocessintl.com/) , 2013(Accessed at 6 July, 2020).

- [26] I. Bjork, B.A. Petersson, J. Sjoquist, Some physiochemical properties of protein A from *Staphylococcus aureus*, *Eur. J. Biochem.*, 29 (1972), pp. 579-584
- [27] T. Arakawa, J.S. Philo, K. Tsumoto, R. Yumioka, D. Ejima, Elution of antibodies from a Protein A column by aqueous arginine solutions, *Protein Expr. Purif.*, 36 (2004), pp. 244-248
- [28] A.W. Vermeer, W. Norde, The thermal stability of immunoglobulin: unfolding and aggregation of a multi-domain protein, *Biophys. J.*, 78 (2000), pp. 394-404
- [29] S. Ghose, M. Jin, J. Liu, J. Hickey, Integrated polishing steps for monoclonal antibody purification, U. Gottschalk (Ed.), *Process Scale Purification of Antibodies*, JWS, New York (2009), pp. 145-167
- [30] H. Pan, K. Chen, M. Pulisic, I. Apostol, G. Huang, Quantitation of soluble aggregates in recombinant monoclonal antibody cell culture by pH-gradient protein A chromatography, *Anal. Biochem.*, 388 (2009), pp. 273-278
- [31] L. Wang, G. Hale, R. Ghosh, Non-size-based membrane chromatographic separation and analysis of monoclonal antibody aggregates, *Anal. Chem.*, 78 (2006), pp. 6863-6867
- [32] S.M. Yoo, R. Ghosh, Simultaneous removal of leached protein A and aggregates from monoclonal antibody using hydrophobic interaction membrane chromatography, *J. Membr. Sci.*, 390–391 (2012), pp. 263-269
- [33] Y. Tao, A. Ibraheem, L. Conley, D. Cecchini, S. Ghose, Evaluation of high-capacity cation exchange chromatography for direct capture of monoclonal antibodies from high-titer cell culture processes, *Biotechnol. Bioeng.*, 111 (2014), pp. 1354-1364
- [34] R. Hahn, K. Shimahara, F. Steindl, A. Jungbauer, Comparison of protein A affinity sorbents III. Lifetime study, *J. Chromatogr. A*, 1102 (2006), pp. 224-231

- [35] K. Brorson, J. Brown, E. Hamilton, K.E. Stein, Identification of protein A media performance attributes that can be monitored as surrogates for retrovirus clearance during extended re-use J. Chromatogr. A, 989 (2003), pp. 155-163
- [36] C. Jiang, J. Liu, M. Rubacha, A.A. Shukla, A mechanistic study of Protein A chromatography resin lifetime, J. Chromatogr. A, 1216 (2009), pp. 5849-5855
- [37] J. Thömmes, M. Etzel, Alternatives to chromatographic separations, Biotechnol. Prog., 23 (2007), pp. 42-45
- [38] A.M. Ramos-de-la-Peña, J. González-Valdez, O. Aguilar, Protein A chromatography: challenges and progress in the purification of monoclonal antibodies, J. Sep. Sci., 42 (2019), pp. 1816-1827
- [39] Alternatives to Protein A: who's investigating? Gen. Eng. And Biotech., (2016). <<https://www.genengnews.com/magazine/265/alternatives-to-protein-a-whos-investigating/>> , (Accessed on 9/8/2020).
- [40] S. Fekete, A. Beck, J. Fekete, D. Guillarme, Method development for the separation of monoclonal antibody charge variants in cation exchange chromatography, Part I: salt gradient approach, J. Pharm. Biomed., 102 (2015), pp. 33-44
- [41] H.L. Knudsen, R.L. Fahrner, Y. Xu, L.A. Norling, G.S. Blank, Membrane ion-exchange chromatography for process-scale antibody purification, J. Chromatogr. A, 907 (2001), pp. 145-154
- [42] R. Ghosh, Protein separation using membrane chromatography: opportunities and challenges, J. Chromatogr. A, 952 (2002), pp. 13-27
- [43] E. Lalli, J.S. Silva, C. Boi, G.C. Sarti, Affinity membranes and monoliths for protein purification, Membranes, 10 (2019), p. 1

- [44] S. Fekete, A. Beck, J.L. Veuthey, D. Guillarme, Ion-exchange chromatography for the characterization of biopharmaceuticals, *J. Pharm. Biomed. Anal.*, 113 (2015), pp. 43-55
- [45] T.N. Warner, S. Nochumson, Rethinking the economics of chromatography: new technologies and hidden costs, *BioPharm. Int.*, 16 (2003), pp. 58-60
- [46] A.S. Rathore, R.M. Kennedy, J.K. O'donnell, I. Bemberis, O. Kaltenbrunner, Qualification of a chromatographic column: why and how to do it, *Biopharm. Int.*, 16 (2003), pp. 30-40
- [47] J.X. Zhou, T. Tressel, Basic concepts in Q membrane chromatography for large-scale antibody production, *Biotechnol. Progr.*, 22 (2006), pp. 341-349
- [48] P. Madadkar, Q. Wu, R. Ghosh, A laterally-fed membrane chromatography module, *J. Membr. Sci.*, 487 (2015), pp. 173-179
- [49] P. Madadkar, R. Ghosh, High-resolution protein separation using a laterally-fed membrane chromatography device, *J. Membr. Sci.*, 499 (2016), pp. 126-133
- [50] P. Madadkar, U. Umatheva, G. Hale, Y. Durocher, R. Ghosh, Ultrafast separation and analysis of monoclonal antibody aggregates using membrane chromatography, *Anal. Chem.*, 89 (2017), pp. 4716-4720
- [51] R. Sadavarte, P. Madadkar, C.D. Filipe, R. Ghosh, Rapid preparative separation of monoclonal antibody charge variants using laterally-fed membrane chromatography, *J. Chromatogr. B Anal. Technol. Biomed. Life Sci.*, 1073 (2018), pp. 27-33
- [52] K. Kawka, P. Madadkar, U. Umatheva, S. Shoaebargh, M.F. Medina, B.D. Lichty, R. Ghosh, D.R. Latulippe, Purification of therapeutic adenoviruses using laterally-fed membrane chromatography, *J. Membr. Sci.*, 579 (2019), pp. 351-358

- [53] P. Madadkar, R. Sadavarte, R. Ghosh, Performance comparison of a Laterally-Fed Membrane Chromatography (LFMC) device with a commercial resin packed column, *Membranes*, 9 (2019), p. 138
- [54] R. Ghosh, G. Chen, U. Umatheva, P. Gatt, A flow distribution and collection feature for ensuring scalable uniform flow in a chromatography device, *J. Chromatogr. A*, 1618 (2020), Article 460892
- [55] R. Ghosh, G. Chen, R. Roshankhah, U. Umatheva, P. Gatt, A z^2 laterally-fed membrane chromatography device for fast high-resolution purification of biopharmaceuticals, *J. Chromatogr. A*, 1629 (2020), Article 461453
- [56] U. Laemmli, Cleavage of structural proteins during the assembly of the head of bacteriophage T4, *Nature*, 227 (1970), pp. 680-685
- [57] G. Jagschies, E. Lindskog, K. Lacki, P.M. Galliher, *Biopharmaceutical Processing: Development, Design, and Implementation of Manufacturing Processes (First ed.)*, Elsevier, Cambridge MA (2018)
- [58] A.R. Mazzer, X. Perraud, J. Halley, J. O'Hara, D.G. Bracewell, Protein A chromatography increases monoclonal antibody aggregation rate during subsequent low pH virus inactivation hold *J. Chromatogr. A*, 1415 (2015), pp. 83-90
- [59] R. Wälchli, M. Ressurreição, S. Vogg, F. Feidl, J. Angelo, X. Xu, S. Ghose, Z.J. Li, X. Le Saoût, J. Souquet, H. Broly, M. Morbidelli, Understanding mAb aggregation during low pH viral inactivation and subsequent neutralization, *Biotechnol. Bioeng.*, 117 (2020), pp. 687-700
- [60] W. Riordan, S. Heilmann, K. Brorson, K. Seshadri, Y. He, M. Etzel
Design of salt-tolerant membrane adsorbers for viral clearance
Biotechnol. Bioeng., 103 (2009), pp. 920-929

[61] D. Yu, R. Ghosh, Integrated fragmentation of human IgG and purification of Fab using a reactant adsorptive membrane bioreactor separator system, *Biotechnol. Bioeng.*, 104 (2009), pp. 152-161

[62] D. Yu, R. Ghosh, Enzymatic fragmentation of cation exchange membrane bound immunoglobulin G, *Biotechnol. Prog.*, 27 (2011), pp. 61-66

[63] U. Umatheva, P. Madadkar, P.R. Selvaganapathy, R. Ghosh, Computational fluid dynamic (CFD) simulation of laterally-fed membrane chromatography, *Chem. Eng. Res. Des.*, 137 (2018), pp. 412-420

Chapter 3

Optimization of Laterally-fed Membrane Chromatography Devices using Computational Fluid Dynamic Simulations.

Earlier, a new technique was discussed and was called z^2 laterally-fed membrane chromatography (or z^2 LFMC). This method combines high-resolution separation with high productivity. It is, therefore, suitable for monoclonal antibody purification.

In this chapter by computational fluid dynamics (CFD) simulations, the reason behind its superior separation is discussed. This work aims to optimize z^2 LFMC device configurations using CFD simulation software. Different designs were curated and tested based on two COMSOL physics. For this part of the thesis, the Sartobind z^2 LFMC with different channels and formats, including square and rectangular shapes, were tested to obtain the optimized design. The results are extensively compared with traditional devices, including stacked disk and radial flow membrane chromatography.

In this research, I conducted the simulations, Umatheny Umatheva assisted me with the initial understanding of the simulation's setup. Dr. Robert Pelton and Dr. Raja Ghosh supervised the project.

Optimization of Laterally-fed Membrane Chromatography Devices using Computational Fluid Dynamic Simulations

Abstract:

The purification of biopharmaceuticals is considered the chief part of the production process, and the efficiency and resolution of the used equipment are impacted by the design and flow distribution. This thesis previously explained the new z^2 LFMC structure, in which, the flow distribution is a combination of two z-shaped flows, leading to significant increase in the biopharmaceuticals' purification efficiency. In z^2 LFMC, the number of theoretical plates per unit membrane bed height is higher than its membrane chromatography devices counterparts. In an attempt to redesign the previously proposed structure, this study compares LFMC and z^2 LFMC, proposing several modifications, changing the stacked discs and radial flow membrane chromatography in a scaled-up fashion. This part of the thesis demonstrates the enhancement in the separation efficiency based on CFD simulations. The validity and practicality of several designs are demonstrated by comparing and analyzing COMSOL Multiphysics modelling.

Introduction

Purification of biological macromolecules has been the focus of research for decades, with significant efficiency and resolution improvements [1]. Chromatography as the foundation of the purification process, was highly prioritized, particularly on an industrial scale. This is contributed to the unique scalability, stability, accuracy, and selectivity, that chromatography offers in comparison with its peers [2][3]. It has been proved that resin-based column chromatography gives an excellent resolution. Particularly, It is the go-to industrial technique used to purify biological products, such as virus/VLP proteins, among other biopharmaceuticals. While there are numerous designs for membrane chromatographies, such as flat sheet systems and stacks of membranes, hollow fibers, and radial flow cartridges.

For each membrane category, multiple designs and geometries have been commercialized [7][8][9]. For instance, several axial and radial flow membrane chromatography devices are

fabricated to understand whether the device dimensions affect the adsorption performance [10]. The literature highlighted that there is an inefficient use of the whole membrane in a stacked disc device, resulting in lower quality and resolution, as the middle part of the stack is saturated with solute significantly sooner than the outer regions [5][11]. This kind of design is very similar to the old method of resin-based columns. A radial flow device is another layout configurational option. Due to the spiral nature of the membrane sheets, there are large dead volumes on both the feed and permeate sides of the membrane roll. However, the fouling is noticeably reduced on both laboratory and industrial scales [12]. Fouling typically happens in narrow paths with small diameters. For instance, hollow fiber membranes are one of the designs with this disadvantage [13][14]. It can be concluded that separation resolution and membrane chromatography efficiency depend entirely on the device's flow distribution [15]. The main reason for the low resolution for other designs of membranes is dispersion, which highly affects the quality of the resolution. Note that this phenomenon is referred to as band spreading or peak broadening in chromatographs.

Overcoming the limitations of these design choices, including cost, speed, and most importantly, dispersion, a new design is proposed (i.e., LFMC). In particular, the productivity of protein separation is increased in one-step purification [16][17][18][19][20]. LFMC has higher theoretical plates, especially in higher flow rates, reducing theoretical plates in other designs [6] [21]. The LFMC device is based on using a stack of rectangular flat sheet membranes. The design allows the fluid to enter from the top channel, pass through tapers, then go through the membrane stack at different locations along its length. Afterward, the fluid comes out on the other side of the membrane stack symmetry to the entering stage and is collected at the bottom channel and directed towards the device outlet.

The LFMC shows promising results in regard to resolution and stability for protein separation process, as well as higher theoretical plates in comparison with resin-based and membrane-stacked disks [6] [16] [17] [18]. Toward enhancing the resolution, the second LFMC generation (referred to as z^2 LFMC) came to light by ignoring the tapered design in LFMC. As a result, there is a noticeable improvement in the uniformity of flow and separation efficiency [22] [23]. The basic fabricated z^2 LFMC design consists of top and bottom plates with primary channels, a circular cross-section of 0.75 mm diameter, connected to a network of semi-circular secondary channels of 0.75 mm diameter. While there is still space for improvements, by tackling the design

configurations of z²LFMC to optimize its efficiency. The experimental evaluation shows promising results regarding the purification process [24][25]. Note that improvements within the ratio of the plates, dimensions of membrane cuts, and cross-section of primary and secondary channels can result in higher purification efficiency. This work shed lights on the improvements in the curvature connection of the channels. In particular, this work examines the fluid dynamics within the updates of the z²LFMC device, comparing them with traditional membrane chromatographies using CFD software to simulate z²LFMC. CFD is an essential tool for understanding and testing the basic transport phenomenon in membrane materials. This study focuses on utilizing CFD to compare various combinations of z²LFMC with conventional methods of membrane chromatography.

Materials

CFD simulates equipment used in the pharmaceutical industry toward optimizing efficiency and performance. With a slight increase in efficiency, industries can increase revenue and decrease production costs [27][28][29]. Further, CFD enables large-scale experimental designs, without the need of conducting the experiments in a wet lab, reducing the operational cost of the experimental research.

For the purpose of this study, COMSOL Multiphysics 5.6 was used to model the experiments. The COMSOL Multiphysics'® Transport of Diluted Species physics interface developed a steady-state model, alongside the Brinkman Equations. When solving models in COMSOL Multiphysics, the finite element technique (FEM) was used.

The equations that were used in these simulations are Navier–Stokes equation (Equation 1), and the Brinkman equations (Equation 2). Brinkman equations are the extensions of the Navier–Stokes and continuity equations in a porous media.

$$\left(\frac{\partial \rho \mathbf{u}}{\partial t} + \rho \mathbf{u} \cdot \nabla \mathbf{u}\right) = \nabla P + \nabla \cdot (\mu(\nabla \mathbf{u} + (\nabla \mathbf{u})^T)) - \frac{2}{3}\mu(\nabla \mathbf{u}) + \mathbf{F} \quad (1.a)$$

$$\rho \left(\frac{\partial \mathbf{u}}{\partial t} + \mathbf{u} \cdot \nabla \mathbf{u}\right) = \nabla P + \nabla \cdot (\mu(\nabla \mathbf{u} + (\nabla \mathbf{u})^T)) + \mathbf{F} \quad (1.b)$$

$$\frac{\rho}{\epsilon} \left(\frac{\partial \mathbf{u}}{\partial t} + (\nabla \cdot \mathbf{u}) \frac{\mathbf{u}}{\epsilon}\right) = -\nabla P + \nabla \cdot \left(\frac{1}{\epsilon}(\mu(\nabla \mathbf{u} + (\nabla \mathbf{u})^T))\right) + \left(\frac{\mu}{K_b} + Q_{in}\right)\mathbf{u} \quad (2.a)$$

$$\frac{\partial(\epsilon \rho)}{\partial t} + \nabla \cdot (\rho \mathbf{u}) = Q_{in} \quad (2.b)$$

The Navier-Stokes equation can be simplified because in these simulations the fluid in the devices is incompressible (Equation 1.b).

In these equations:

- μ is the dynamic viscosity of the fluid
- K is the permeability of the porous medium
- ρ is the density of the fluid
- p is the pressure
- ϵ is the porosity
- F is force

These study's devices were modeled with tetrahedral mesh, with fine size for plates for devices that have outer plates over membranes, such as Z²LFMC and LFMC, and coarser size for membranes. For Z²LFMC and LFMC, the length and width of the membrane stack in each of these devices in earlier works were 70 mm and 20 mm, respectively. The membrane bed height was set to 7.2 mm for all designs. However, the configurations were changed for the aim of this study, proposing two new designs of Z²LFMC. The main design dimensions and CFD properties of the membrane devices and tracer solute used in this study are reported in Table 1.

Table 1. Parameters used in chapter 3

Parameter		Value	
		Condition A (Rectangle)	Condition B (Square)
Length (m)	L	0.07 x sqrt(10)= 0.2213	0.1179
Width (m)	W	0.02 x sqrt(10)= 0.0632	0.1179
Stacked Disk Radius (m)	R	0.0665	
Channel height for LFMC (m)	H _c	0.00158	
Bed Height (m)	H _b	0.0072	
Flow Rate (mL/min)	Q _{in}	100,500	
Mustang Q/S Porosity (-)	ϵ	0.65	
permeability (m ²)	K _b	1.18 x 10 ⁻¹⁴	
Temperature (K)	T	298.15	
Diffusion coefficient of NaCl in water (m ² /s)	D	2.9 x 10 ⁻⁹	
Loop (mL)		2	
Relative tolerance (-)	-	10 ⁻³	

Results and Discussion

The efficiency of the chromatograph has a direct relation with the broadness of the tracer peak. Toward checking the efficiency of the chromatography, several approaches were proposed in the literature, including the commonly used Van Deemter equation. Van Deemter equation considers details regarding the factors that shape the peaks of the chromatograph and the efficiency of the device. The equation is as follows:

$$\text{HETP} = A + B/u + C.u \quad (3)$$

As shown in Equation 3, the chromatograph's shape depends on three main factors: (i) Eddy diffusion; (ii) Axial diffusion; and (iii) Resistance to mass transfer. Notice that A is the Eddy diffusion factor, B is the Axial diffusion sign, and C is the mass transfer resistance. It is worth mentioning that dispersion in membrane chromatographies is a combination of eddy diffusion and axial diffusion.

Further, optimizing membrane chromatographies toward a smaller HETP value (m/N) is desirable. Here, HETP is the height equivalent of a theoretical plate (i.e., the inverse of N/m). In the equation, u represents the superficial velocity, calculated as the flow rate over the membrane area.

To compare the efficiency of different designs of membrane chromatographies, two famous industry-based devices were used which are mainly used in downstream processes in the biopharmaceutical and biotechnological industries, namely, stacked disk membrane and radial flow membrane chromatography. The utilized stacked disk membrane chromatography and radial flow membrane chromatography are shown in Fig. 1. In Fig. 1 COMSOL Multiphysics was used to model them.

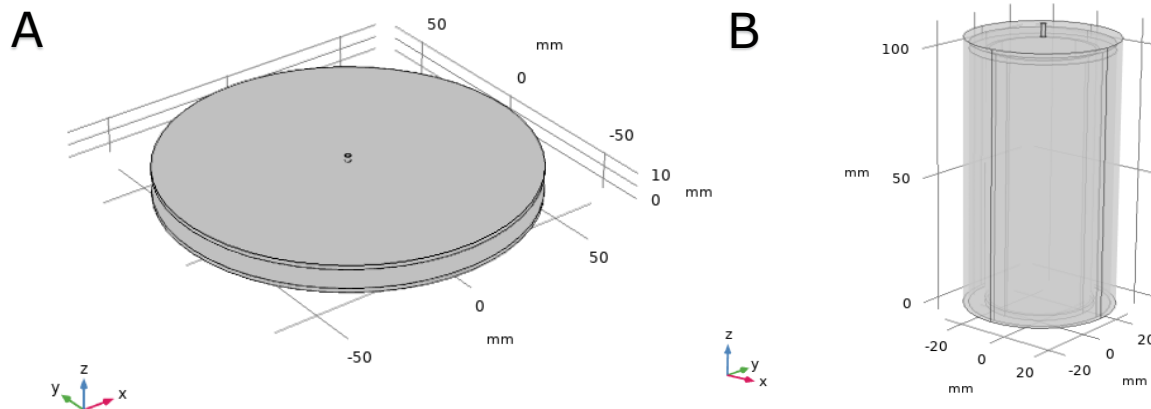


Fig 1. Membrane chromatography devices with equal bed height. A) Stacked disk membrane B) Radial flow membrane chromatography

Moreover, the different generations of the Laterally Fed Membrane Chromatography (LFMC) are shown in Fig. 2. The first generation is shown in Fig. 2A. Moreover, the different shapes of the second generation of LFMC, z^2 LFMC, are shown in Fig. 2B and C (rectangular and square). Note that the z^2 laterally-fed membrane chromatography (z^2 LFMC) has been developed to address concerns associated with prior designs, including increased manufacturing expenses and high fluid dispersion.

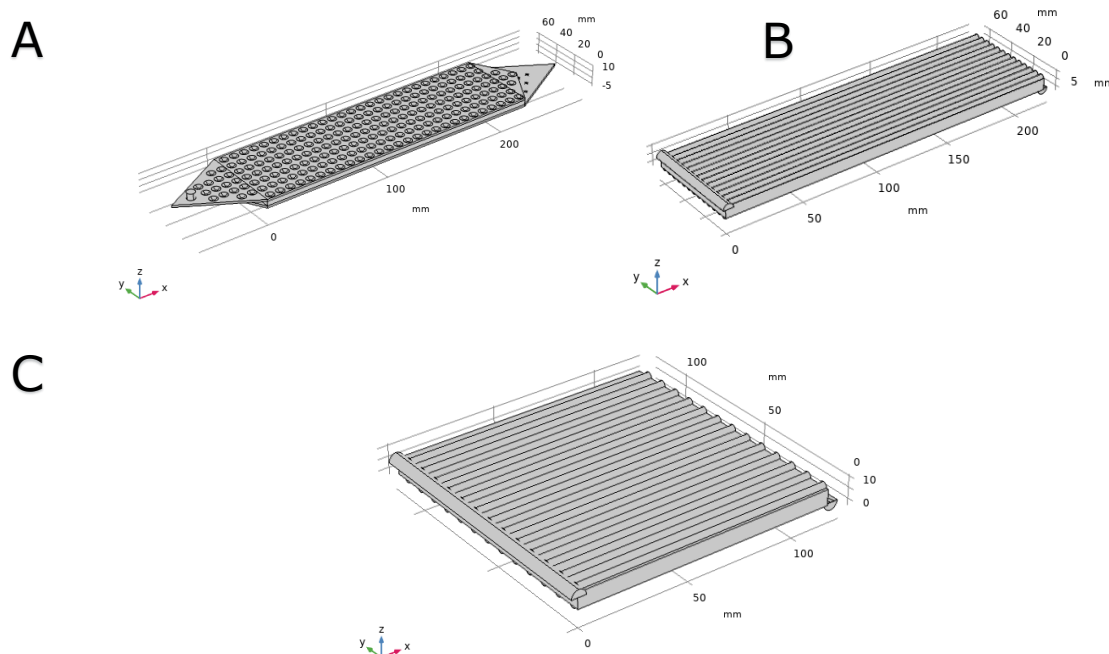


Fig 2. Laterally fed membrane chromatography over three different generations.

The LFMC is well explored [19][20] as an alternative to radial-flow membrane chromatography and stacked disk membrane chromatography. LFMC is shown to be suitable for carrying out fast, high-resolution separations. In this study, two updates to LFMC were applied in the form of z^2 LFMC optimizations (rectangle/square to compare the efficiency by COMSOL Multiphysics), as shown previously in Fig. 2B and Fig. 2C. To have a better understanding of the tracer movements around membrane chromatography, this study gives an in-depth explanation of the design effects on the tracer resolution performance.

Fig. 3 shows the difference in timing for solutes. The solute molecule moving closer to the axis of a stacked disk would have a shorter flow path than the periphery, which results in the time difference between the solutes. This process is known as axial dispersion, and it is considered one of the factors which increase the HETP and peak broadness [30]. Fig. 3 shows the solute movement within the stacked disk at the time of 15 seconds by COMSOL Multiphysics'®.

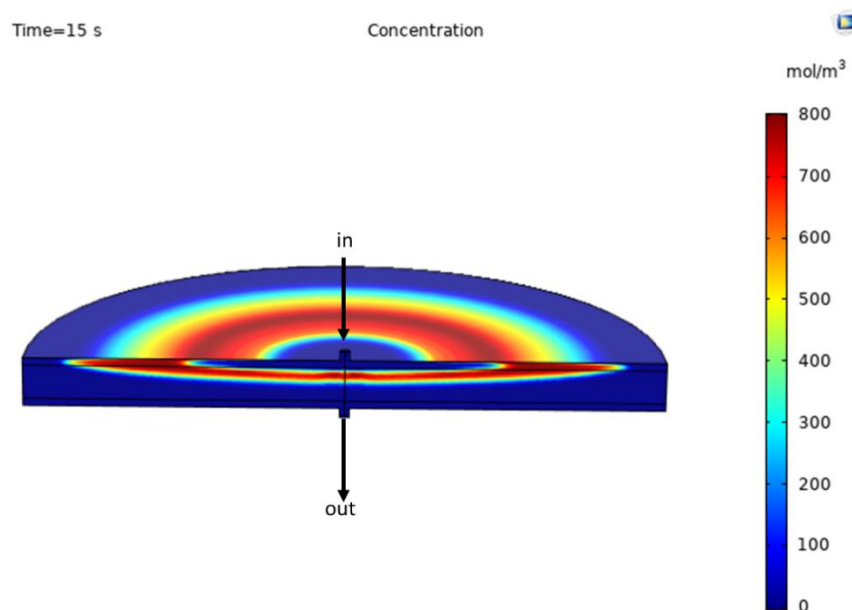


Fig 3. Concentration of solute (mol/m³) on stacked-disk device on the time of 15 seconds. The detailed configurations and specifics are mentioned in table 1.

The dimensions of the stacked disk are shown in table 1. The flow rate of this experiment is 100 mL/min. Feed enters the membrane module centrally in the axial flow stacked-disk membrane module. Consequently, the material/liquid is distributed radially in an outward

direction over the membrane bed. Then, fluid flows through the membrane bed. Finally, permeate is collected at a centrally located outlet.

As aforementioned, radial flow membrane chromatography devices have significant advantages over stacked disk devices. However, these devices have complicated flow paths. For instance, the materials and liquid are first distributed in a radial surrounding the device and then flow in an axial direction within the annular space surrounding the membrane, followed by radially inward flow within the membrane and finally axial flow over the collecting cylindrical core. In radial flow chromatography, when the fluid reaches the periphery, the velocity magnitude decreases as the cross sectional area increases. Consequently, In the radial flow configuration, the high dead volume on both the feed and membrane's permeate side leads to sample dilution and shallower peaks. Fig. 4 shows the solute concentration on the radial flow device for the time of 15 seconds and the paths of the solute over time. As shown, at the mark of 15 second, the solute diluted noticeably before reaching the membrane. This is mainly contributed to the large dead volume in both the header and shell. The diffusion process clears the remaining solute from the module, resulting in peak asymmetry values.

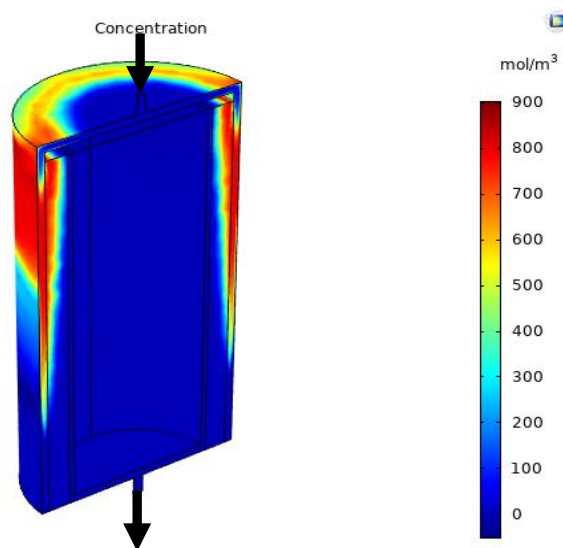


Fig 4. Concentration of solute (mol/m³) on radial flow device at the 15 seconds mark. The specifics are mentioned in table 1.

Fig. 5 and 6 show the movement of the same solute during its transit in the LFMC and z^2 LFMC rectangular design (the primary channel is 2.37 mm and the secondary channel is 0.87 mm).

In LFMC, the inlet region of the LFMC module was designed specifically so the fluid coming from the external piping has time for flow development before entering the channel regions which are above the membrane bed. Due to the lateral flow distribution, the dispersion is negligible. Therefore, it could be anticipated that the difference in time spent by the fastest and the slowest salt solute molecules within the membrane would be significantly lower than that in the stacked disk and radial flow devices.

In our earlier studies it was mentioned that due to low dispersion effects, the residence time along each hypothetical flow path within the z^2 LFMC device is expected to be the same. In z^2 LFMC, same as LFMC, the dispersion is lower than in the other two conventional membrane chromatographies. In both LFMC and z^2 LFMC the fluid did not “short-circuit” through the membrane stack, which makes them perform perfectly.

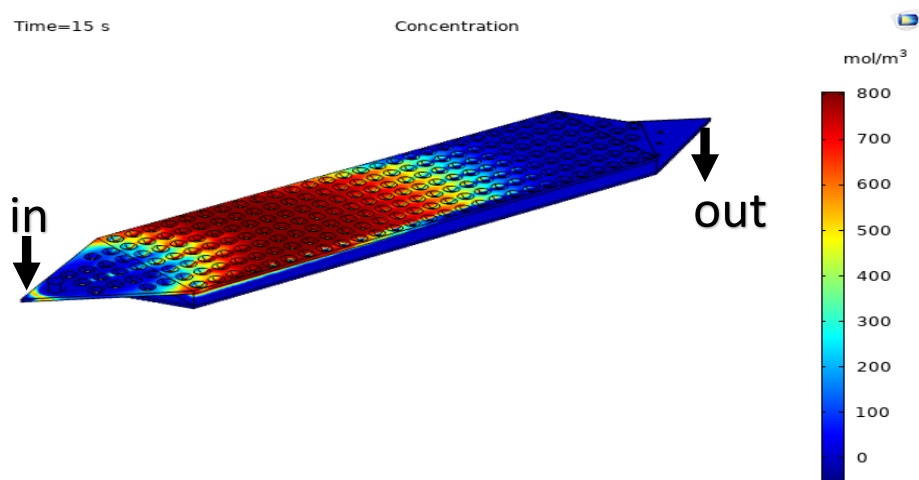


Fig 5. Concentration of solute (mol/m³) on LFMC device at the 15 seconds mark. The specifics are mentioned in table 1.

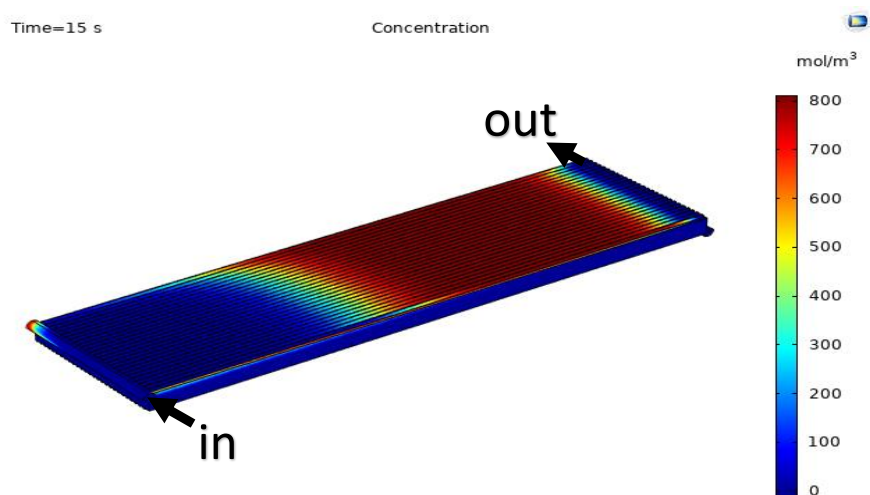


Fig 6. Concentration of solute (mol/m^3) on z^2 LFMC-rectangular design device at the 15 seconds mark. The specifics are mentioned in table 1. The primary channel is 2.37 mm and secondary channel is 0.87 mm.

In this experiment, diameters of the z^2 LFMC channels were changed to observe the effect of diameter configuration on the resolution and efficiency of z^2 LFMC. One study elucidated that for an LFMC device's efficient functioning, the lateral channels' hydraulic resistance must be identical. In turn, the lateral channels' hydraulic resistance has to be significantly lower in magnitude than the one in the membrane stack. If there is a tendency to lose less pressure through a series of pipes and fittings, the pipes' size should be increased, indicating that the primary channel should have a higher diameter than the secondary channel. In earlier work [23], both diameters were similar, whereas, in this study, the optimized diameters ratio is concluded following experimental evaluation of different channels' proportions. In this experiment, the control channels are set to 0.75 mm and 0.5 mm for primary and secondary, respectively. Then, the channels were configured using several mathematical ratios. Table 2 shows the dimensions for five different designs for both rectangular and square devices, and the chromatographs for the tracer test are shown in Fig. 7.

Table 2 Diameter of primary and secondary channels in the rectangular and square z²LFMC devices

Primary channel diameter (mm)	Secondary channel diameter (mm)	Rectangular device	Square device
1.84	0.87	z ² LFMC R1	z ² LFMC S1
2.90	1.58	z ² LFMC R2	z ² LFMC S2
3.35	1.93	z ² LFMC R3	z ² LFMC S3
2.37	1.32	z ² LFMC R4	z ² LFMC S4
2.37	0.87	z ² LFMC R5	z ² LFMC S5

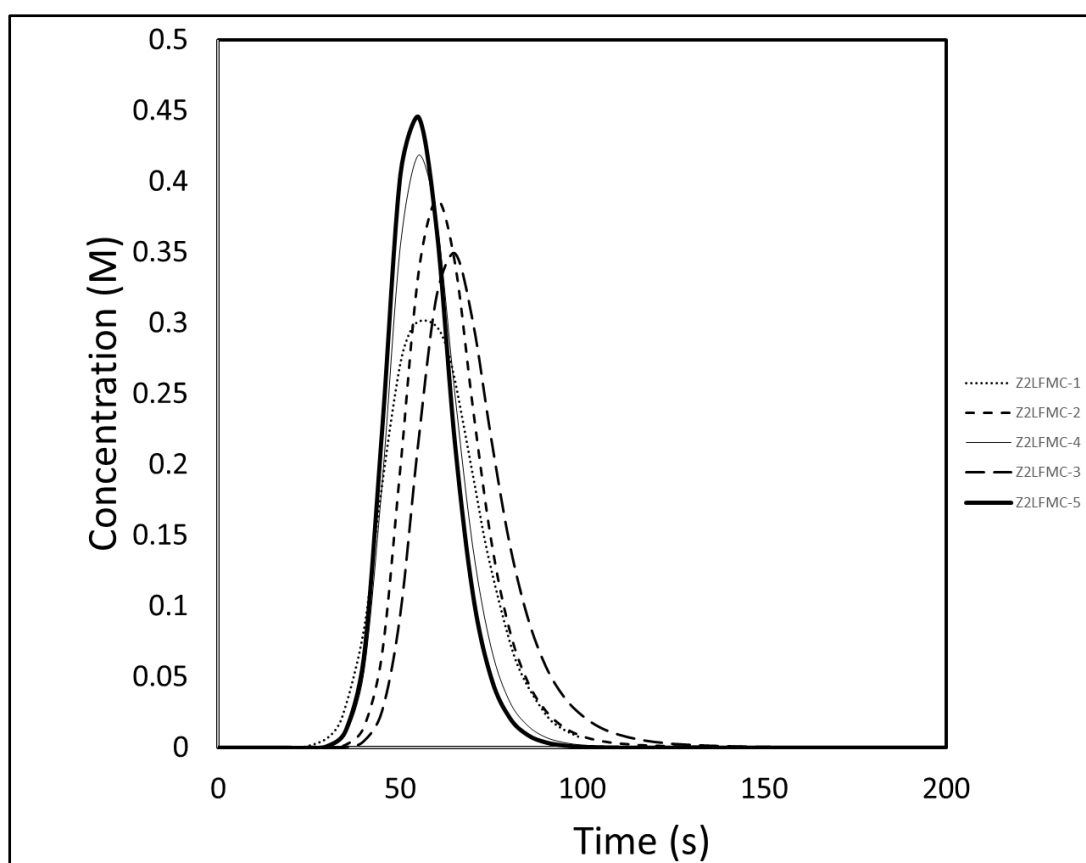


Fig 7. Comparing all z²LFMC rectangular designs for 100mL/min. z²LFMC R1 dotted, z²LFMC R2 small dash, z²LFMC R3 large dash, z²LFMC R4 thin solid and z²LFMC R5 thick solid.

In this experiment, buffers of 0.4 and 0.8 M sodium chloride were used at room temperature. As shown in Fig. 7, the z²LFMC R5 has the best result, followed by z²LFMC R4, z²LFMC R2, z²LFMC R3, and z²LFMC R1, respectively. The experimental evaluation highlights a strong relationship

between the configurations of primary and secondary channels, such as the difference in diameter between primary and secondary channels should not be significant. For example, in the second and third designs, this phenomenon is evident, which makes the concentration profile weak. Pressure drop changes should be uniform throughout the device and making a sudden change can be inappropriate. Furthermore, if the primary channel becomes very large, it does not have a good effect (such as in the second and third designs). Given that the z^2 LFMC R5 and z^2 LFMC R4 show the best results, it can be concluded that 2.37 mm is the best diameter for the primary channel. For secondary channel, the 1.32 mm diameter achieves better result than the 0.87 mm diameter. This is mainly contributed to the fact that 0.87 mm is too small for the solutes to pass the channels.

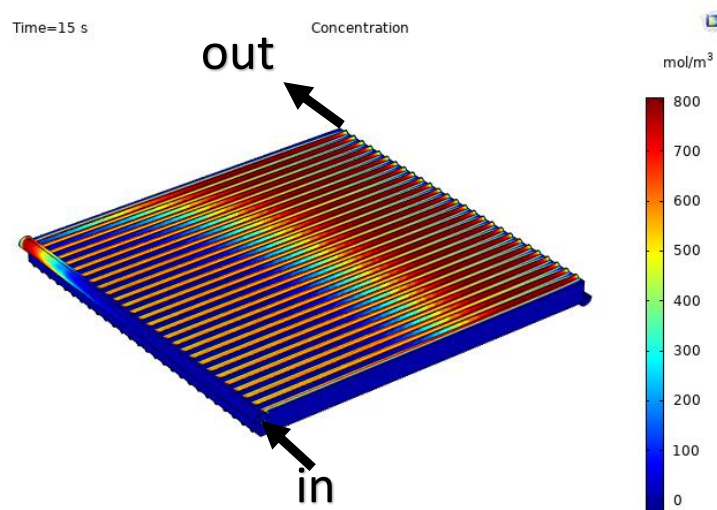


Fig 8. Concentration of solute (mol/m³) on z^2 LFMC-square design device at the 15 seconds mark. The specifics are mentioned in table 1. The primary channel is 2.37 mm and secondary channel is 0.87 mm.

Fig. 8 shows the movement of the same solute during its transition in the z^2 LFMC square design. It was expected same the results as the previous design. It can be concluded that the fastest and the slowest molecules within z^2 LFMC-square design device would be significantly lower than that in the column or radial flow membrane chromatography. However, in this design choice, the difference in time spent by the fastest and the slowest salt solute molecules within the membrane is expected to be less than that in a rectangular design, this is due to that the dimensions of the plates are similar.

Similar to the rectangular z^2 LFMC, this experiment investigated various channels diameters to study the effect of channel's diameter in the resolution and efficiency of z^2 LFMC. Fig. 9 shows the performance of 5 different designs of square z^2 LFMC. As shown, the z^2 LFMC S5 holds the best results in comparison to other design choices because the flow-through salt peak obtained with the latter was narrower and sharper. This indicated that better separation efficiency could be expected with z^2 LFMC S5 configuration. Further, it can be concluded that a rectangular design outperforms the square design, as reported in the results (0.45 M vs 0.4 M).

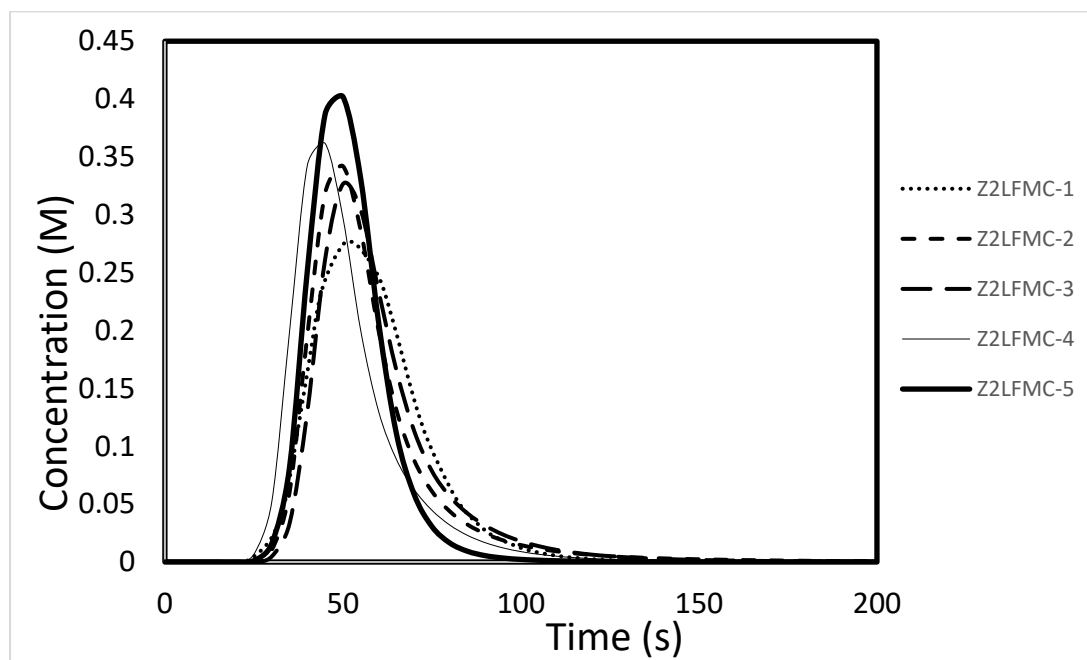


Fig 9. Comparing all z^2 LFMC square designs for 100mL/min. z^2 LFMC S1 dotted, z^2 LFMC S2 small dash, z^2 LFMC S3 large dash, z^2 LFMC S4 thin solid and z^2 LFMC S5 thick solid.

Fig.10 shows the salt flow-through peaks obtained by carrying out experiments using the stacked disk membrane chromatography, radial flow membrane chromatography, LFMC, z^2 LFMC R5, and z^2 LFMC S5, at a flow rate of 100 mL/min, using 0.4 M NaCl as mobile phase, and 0.8 M NaCl solution as the tracer. These results are from the dry experiments by salt tracer (simulation).

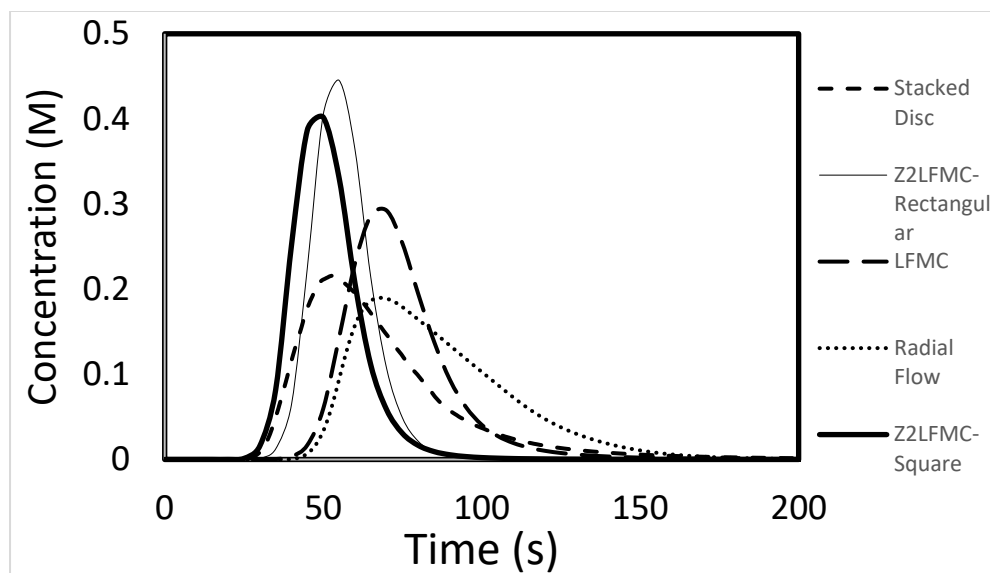


Fig 10. Tracer profiles for five different membrane chromatography at 100mL/min radial flow is dotted, stacked disc is small dash, LFMC is large dash, z^2 LFMC rectangular is thin solid, z^2 LFMC square is thick solid.

As aforementioned, stacked disk and radial flow designs have the broadest peaks, which is inline with the van Deemter equation. At 100 mL/min, the resolution obtained with the z^2 LFMC rectangular device was higher than that obtained with the LFMC. Recall that the z^2 LFMC device couples high speed with higher resolution than LFMC and the chromatographs also show similar results. However, the rectangular design of z^2 LFMC device, outperforms the square design one. Fig. 11 has the same trend as Fig. 10, as the flow rate increased up to five times. The z^2 LFMC R5 resulted in a taller and narrower flow-through peak compared to other devices. The NaCl tracer, having high diffusivity, led to shorter peaks in other devices; moreover, it was more pronounced in the radial flow and stacked disk module.

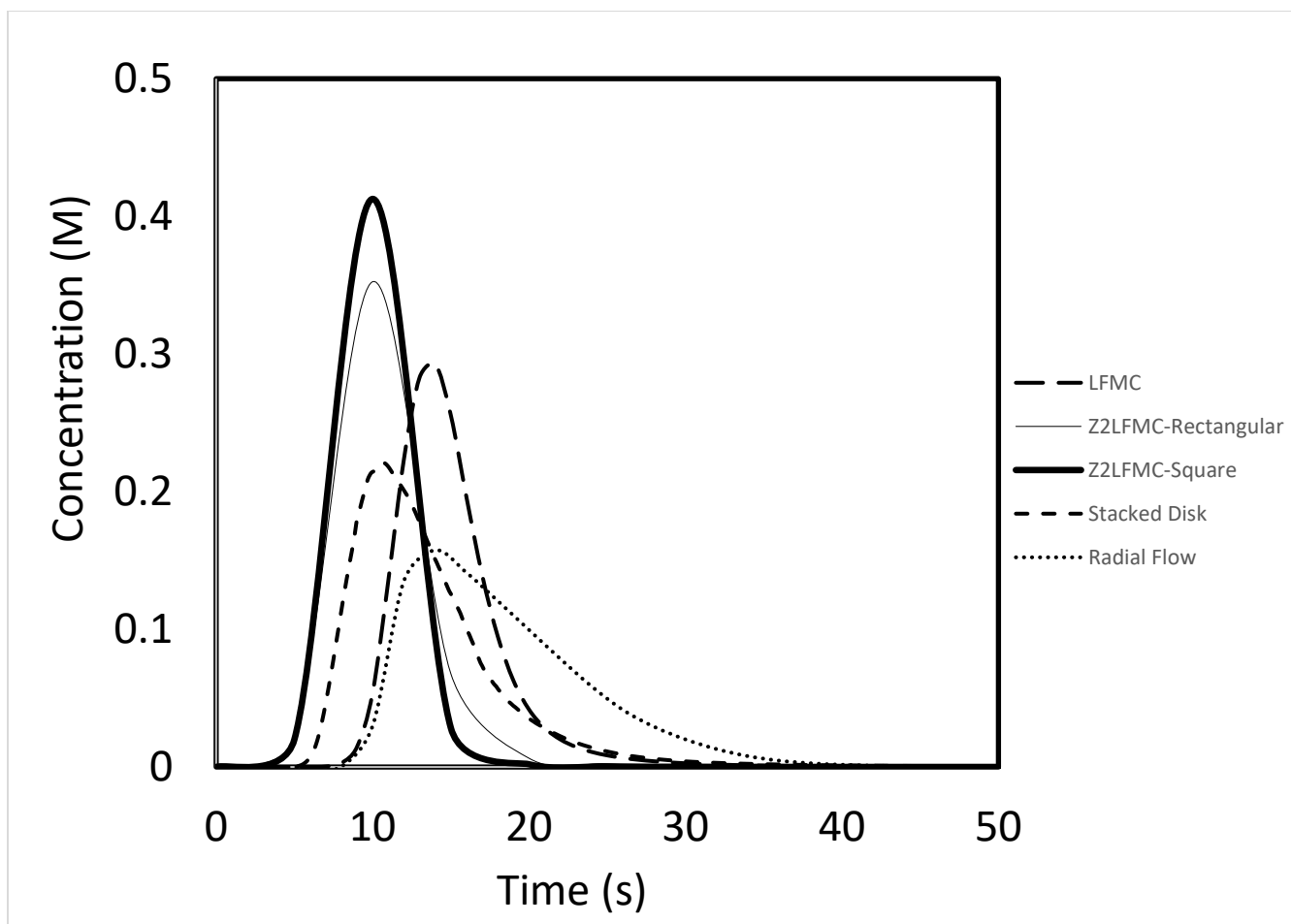


Fig 11. Tracer profiles for 5 different membrane chromatography at 500mL/min radial flow is dotted, stacked disc small dash, LPMC large dash, z²LFMC rectangular thin solid, z²LFMC square thick solid.

Further investigating possible improvements to z²LFMC. The effect of the curvature on the tracer profile is studied. In this study, the connection of primary and secondary channels to each other can lead to changes in the resolution of chromatographs. The Primary channel can connect to secondary channels with the array of the knees as shown in Fig. 12B.

Fig. 12 highlights that with the inclusion of the curve, there is a slight improvement in the efficiency, as the fluid always works better in curved knee pipes, in comparison with the 90 degrees pipes. This is contributed to the drop in the pressure resulting from the sharp knees.

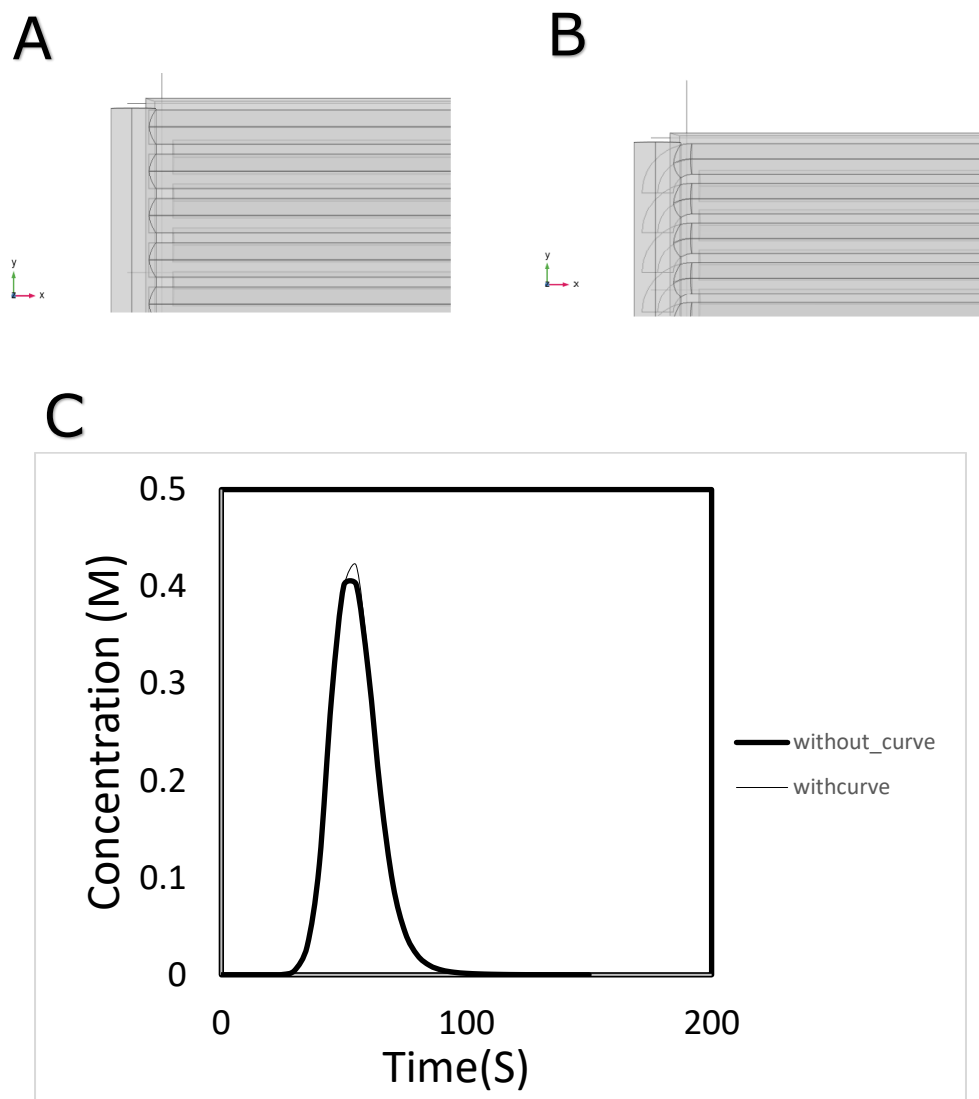


Fig 12. Effect of the curvature on tracer profile at 100 mL/min.

Conclusion

CFD simulations are widely leveraged to conduct preliminary experiments before embarking on actual device fabrication, lowering the manufacturing and research costs. Using CFD simulations, this chapter put under the test the efficiency of z^2 LFMC device for biopharmaceuticals purification. The experimental results highlight that z^2 LFMC device is suitable for the separation and purification of biopharmaceuticals compared to traditional membrane chromatography devices when considering large volumes (i.e., 100 mL). While the observations of this work show the superiority of z^2 LFMC design, more detailed and rigorous experiments are required to consider z^2 LFMC as an industrial alternative to the traditional approaches. This is evident given the room for improvements that z^2 LFMC device still has. The experimental results

demonstrated that by slightly modifying the design of z²LFMC device, the resolution in biopharmaceutical separation is significantly increased. This is more evident in the case of the biopharmaceutical separation process, where z²LFMC R5 device outperformed its counterparts, providing the best resolution.

Acknowledgment

We acknowledge the support of the Natural Sciences and Engineering Research Council of Canada (NSERC).

References

- [1] J.C. Janson, Protein Purification: Principles, High-Resolution Methods, and Applications third ed., Wiley, 2011
- [2] Y. Wan, T. Zhang, Y. Wang, Y. Li, Comparing the relative robustness of byproduct removal by wash and by elution in column chromatography for the purification of a bispecific antibody Protein, *Expr. Purif.*, 177(2021), pp. 105762
- [3] A.S. Rathore, D. Kumar, N. Kateja, Recent developments in chromatographic purification of biopharmaceuticals, *Biotechnol. Lett.*, 40(6)(2018), pp. 895-905
- [4] T.M. Przybycien, N.S. Pujar, L.M. Steele, Alternative bioseparation operations: life beyond packed-bed chromatography, *Curr. Opin. Biotechnol.*, 15(5)(2004), pp. 469-78
- [5] V. Orr, L. Zhong, M. Moo-Young, C.P. Chou, Recent advances in bioprocessing application of membrane chromatography, *Biotechnol. Adv.*, 31(4)(2013), pp. 450-65
- [6] P. Madadkar, R. Sadavarte, R. Ghosh, Performance Comparison of a Laterally-Fed Membrane Chromatography (LFMC) Device with a Commercial Resin Packed Column, *Membranes.*, 9(11)(2019), pp. 138
- [7] R. Ghosh, T. Wong, Effect of module design on the efficiency of membrane chromatographic separation processes, *J. Membrane. Sci.*, 281(2006), pp. 532-540
- [8] S. Bower, R. Wickramasinghe, Elimination of non-uniform, extra-device flow effects in membrane adsorbers, *J. Membrane. Sci.*, 330(2009), pp. 379-387
- [9] P. Ghosh, K. Vahedipour, M. Leuthold, E.V. Lieres, Model-based analysis and quantitative prediction of membrane chromatography: extreme scale-up from 0.08 ml to 1200 ml, *J. Chromatogr. A.*, 1332(2014), pp. 8-13

[10] C. Teepakorn, K. Fiaty, C. Charcosset, Effect of geometry and scale for axial and radial flow membrane chromatography-Experimental study of bovin serum albumin adsorption, *J. Chromatogr. A.*, 1403(2015), pp. 45-53

[11] M.A. Teeters, T.W. Root, E.N. Lightfoot, Performance and scale-up of adsorptive membrane chromatography, *J. Chromatogr. A.*, 944(2002), pp.129-39

[12] U. Umatheva, P. Madadkar, P. R. Selvaganapathy, R. Ghosh, Computational fluid dynamic (CFD) simulation of laterally-fed membrane chromatography, *Chem. Eng. Res. Des.*, 137(2018), pp. 412-420

[13] E. Akhondi, F. Zamani, K.H. Tng, G. Leslie, W.B. Krantz, A.G. Fane, J.W. Chew, The Performance and Fouling Control of Submerged Hollow Fiber (HF) Systems: A Review, *Appl. Sci.*, 7(8)(2017), pp. 765

[14] S.Y. Suen, Y.C. Liu, C.S. Chang, Exploiting immobilized metal affinity membranes for the isolation or purification of therapeutically relevant species, *J. Chromatogr. B. Analyt. Technol. Biomed. Life. Sci.*, 797(1-2)(2003), pp. 305-319

[15] J. Marriott, E. Sørensen, A general approach to modelling membrane modules, *Chem. Eng. Sci.*, 58(22)(2003), pp. 4975-4990

[16] P. Madadkar, R. Ghosh, High-resolution protein separation using a laterally-fed membrane chromatography device, *J. Membr. Sci.*, 499 (2016), pp.126-13

[17] P. Madadkar, S.L. Nino, R. Ghosh, High-resolution, preparative purification of PEGylated protein using a laterally-fed membrane chromatography device, *J. Chromatogr. B. Analyt. Technol. Biomed. Life. Sci.*, 1035(2016), pp. 1-7

[18] P. Madadkar, U. Umatheva, G. Hale, Y. Durocher, R. Ghosh, Ultrafast Separation and Analysis of Monoclonal Antibody Aggregates Using Membrane Chromatography, *Anal. Chem.*, 89(8)(2017), pp. 4716-4720

[19] P. Madadkar, Q. Wu, R. Ghosh, A laterally-fed membrane chromatography module, *J. Membr. Sci.*, 487(2015), pp. 173-179

[20] R. Ghosh, P. Madadkar, Q. Wu, On the workings of laterally-fed membrane chromatography, *J. Membr. Sci.*, 516(2016), pp. 26-32

[21] R. Sadavarte, P. Madadkar, C.D. Filipe, R. Ghosh, Rapid preparative separation of monoclonal antibody charge variants using laterally-fed membrane chromatography, *J. Chromatogr. B. Analyt. Technol. Biomed. Life. Sci.*, 1073(2018), pp. 27-33

[22] R. Ghosh, G. Chen, U. Umatheva, P. Gatt, A flow distribution and collection feature for ensuring scalable uniform flow in a chromatography device, *J. Chromatogr. A.*, 1618(2020), pp. 460892

[23] R. Ghosh, G. Chen, R. Roshankhah, U. Umatheva, P. Gatt, A z^2 laterally-fed membrane chromatography device for fast high-resolution purification of biopharmaceuticals, *J. Chromatogr. A.*, 1629(2020), pp. 461453

[24] R. Roshankhah, G. Chen, Y. Xu, N. Butani, Y. Durocher, R. Pelton, R. Ghosh, Purification of monoclonal antibody using cation exchange z^2 laterally-fed membrane chromatography – A potential alternative to protein A affinity chromatography, *Biochem. Eng. J.*, 178(2022), pp. 108293

[25] G. Chen, J. Pagano, D. Yu, S. Ghose, Z. Li, R. Ghosh, Fast and high-resolution purification of a PEGylated protein using a z^2 laterally-fed membrane chromatography device, *J. Chromatogr. A.*, 1652(2021), pp. 462375

- [26] S.D. Miles, S. Kumar, G. Cox, Comparisons Of 'blind Predictions' Of A Cfd Model With Experimental Data, *Fire. Saf. Sci.*, 6(2000), pp. 543-554
- [27] P. Pandey, R. Bharadwaj, X. Chen, 1 - Modeling of drug product manufacturing processes in the pharmaceutical industry, in: P. Pandey, R. Bharadwaj, *Predictive Modeling of Pharmaceutical Unit Operations*, Woodhead Publishing, 2017, pp. 1-13
- [28] H.S. Pordal, C.J. Matice, T.J. Fry, The role of computational fluid dynamics in the pharmaceutical industry, *Pharm. Technol.*, 26(2002), pp. 72-79
- [29] D.M. Kremer, B.C. Hancock, Process simulation in the pharmaceutical industry: a review of some basic physical models, *J. Pharm. Sci.*, 95(3)(2006), pp. 517–529
- [30] J.E. Baur, E.W. Kristensen, R.M. Wightman, Radial dispersion from commercial high-performance liquid chromatography columns investigated with microvoltammetric electrodes, *Anal. Chem.*, 60(21)(1988), pp. 2334-2338

Chapter 4

Purification of T7 Bacteriophage using Anion Exchange z^2 Laterally-fed Membrane Chromatography

Bacteriophage is a virus that infects and replicates within bacteria and archaea, and has been recently used in the treatment of localized infections. Phage particle purification is crucial for therapeutic applications of bacteriophages. The purification of bacteriophages for phage therapy purposes is considered a straightforward exercise of removal of bacterial debris by filtration, centrifugation, or membrane chromatography, and their combinations. However, older techniques are cumbersome, elaborate, and expensive. Moreover, they are not suitable for purifying large quantities of phages.

The aim of this chapter is to explore the possible replacement of conventional purification methods. In particular, Q z^2 LFMC is studied toward high-speed and high-resolution purification of bacteriophage. The protocol described here, uses anion-exchange chromatography (Q z^2 LFMC) to bind phages to a stationary phase. This is done using an HPLC system, combined with z^2 LFMC.

In this project, I am the primary author of the manuscript and conducted the experiments. Kyle Jackson assisted me with phage propagation, titer assay, and endotoxin quantification assay. Ngoc Nguyen Truong assisted me with part of the experiments during my internship, as I was remotely working with him to ensure the on-time completion of the experimental design.

Dr. Robert Pelton and Dr. zeinab hosseini-doust provided their kind advice and help throughout the entire project. Dr. Raja Ghosh supervised the project.

Purification of T7 Bacteriophage using Anion Exchange z^2 Laterally-fed Membrane Chromatography

Abstract

The antibiotic resistance to bacterial pathogens is on the rise in recent years. This necessitates developing novel infection-control strategies to counter this phenomenon. Despite the concerns around bacteriophages (phages), as they are still not approved as a treatment in western medicine, a massive number of patients have been successfully treated in other countries using this technique, namely, Eliava Institute. On yearly bases, Eliava Institute continues to treat hundreds of international patients. However, the bacteriophages produced following their lysis procedure contain many impurities, including endotoxins produced by gram-negative bacteria, which are harmful to humans. To have functional bacteriophages, purification of these infectious particles is required. This can only be ensured if the activity and the number of phages in the entire mixed community are maintained under a certain threshold during the whole process.

This chapter proposes a two-steps process, using a combination of modern membrane purification processes and ultrafiltration. The advantage of this process is the absence of organic and inorganic solvents. The proposed method is tested on real case studies, such as the removal of monoclonal antibody aggregates, the purification of PEGylated proteins, and the purification of monoclonal antibodies. This chapter further extends the applications to the purification of bacteriophages. The findings, among others, show that the combination of ultrafiltration with z^2 LFMC device results in an efficient bacteriophage purification.

Introduction

Since the discovery of penicillin, there have been rapid and promising research directions within antibiotics and their efficiency. However, this pace has significantly decreased, and several concerns have been raised regarding bacterial resistance to antibiotics [4]. The clinical reports of antibiotic resistance noticeably increased [1]. Clinical studies for streptomycin efficacy in tuberculosis treatment evidenced the emergence of resistance to Mycobacterium tuberculosis [2][3]. In recent years, there has been a vast interest in industrial and academic research toward

producing non-antibiotic products in scale, namely bacteriophage-based medicines [5][1]. This is beneficial, as patients who did not respond to penicillin therapy in various Western nations were treated with bacteriophage as an alternative solution. The results on 223 individuals with lung and pleural infections treated with phages were compared to 117 patients treated with antibiotics. In the phage-treated group, 82% of the patients recovered completely, compared to only 64% of the patients in the antibiotic-treated group [6]. However, the efforts in phage treatment have only been the focus of the research recently, in comparison with antibiotic research [7]. To unleash the capabilities of phage treatment, low endotoxin and highly concentrated phage solutions are required for several applications, such as phage therapy, agricultural, or veterinary applications [8][9]. The impurities within phages are categorized into three types: (i) harmful bacterial, defined as the protein toxins produced by several pathogenic bacterial species, which are harmful to humans, (ii) culture medium components, e.g., bacterial endotoxins and animal products, (iii) non-biologic molecules, including small molecules. Most of the contamination is caused by the preparation step, as the culture media are contaminated with the macromolecules produced by the host bacteria.

The focus of impurities purification in bacteriophages is the elimination of endotoxin. Endotoxin is a pyrogen made of the lipopolysaccharide LPS, consisting of the lipid A, fatty acids and disaccharide phosphates, core polysaccharides and the O-antigen. Endotoxins are considered immunogenic in the human body. Septic shock following intravascular coagulation, multiple organ failure, and even death are common symptoms of entering endotoxin in the human body [10][11][12][13]. The main reason is that endotoxins are amphipathic molecules that can suddenly form large aggregates [14]. Endotoxins should be eliminated from phage preparations while researching or utilizing phage in human systems, mainly due to the potentiation complications of using phage treatment. The amount of endotoxin is calculated using Endotoxin Unit (EU), defined as the activity of 100 pg of *E. coli* lipopolysaccharide. The Endotoxin limit for intravenous and oral administration are $5 \text{ EU} \cdot \text{kg} \cdot \text{hr}^{-1}$ and $20 \text{ EU} \cdot \text{ml}^{-1}$, respectively [15][16].

The traditional approach for purification is by using polyethylene glycol precipitation and subsequent CsCl gradient ultracentrifugation. These methods have been tested and approved in the industry and are feasible for most of the bacteriophage strains, and their efficiency is not sensitive to pH. For instance, it has been proved [17][18] that with the appropriate procedure in

purification, a 65-95% of the crude lysate plaque-forming units (PFU) can be achieved. The main advantage is that this method is mostly independent of the initial concentration of the bacteriophages in suspension. However, many phages are destroyed by centrifugal pressures and their interaction with CsCl, losing their infectivity [19]. Although there are several approaches in which the problem can be tackled, such as sucrose gradient. However, gradient separations are cumbersome [20]. Another purification method is Tangential Flow Filtration (TFF). This method is easy to set up, fast, efficient, and economical. However, it is not recommended due to its rotor limitations, resulting in difficulties in using this method on a large scale [21][22]. A new alternative method for purifying bacteriophages is chromatography [24][25]. The literature on the conventional purification methods (precipitation and centrifugation) shows that the suspended time for the entire process exceeded 18.5 hours, including 16 hours spent on the overnight precipitation. An additional hour for the second precipitation, and a total of one hour and 25 min dedicated to centrifugation. In comparison, the time spent for the whole process in chromatography was overall 228 minutes (i.e., 3.8 hours) [25].

Despite the breadth of affinity chromatography purification device configurations and choices, this approach is not recommended, in most cases, due to its high time consumption and low yield. Additionally, SEC has limited capacity and selectivity. Overall, AEC is the preferred chromatography technique due to its high selectivity, rapid separation, and reproducibility.

The previous work in this thesis attempted to improve resolution by neglecting the tapering design in LFMC, leading to the development of the second generation of LFMC (z^2 LFMC). As a result, the flow homogeneity and separation efficiency have both been improved [31][32].

This work further discusses the possibility of using anion exchange z^2 LFMC device for bacteriophage purification in the bind-and-elute mode. The z^2 LFMC device used in this study had a membrane bed volume of 5 mL and contained a stack of strong anion exchange (Sartobind Q) membranes. The purified bacteriophage was obtained from the eluate for further investigations.

Materials and Methods

Phage Propagation and Filtering

T7 phage was propagated using a host, *Escherichia coli* strain K12 BL21 (Sigma-Aldrich, CMC001). A pre-culture of *E. coli* in LB-Miller broth was cultured overnight in a shaking incubator

set at 180 rpm and 37 °C. The next day, using fresh LB-Miller broth, a 1:200 subculture was made and allowed to grow until an OD 600nm of 0.6 was reached. 10 mL of T7 phage (~ 10¹⁰ PFU/mL) was subsequently added to the subculture. 50 mL of 1M CaCl₂ solution was added to the subculture to assist in phage infectivity. The T7-subculture solution was then incubated in a shaking incubator set at 180 rpm and 37 °C for 14 hours. The culture was then centrifuged at 7000xg for 15 minutes. The bacteria pellets were discarded, and the phage-containing supernatant was retained and filtered through a 0.2 µm filter (Fisher Scientific, 13100106) to remove residual bacteria. The filtered supernatant was stored at 4 °C.

Double Overlay Phage Titer Assay

T7 phage was quantified using the agar overlay technique. Briefly, 200 mL of E. coli K-12 BL21 and 100 mL of diluted T7 phage solution were added to liquefied LB-Miller Soft Agar (2.5% LB; 0.6% Agar), vortexed, and poured on top of LB-Miller Agar (2.5% LB; 1.5% Agar) plates (Fisher Scientific, Sterile 100mm x 15mm Polystyrene Petri Dishes, FB0875712). Plates were placed in a stationary incubator set at 37 °C for 6 hours and then incubated at room temperature for 12 hours. The number of resulting plaques were counted, and a total concentration was determined using the following equation: (# of plaques / ((dilution factor) * (phage volume added))).

Endotoxin Quantification Assay

Endotoxins were quantified using the Pierce LAL Chromogenic Endotoxin Quantification Kit (Thermo Scientific, 88282). Assay was performed as instructed in the user manual. Briefly, endotoxin standard stock solutions were prepared by combining the endotoxin standard vial with the desired amount of endotoxin-free water, as instructed. Endotoxin standard stock solutions were diluted as instructed to required concentrations. Limulus Amebocyte Lysate (LAL) and Chromogenic Substrate solutions were prepared by suspending dehydrated contents with the desired volume of endotoxin-free water, as instructed. A 96-well microplate (Fisher Scientific, 08-772-54). was equilibrated to 37 °C on a hot plate. 50 µL of endotoxin standard solutions and test solutions were dispensed into desired wells. 50 µL of LAL was then immediately dispensed into all wells containing solutions and left to incubate for 10 mins at 37 °C. At exactly 10 mins, 100 µL of chromogenic substrate solution was gently added to each well and left to incubate for 6

mins at 37 °C. At exactly 16 mins, 100 mL of stop reagent (25% Acetic Acid) was added to each well. The absorbance readings of the plate were then taken on a plate reader (Synergy Neo2, 1351000) at 405nm. A standard curve was established based on the absorbance values of the standard stock solutions and the resulting linear regression determined the concentration of endotoxins (EU/mL) of the test solutions.

Materials

Usually, two different buffer systems were used for loading and unloading the phages on the z²LFMC. Tris HCl buffer (10 mM) (plus 0.5 M NaCl) was added to the loading buffer. Sartobind Q anion-exchange membrane sheets (94IEXQ42-001) were purchased from Pall Corporation (New York, USA) and 5 mL bed volume z²LFMC was manufactured internally. Tris HCl (S7653) was purchased from Sigma-Aldrich (St. Louis, MO, USA). All buffers and the solutions used in our experiments were prepared using ultra-pure water (18.2 MΩ cm) obtained from Millipore's SIMPLICITY 185 water purification unit (Molsheim, France). MF-Millipore™ Membrane Filter, 0.45 μm pore size (Catalogue Number: HAWP04700) was used for micro-filtering and degassing buffers. Freeman 1085 Polyurethane Elastomer (Batch # 77032), consisting of the resin (part A) and hardener (part B) was purchased from Freeman Manufacturing and Supply Company, Avon, OH, USA. The membrane-based chromatography experiments were carried out using an AKTA Prime liquid chromatography system (GE Healthcare Biosciences, Montreal, QC, Canada).

Using the proper sample loops, the phage feed solutions were injected. In these experiments, two types of the loops (e.g., small loops and super loops) were used to fully investigate the z²LFMC device. At a wavelength of 280 nm in AKTA Prime liquid chromatography system, chromatograms were obtained by measuring the flowthrough and eluate peaks. During this process, samples matching the distinct, separated peaks were collected in falcon tubes by measuring the exact mass with 0.01 g error and were evaluated by using Pierce LAL Chromogenic Endotoxin Quantification Kit, Bradford Assay and Double Overlay Phage Titer Assay.

Results and Discussion

Flow distribution in a z²LFMC device comprises two sets of primary and secondary flow channels, as shown in Fig. 1. Fig. 1A shows how the fluid flowing through a z²LFMC device has three levels

of hierarchy, i.e., primary flow through the primary channels, secondary flow through the secondary channels, and tertiary (or regular) flow through the membrane stack. Based on the type of the mobile and stationary phase of the feed and ion-exchange chromatography, the chromatograph is different. The mobile phase is a complex mixture of many proteins and the target (i.e., phage). During binding, the target protein (phage) creates a uniquely strong affinity to the membrane and the impurities pass from the membrane and the results are observed on the chromatograph. Elution, the final step, now releases the purified protein from the membrane so it can be collected for further processing. Fig. 1B shows the details regarding the concept.

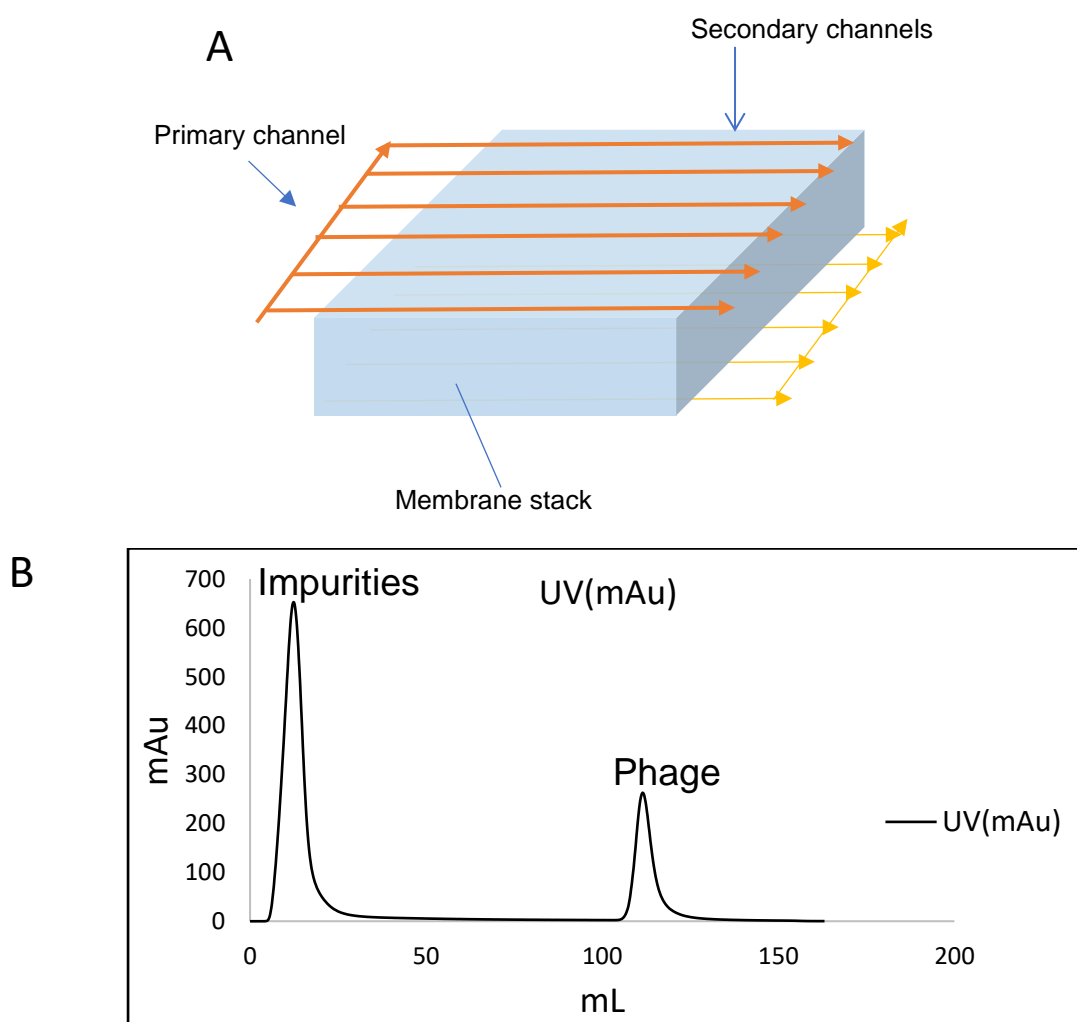


Fig. 1. A) z^2 LFMC. Explanation regarding how it works and why it was chosen based on its geometry. B) Explanation how chromatography works.

There is a necessity for optimizing chromatographic devices. Optimization of anion-exchange chromatography, like any chromatography, should be done step-by-step by testing different parameters, which can significantly affect the process. The first step is to fix the size of the LFMC and iterate over several parameters' configurations. The z²LFMC device used in this study has a bed volume of 5 mL. The experiments were conducted using a 5 mL loop. However, within two of the experiments, a superloop was used. Toward understanding the optimized flow rate, the efficiencies of the z²LFMC devices were compared at 5, 10, 12, 15 mL/min flow rates by theoretical plates. Theoretical plate measurement was performed using 50 μ L injection with 0.4 M NaCl solution as mobile phase and 0.8 M NaCl solution as tracer. The number of theoretical plates (N) was calculated using the equation 1 in chapter 2. At the flow rate of 10mL/min, the number of plates/m obtained with the z²LFMC device was more significant than the other flow rates. Table 1 shows the summary of the tests.

Table 1. Number of plates/m obtained with the 5 mL Q z²LFMC device in different flowrates (5, 10, 12 and 15 mL/min)

Flowrate (mL/min)	N/m
5	31381.8
10	52782.1
12	49161.2
15	50788.9

In Ion exchange chromatography the separation of molecules is based on their total charge. This technique is reasonable for the separation of molecules that would be difficult to separate by other separation techniques because the charge of the molecule of interest can be manipulated by changing buffer pH. In the evaluation process, a preliminary experiment was conducted to determine the best pH and gradient length, where pH values of 7.5, 8.0 and 8.5 were selected based on the pI of the phage. Based on the experimental observations, the pI was assumed to be around 7. The selected pH for investigations is higher than pI, therefore, the phage will bind to Q membrane while impurities, including proteins, are expected to flow through. By changing the buffer with the proper salt concentration, the phage from eluate was gathered for further investigation. Experiments carried out at three different pH values with three gradient lengths are shown in Fig. 2 and Fig. 3.

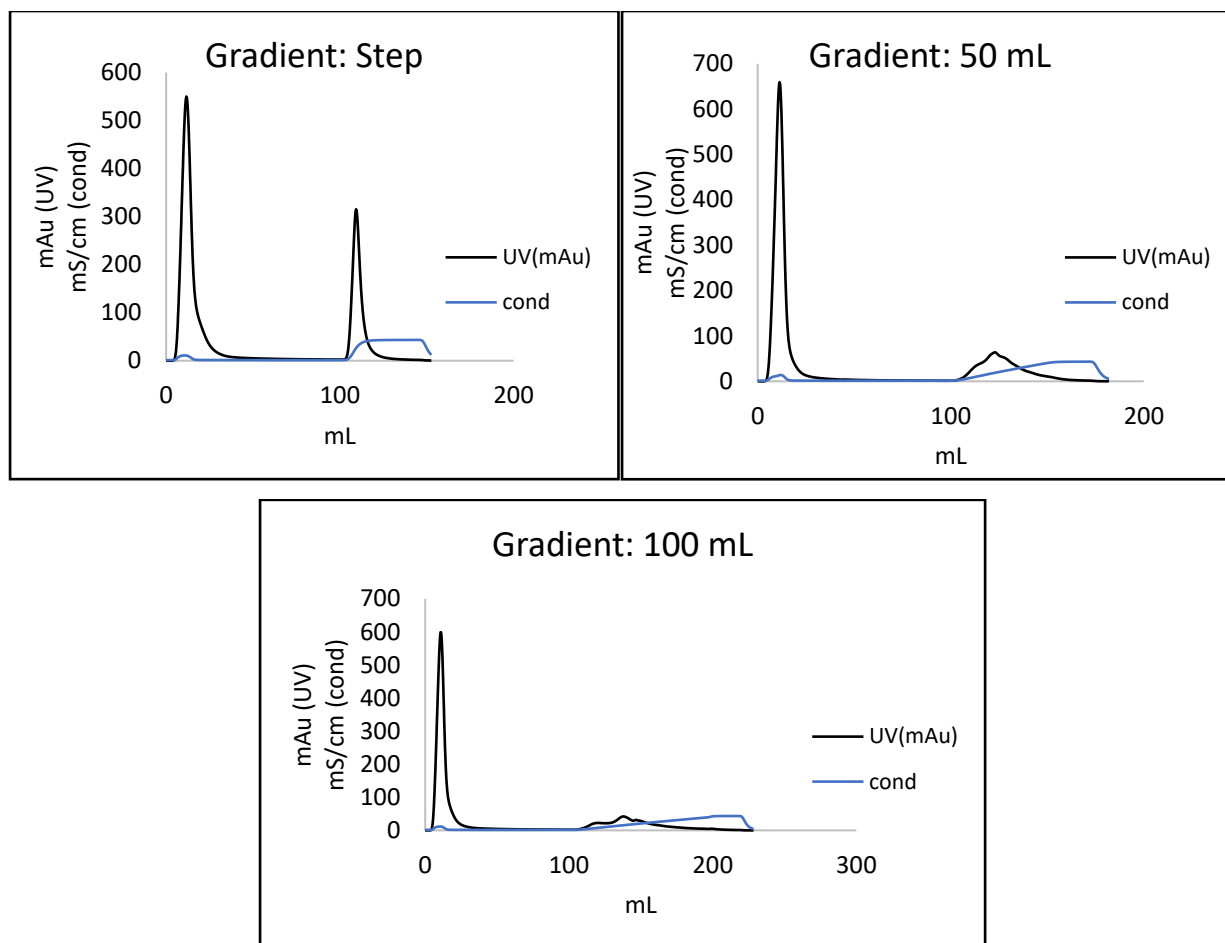


Fig. 2. Optimizing the gradient for releasing pure phage

Device: 5 mL, Flow rate: 10 mL/min, loop: 5 mL, Gradient: Shown in Graphs, Buffers: Tris HCl: 10mM, pH 7.5 (+0.5M NaCl). Phage diluted 2 times.

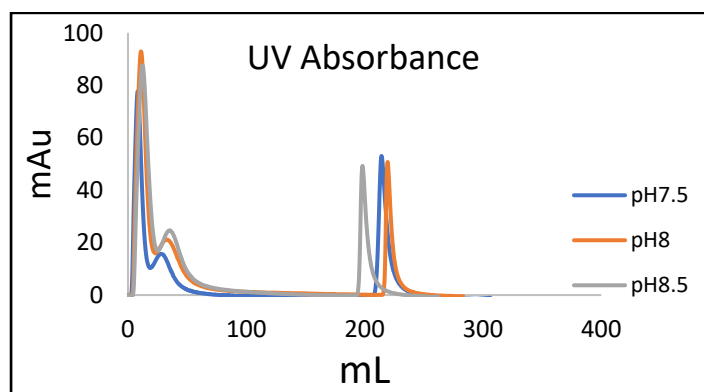


Fig. 3 Optimizing pH for releasing pure phage. Device: 5 mL, Flow rate: 10 mL/min, loop: 5 mL, Gradient: Step, Buffers: Tris HCl: 10mM, (+0.5M NaCl). Phage diluted 20 times.

The main goal of these experiments is to explore potential relationships between other proteins and impurities. The gradient helped to separate these from the phage. However, the peaks obtained with longer gradients indicated that the phage was the main target bound and even if other impurities were bound, the amount was low and can be neglected. So, an extended gradient would not be required as there should be a buffer usage trade-off. In this case, an extended gradient would affect the peaks, resulting in broad and diluted elution peaks. A step change is therefore recommended. When a gradient of 50 mL or 100 mL length was used, the shoulders followed the main peak very closely. With the decrease in the gradient length (step), the shoulder moved away, indicating better resolution. By observing the chromatograms, the difference in binding at the three specified pH values is not significant. However, as the pH value of 7.5 has the sharpest eluate peak, it can be chosen as desirable pH. In order to select the best pH and gradient, the quantitative analysis of the binding and elution portions was performed and graph analysis of the peak area ratio was calculated.

The calculations based on the elution peak ratio is shown in Fig. 4A. As shown, a pH value of 7.5 has a higher elution peak ratio, in comparison with other pH values for 0 mL gradient length, therefore motivating for using the step gradient. The elution peak ratio is measured by calculating AUC of the elution peak divided by the total AUC of the chromatograph.

Fig. 4B shows the PFU/mL recovery data (based on double overlay phage titer assay) for flow-through and elution at different pH values. In this experiment, samples corresponding to the flow through, and the elution peak from the phage purification experiment carried out with the Q z²LFMC device at the optimized conditions (flow rate: 10 mL/min, gradient length: 0 mL) were analyzed by double overlay phage titer assay and the phage recovery was calculated. The results obtained by double overlay phage titer assay analysis are summarized in Fig. 4B.

As shown, a pH value of 7.5 has the best result with 35% recovery, which is selected as the baseline for the remaining of the experiments.

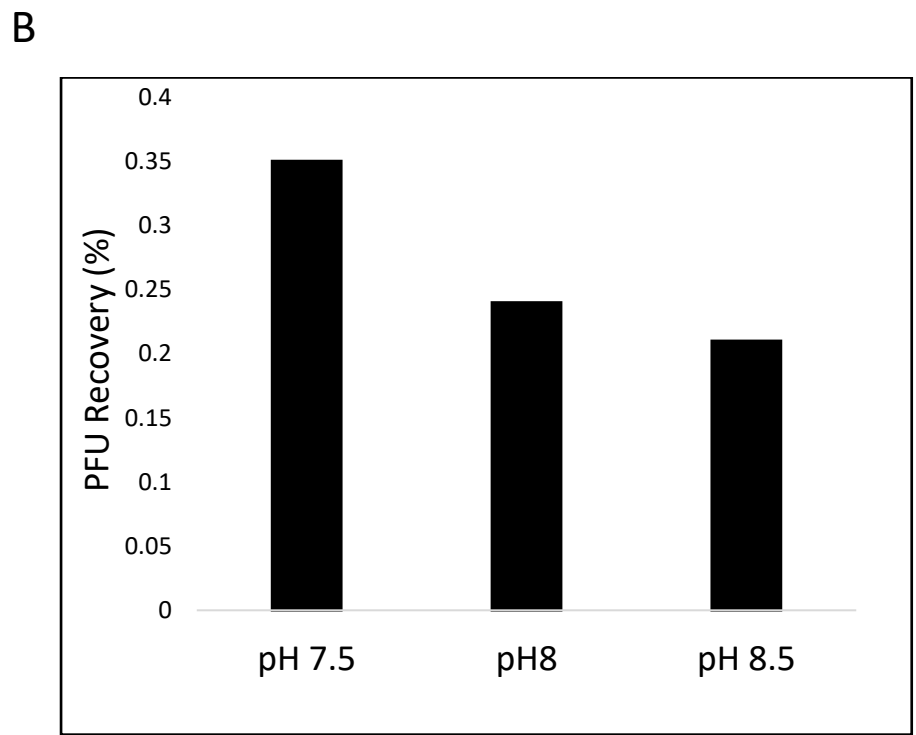
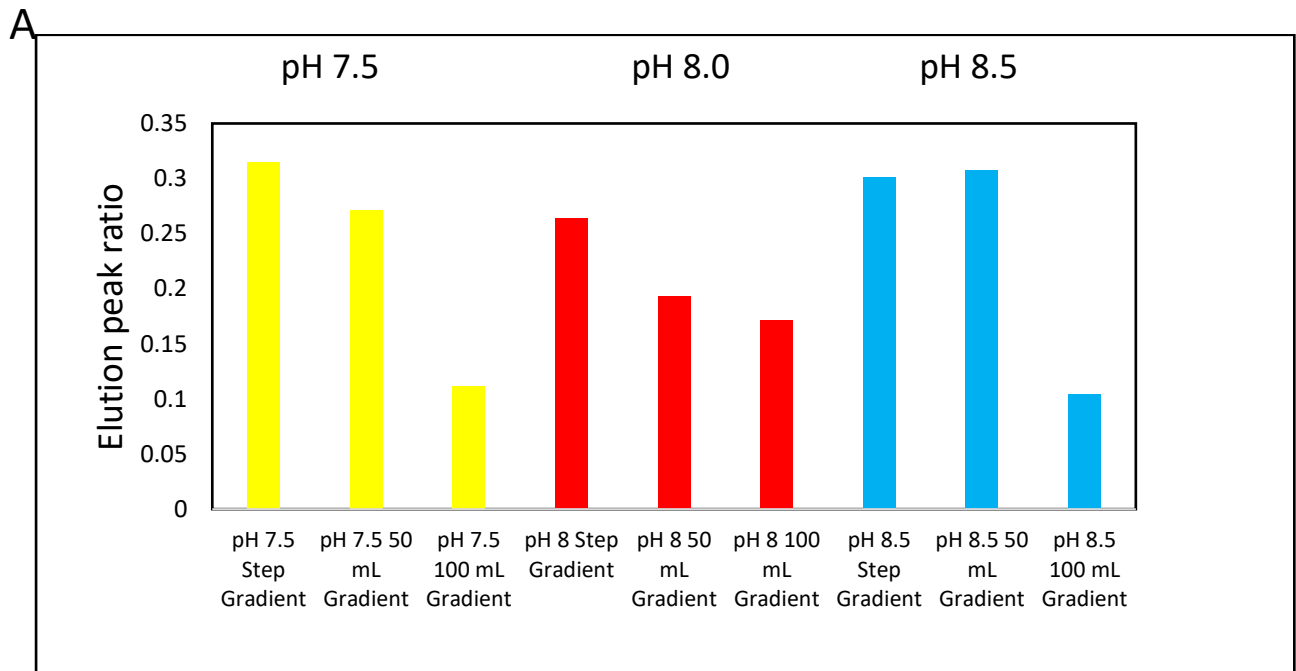


Fig. 4. Optimization regarding the pH and Gradient. Further investigation on A) Eluate peak ratio (Device: 5 mL, Flow rate: 10 mL/min, loop: 5 mL, Buffers: Tris HCl 10mM, (+0.5M NaCl)) and B) PFU Recovery. Device: 5 mL, Flow rate: 10 mL/min, loop: 5 mL, Gradient: Step, Buffers: Tris HCl 10mM, (+0.5M NaCl).

In some cases, the feed could contain salt and a high salt concentration could reduce the phage binding on Q membrane. Salt concentration has a direct effect on the success of any ion-exchange chromatography experiments.

By experimenting feed on different dilutions and checking the conductivity of the AKTA system, the existence of salt has been confirmed. Fig. 5 shows the conductivity (mS/cm) in different dilutions by injecting feed in the mobile phase of the membrane. As shown, there is salt in the feed. In some cases, the feed could contain salt, and a high salt concentration could reduce the phage binding on Q membrane. However, due to the potential effects of this phenomenon on the binding, further examination was required.

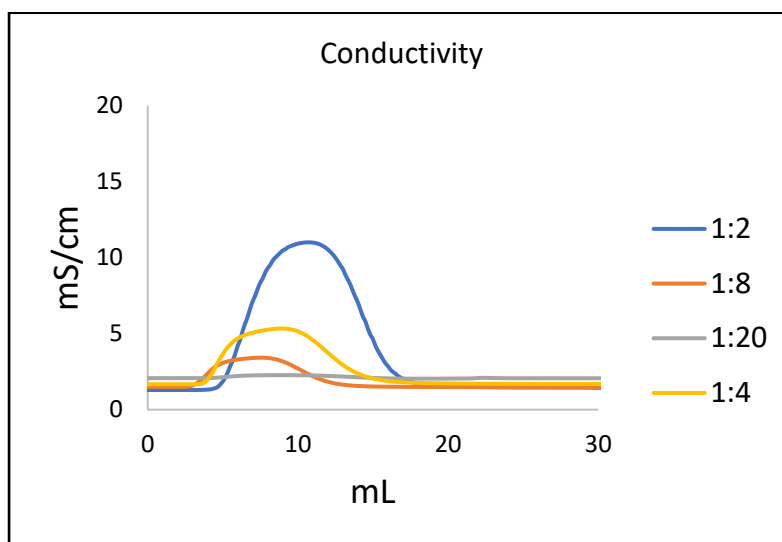


Fig. 5. Conductivity in AKTA of different dilutions (1 in 2, 1 in 4, 1 in 8, 1 in 20) of phage in FT.

Experiments were carried out using different dilutions, 1 in 2, 1 in 4, 1 in 8 and 1 in 20 at pH value of 7.5 with step gradient. It is given the elution peak area/total area data for the 4 dilutions in Fig. 6.

Based on fig. 6 it can be concluded that diluting phages does not have that much effect on the efficiency of the membrane chromatography. At all dilution factors, the extent of phage binding was negligibly affected by the high ionic strengths of the feed solutions. For instance, the fraction of phage recovered at a dilution factor of 1 in 2 was 0.31, the phage binding was negligibly lower than that at 1 in 8 dilution factor and negligibly higher than other dilutions.

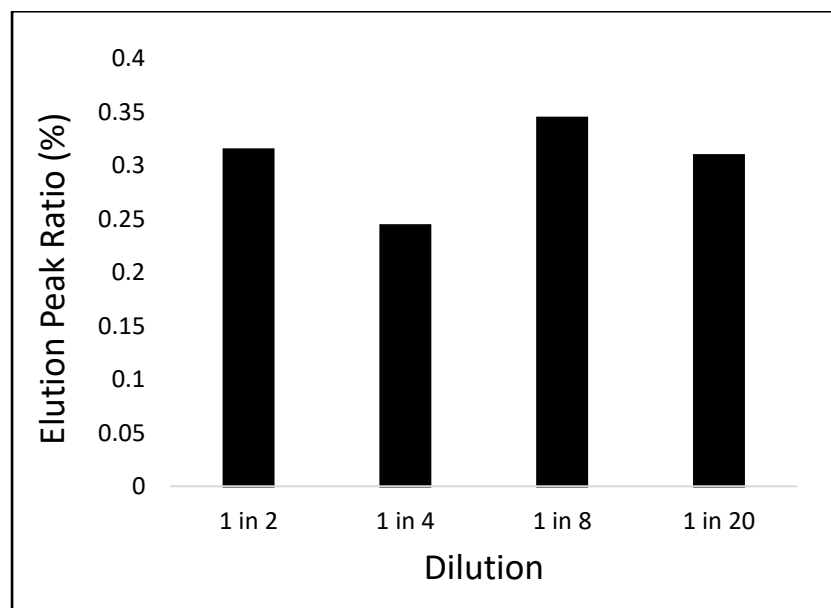


Fig. 6. Effect of dilution (1 in 2, 1 in 4, 1 in 8, 1 in 20) on peak area ratio.

To check the efficiency of the membrane chromatography, two different dilutions were randomly selected to proceed with the experimental evaluation, in particular, dilutions 1 in 4 and 1 in 20 have been selected for further investigations.

Fig. 7 shows the chromatogram obtained during purification of T7 bacteriophage using the Q z²LFMC. This experiment was carried out at a flow rate of 10 mL/min, the conditions being identical to that optimized for phage purification using the 5 mL Q z²LFMC device, i.e., 5 mL of 1 in 4 diluted phages. The binding, the eluting buffers were also the same as those mentioned earlier, i.e., 10mM Tris-HCl (pH 7.5) and 0.5 M NaCl solution (prepared in binding buffer) respectively. The elution was carried out using a 0 mL linear gradient (step gradient) from binding to eluting buffer. The impurities appeared in the flow through peak between 5 and 81 mL effluent volume while the phage was eluted as a single peak around 112 mL effluent volume. In order to qualify the device for larger volumes of phages, multiple injections of same feed were tested in this experiment as well. The chromatograms and recovery data are shown in Fig. 7 and Fig. 8. In a single injection, only 5 mL of feed was injected over the membrane and a phage recovery rate of 74.9% was achieved. For multi-injection, a total of 110 mL of feed was injected, which

was conducted over 22 doses (i.e., 22 x 5 mL injections), and a 35.3% phage recovery rate in the eluate was observed.

In this experiment, samples corresponding to the flow through peak, and the elution peak from the 5 mL and 110 mL phage purification experiment collected and were analyzed by double overlay phage titer assay. In both experiments no phage was collected from the flow through peaks, however, the phage recovery in 5 mL phage purification experiment is 2 times more than another experiment.

It can be concluded that phage recovery can be expected to be higher in the smaller amount of the feed flowing through the membrane chromatography.

At the same time, the endotoxin removal for both conditions were close to 70%.

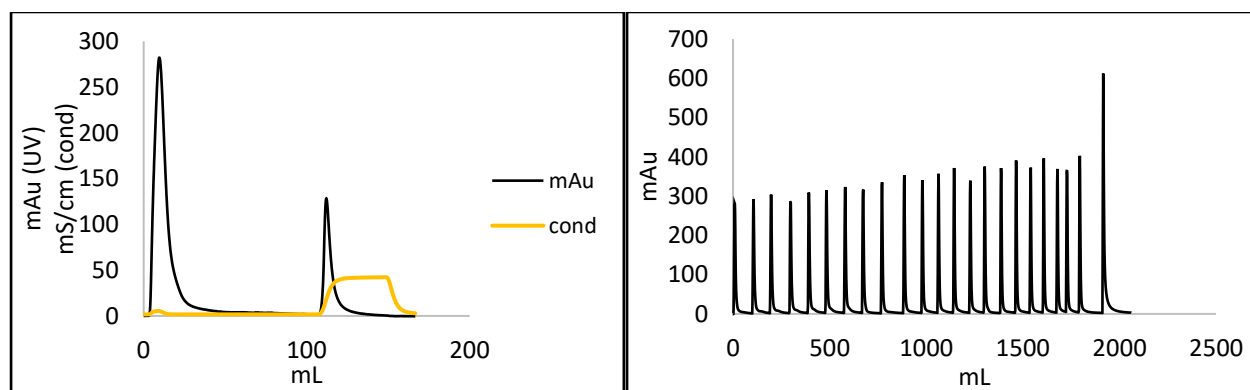


Fig. 7. Single and multi-injection phage on z²LFMC. Device 5 mL sartobind q (L x W = 20 x 70 mm), Flow rate: 10 mL/min, loop: 5 mL, Gradient: Step, Buffers: Tris HCl 10mM, pH 7.5 (+0.5M NaCl), Sample 1 in 4.

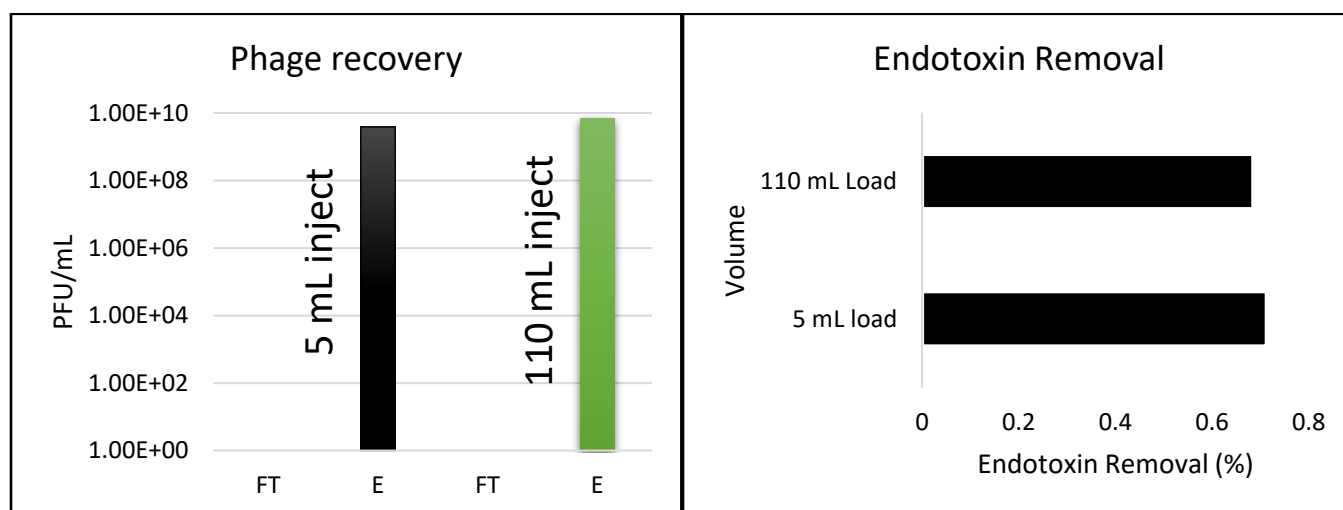


Fig. 8. Phage recovery and endotoxin removal in single and multiple inject. Device 5 mL sartobind Q (L x W = 20 x 70 mm), Flow rate: 10 mL/min, loop: 5 mL, Gradient: Step, Buffers: Tris HCl 10mM, pH 7.5 (+0.5M NaCl), Sample 1 in 4.

In the second set of experiments, the separation process was carried out at 1 in 20 dilutions using single and multiple injections. In a single injection, only 5 mL of feed was injected over the membrane, obtaining a phage recovery rate of 89.0%. For multi-injection, a total of 25 mL and 50 mL feed were injected, which is equal to 5 x 5 mL and 5 x 10 mL, and the achieved phage recovery in the eluate was 77.7% and 65.4%, respectively, while maintaining endotoxin removal rates of higher than 60%. The chromatograms and recovery data are shown in Fig. 9 and 10.

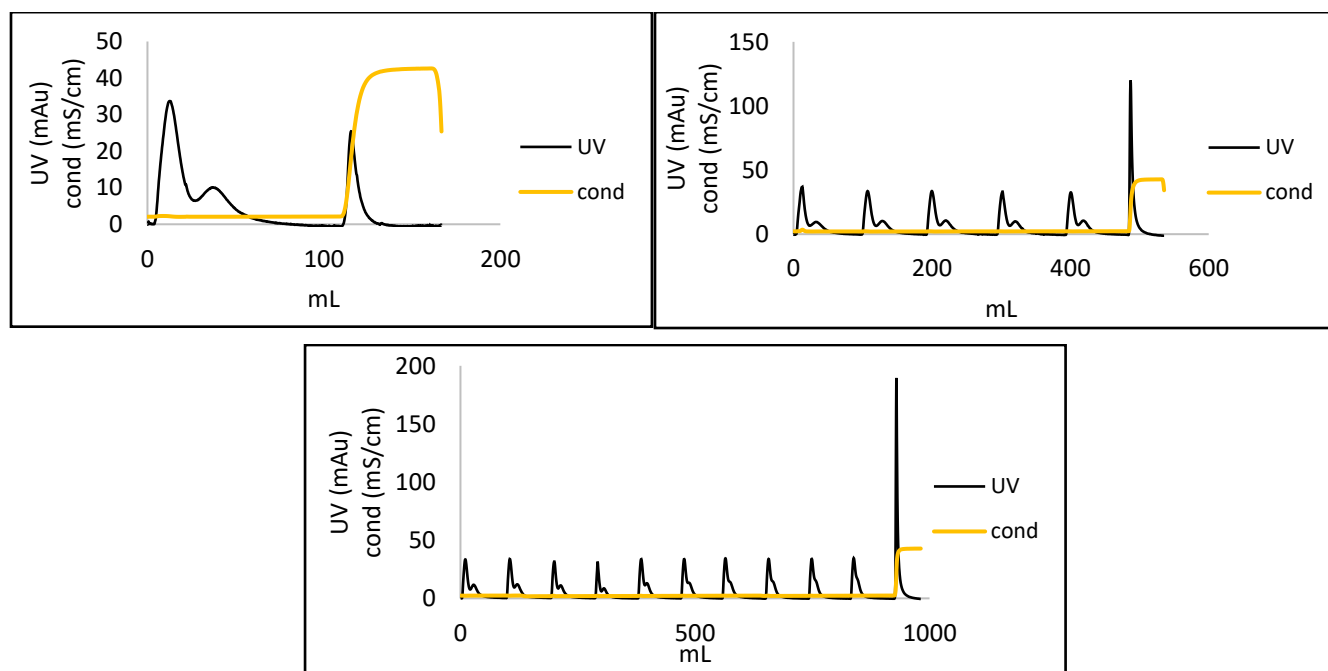


Fig 9. Single and multi-injection phage on z²LFMC. Device: 5 mL Sartobind Q (L x W = 20 x 70 mm), Flow rate: 10 mL/min, loop: 5 mL, Gradient: Step, Buffers: Tris HCl 10mM, pH 7.5 (+0.5M NaCl), Sample 1 in 20.

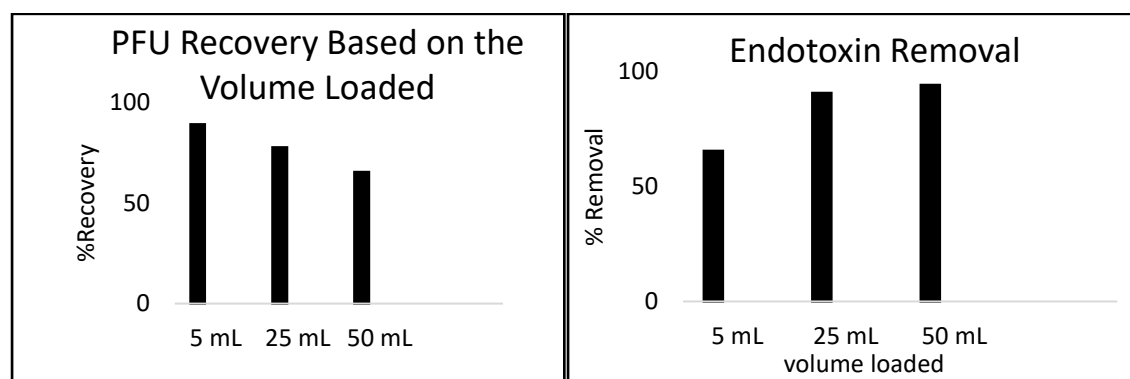


Fig. 10. PFU recovery and Endotoxin removal based on previous chromatographs. Device: 5 mL sartobind q (L x W = 20 x 70 mm), Flow rate: 10 mL/min, loop:5 mL, Gradient: Step, Buffers: Tris HCl 10mM, pH 7.5 (+0.5M NaCl), Sample: 1 in 20.

Phage recovery for 1 in 4 feed diluted is lower than 1 in 20 dilutions. However, a diluted feed would not be required as there should be a buffer usage trade-off.

Using a sample loop, an overall volume of 10 μ l to 100 ml can be injected onto the column. The advantage of sample loops over normal loops is their lower cost, effectiveness, reduced sample loss, and higher reproducibility of the injection [35].

Moreover, the superloop enables a higher amount of injection feed can be loaded on the membrane without being lost within the system. In this experiment, two different superloops were tested to determine the binding capacity. In the first set of experiments, optimized conditions were assumed, and a 100 mL of 1:1 feed was loaded on the 5 mL membrane chromatography. Based on the calculation by Bradford assay, 53.5% of impurities were eliminated, showing a promising direction, as illustrated in Fig. 11A. Note that the superloop's accuracy was checked with a smaller amount of the feed as well. On the other hand, Fig. 11B shows the chromatograph when loading 15 mL 1:1 feed with optimized conditions, with a phage recovery rate of 72.0%.

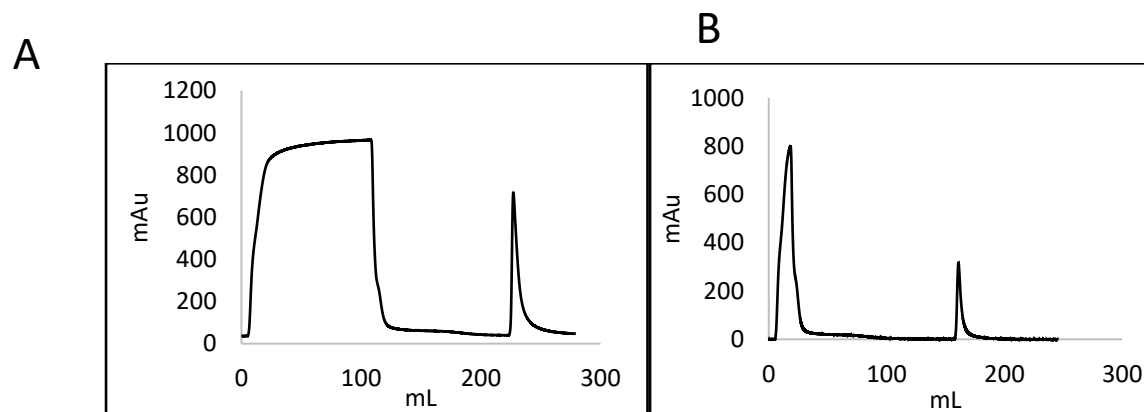


Fig 11. A) Super loop by loading 100 mL phage 1:1 with optimized conditions, B) Super loop by loading 15 mL phage 1:1.

Next, UF centrifuge and UF stirred filtration is utilized for analytical analysis. For UF centrifuge 4 min, 2000 rpm, 4°C, 100 kDa NMWCO conditions were used. Then, the pellet was resuspended in phage buffer (10 mM Tris HCL to 7.5). Note that the phage could also be concentrated from

the UF stirred filtration (1 h, 300 rpm, 25°C). Endotoxin removal was tested for the phage collected from each condition. Given that, ultrafiltration significantly reduced the endotoxins from phage samples, as shown in table 2. Overall, anion exchange chromatography is efficient in endotoxin removal, whereas ultrafiltration can be used as a second step.

Table 2. Comparing endotoxin removal percentage in UF Centrifuge, UF stirred filter and Sartobind Q z²LFMC.

Injection Type	Endotoxin Removal (%)
One Inject	71.2%
UF Centrifuge	63.4%
UF Stirred filter	65.6%

Conclusion

Therapeutic bacteriophage production is a time-consuming operation, including multi-stage processing, starting from phage propagation and filtering, and ending with several combinations of separation and purification processes. Among these, purification is a very crucial step in bacteriophage production. Although Traditional purification processes provide promising results, they are considered defective processes. In this work, Tris–HCl buffer was used as binding and elution buffers. The hand-made z²LFMC with anion exchange membrane was connected to an AKTA HPLC system. The purification process was conducted within one hour and 20 minutes. The infectivity and the recovery percentage of purified phage particles were determined by plaque-forming assay. Membrane chromatography, such as anion exchange z²LFMC, presents promising results with the proposed design, with phage recoveries of 89.0% under perfect conditions. Moreover, the achievable endotoxin removal rate is up to 71.2% under the same conditions. Compared to conventional columns, z²LFMC chromatographic approach presents a much simpler process with an easy and straightforward result in a short time.

Acknowledgement

We thank the Natural Science and Engineering Research Council (NSERC) of Canada for funding this project.

References

- [1] V.V. Vlassov, N.V. Tikunova, V.V. Morozova, Bacteriophages as Therapeutic Preparations: What Restricts Their Application in Medicine, *Biochemistry. Biokhimiia.*, 85(11)(2020), pp. 1350–1361
- [2] STREPTOMYCIN treatment of pulmonary tuberculosis, *Br. Med. J.*, 2(4582)(1948), pp. 769-782
- [3] K.E. Kortright, B.K. Chan, J.L. Koff, P.E. Turner, Phage Therapy: A Renewed Approach to Combat Antibiotic-Resistant Bacteria, *Cell. Host. Microbe.*, 25(2)(2019), pp. 219–232
- [4] R. J. Fair, Y. To, Antibiotics and bacterial resistance in the 21st century, *Perspect. Medicinal. Chem.*, 6(2014), pp. 25–64
- [5] C. Brives, J. Pourraz, Phage therapy as a potential solution in the fight against AMR: obstacles and possible futures, *Palgrave. Commun.*, 6(1)(2020), pp. 1-11
- [6] A. Sulakvelidze, Z. Alavidze, J.G. Jr. Morris, Bacteriophage therapy, *Antimicrob. Agents. Chemother.*, 45(3)(2001), pp. 649–659
- [7] D.M. Lin, B. Koskella, H.C. Lin, Phage therapy: An alternative to antibiotics in the age of multi-drug resistance, *World. J. Gastrointest. Pharmacol. Ther.*, 8(3)(2017), pp. 162-173
- [8] C.R. Raetz, C. M. Reynolds, M.S. Trent, R.E. Bishop, Lipid A modification systems in gram-negative bacteria, *Annu. Rev. Biochem.*, 76(2007), pp. 295–329
- [9] J.J. Gill, P. Hyman, Phage choice, isolation, and preparation for phage therapy, *Curr. Pharm. Biotechnol.*, 11(1)(2010), pp. 2–14

[10] C.R. Raetz, C.M. Reynolds, M.S. Trent, R.E. Bishop, Lipid A modification systems in gram-negative bacteria, *Annu. Rev. Biochem.*, 76(2007), pp. 295–329

[11] D. C. Morrison, R.J. Ulevitch, The effects of bacterial endotoxins on host mediation systems. A review, *Am. J. Pathol.*, 93(2)(1978), pp. 526–618

[12] E.T. Rietschel, T. Kirikae, F.U. Schade, U. Mamat, G. Schmidt, H. Loppnow, A.J. Ulmer, U. Zähringer, U. Seydel, F. Di Padova, Bacterial endotoxin: molecular relationships of structure to activity and function, *FASEB J.*, 8(2)(1994), pp. 217–225

[13] Administration, U.S.F. a. D. Inspection Technical Guides. (2014, Nov 17). Bacterial Endotoxins/Pyrogens. Available online: <https://www.fda.gov/inspections-compliance-enforcement-and-criminal-investigations/inspection-technical-guides/bacterial-endotoxinspyrogens>

[14] P.O. Magalhães, A.M. Lopes, P.G. Mazzola, C. Rangel-Yagui, T.C. Penna, A. Jr. Pessoa, Methods of endotoxin removal from biological preparations: a review, *J. Pharm. Pharm. Sci.*, 10(3)(2007), pp. 388–404

[15] S.T. Abedon, S.J. Kuhl, B.G. Blasdel, E.M. Kutter, Phage treatment of human infections, *Bacteriophage.*, 1(2)(2011), pp. 66–85

[16] N. Bonilla, M.I. Rojas, G. Netto Flores Cruz, S.H. Hung, F. Rohwer, J.J. Barr, Phage on tap- a quick and efficient protocol for the preparation of bacteriophage laboratory stocks, *PeerJ.*, 4(2016), pp. e2261

[17] K.R. Yamamoto, B.M. Alberts, R. Benzinger, L. Lawhorne, G. Treiber, Rapid bacteriophage sedimentation in the presence of polyethylene glycol and its application to large-scale virus purification, *Virology.*, 40(3)(1970), pp. 734–744

[18] R.K. Scopes, *Protein Purification: Principles and Practice* (3rd ed.), New York: Springer (2010)

[19] E.M. Kutter, A. Sulakvelidze, *Bacteriophages: Biology and Application*, Boca Raton, FL: CRC Press (2005)

[20] E.M. Adriaenssens, S.M. Lehman, K. Vandersteegen, D. Vandenneuvel, D.L. Philippe, A. Cornelissen, M.R. Clokie, A.J. García, M. De Proft, M. Maes, R. Lavigne, CIM(®) monolithic anion-exchange chromatography as a useful alternative to CsCl gradient purification of bacteriophage particles, *Virology.*, 434(2)(2012), pp. 265–270

[21] L. Schwartz, K. Seeley, *Introduction to Tangential Flow Filtration for Laboratory and Process Development Applications*

[22] G. W. Rembhotkar, G.S. Khatri, Large scale preparation of bacteriophage lambda by tangential flow ultrafiltration for isolation of lambda DNA, *Anal. Biochem.*, 176(2)(1989), pp. 373–374

[23] S. Reitingner, O.I. Petriv, K. Mehr, C.L. Hansen, S.G. Withers, Purification and quantitation of bacteriophage M13 using desalting spin columns and digital PCR, *J. Virol. Methods.*, 185(1)(2012), pp. 171–174

[24] P. Serwer, P.R. Graef, P.N. Garrison, Use of ethidium bromide fluorescence enhancement to detect duplex DNA and DNA bacteriophages during zone sedimentation in sucrose gradients: molecular weight of DNA as a function of sedimentation rate, *Biochemistry.*, 17(7)(1978), pp. 1166–1170

[25] T.C. Ling, C.K. Loong, W.S. Tan, B.T. Tey, W.M. Abdullah, A. Ariff, Purification of filamentous bacteriophage M13 by expanded bed anion exchange chromatography, *J. Microbiol.*, 42(3)(2004), pp. 228–232

[26] P. Madadkar, R. Ghosh, High-resolution protein separation using a laterally-fed membrane chromatography device, *J. Membr. Sci.*, 499(2015)

- [27] P. Madadkar, S.L. Nino, R. Ghosh, High-resolution, preparative purification of PEGylated protein using a laterally-fed membrane chromatography device, *J. Chromatogr. B. Biomed. Appl.*, 1035(2016), pp. 1–7
- [28] P. Madadkar, U. Umatheva, G. Hale, Y. Durocher, R. Ghosh, Ultrafast Separation and Analysis of Monoclonal Antibody Aggregates Using Membrane Chromatography, *Anal. Chem.*, 89(8)(2017), pp. 4716–4720
- [29] P. Madadkar, Q. Wu, R. Ghosh, A laterally-fed membrane chromatography module, *J. Membr. Sci.*, 487(2015)
- [30] J. Marriott, E. Sørensen, A general approach to modelling membrane modules, *Chem. Eng. Sci.*, 58 (22)(2003), pp. 4975-4990
- [31] R. Ghosh, G. Chen, U. Umatheva, P. Gatt, A flow distribution and collection feature for ensuring scalable uniform flow in a chromatography device, *J. Chromatogr. A.*, 1618(2020), pp. 460892
- [32] R. Ghosh, G. Chen, R. Roshankhah, U. Umatheva, P. Gatt, A z^2 laterally-fed membrane chromatography device for fast high-resolution purification of biopharmaceuticals, *J. Chromatogr. A.*, 1629(2020), pp. 461453
- [33] K. Kawka, P. Madadkar, U. Umatheva, S. Shoaebargh, M.F.C. Medina, B.D. Lichty, R. Ghosh, D.R. Latulippe, Purification of therapeutic adenoviruses using laterally-fed membrane chromatography, *J. Membr. Sci.*, 579(2019), pp. 351-358
- [34] R. Roshankhah, G. Chen, Y. Xu, N. Butani, Y. Durocher, R. Pelton, R. Ghosh, Purification of monoclonal antibody using cation exchange z^2 laterally-fed membrane chromatography – A potential alternative to protein A affinity chromatography, *Biochem. Eng. J.*, 178(2022), pp. 108293

[35] <https://www.knauer.net/>

Chapter 5

Conclusion

Membrane chromatography is a chromatography device that consists of a stack of membranes for antibody separation. In this work, we leverage two membrane chromatography devices, LFMC and z²LFMC. The real-life applications of LFMC were studied in the literature, including the removal of monoclonal antibody aggregates, and the purification of PEGylated proteins. However, it is necessary to validate the characteristics of the second generation of LFMC, namely, z²LFMC. In this thesis, z²LFMC was extensively studied to evaluate its capabilities in removing impurities, endotoxins, and host cell proteins from biopharmaceutical products. For example, in chapter two, using z²LFMC for monoclonal antibodies purification, it was observed that cation exchange z²LFMC was selected to be replaced with protein A resin. Based on this theoretical observation, the second generation of LFMC provided high-speed, high-resolution purification. Moreover, Trastuzumab was purified from cell culture supernatant using the S z²LFMC device. The mAb recovery rate obtained using S z²LFMC device was higher than the recovery rates obtained when using either the MabSelect SuRe resin column or the Capto S ImpAct column. However, it is essential to point out that further investigation is required before generalizing that the S z²LFMC-based method could be a viable alternative to protein A based affinity chromatography for mAb purification. Moreover, this thesis studied T7 bacteriophage as a purification subject. In particular, anion exchange z²LFMC membrane chromatography presented promising results with recovery rates of up to 89.0% of phage under perfect conditions, alongside an endotoxin removal rate of up to 71.2%. Compared to conventional columns, z²LFMC chromatographic approach presents a much simpler process, with easy and straightforward results in a shorter overall time.

Additionally, this thesis highlights the attempt to reengineering the channels and the shape of z²LFMC under different scenarios and applications. For instance, chapter three highlights the scenario based on the computational fluid dynamics, in which, no wet lab work took place. To confirm the efficiency of z²LFMC, various simulations were used to understand the fluid movements within membrane chromatography. Although z²LFMC addresses problems that exist in other conventional chromatography geometries, there can be maldistribution in z²LFMC. The introduced issues can be solved by redesigning taking into account the application requirements

and environment. This is more evident in the case of the biopharmaceutical separation process, where z²LFMC R5 device outperformed its counterparts, providing the best resolution.

Future work

In the future, more detailed, cohesive experiments should take place. This is essential to verify whether z²LFMC method is a feasible alternative to protein A affinity chromatography for mAb purification. This requires more guided quantitative analyses in regard to the endotoxin removal and purity percentage, with scalability is taken in mind.

Moreover, the design of z²LFMC is yet to be optimized, and more alternative designs should be tested. For example, changing the number of channels or the ports' design may significantly affect the device efficiency. In the future, COMSOL projects regarding the purification of monoclonal antibodies or bacteriophages can take place.

Further, z²LFMC is to be compared with other purification devices, including column and TFF, where the binding capacity of z²LFMC can be tested under different conditions.

Appendix

permission for using my paper in thesis [220308-004978]



Permissions Helpdesk <permissionshelpdesk@elsevier.com>



Wed 3/9/2022 7:37 AM

To: Roxana Roshankhah

Dear Roxana Roshankhah

Thank you for reaching out to us.

As the author of this **article** you are allowed to use it in your thesis as part or whole and permission is not required to be obtained. Hence, please go ahead.

Kindly ensure to give credit to the original source.

Let me know if you have any further questions.

Kind regards,

Roopa Lingayath

Senior Copyrights Coordinator

ELSEVIER | HCM - Health Content Management

Visit [Elsevier Permissions](#)